NTNU

Norwegian University of
Science and Technology

Hydrodynamic Interaction Among the Pontoons of a Floating Bridge: Effect of Global Responses

Marius Lien Killi

PROJECT THESIS IN MARINE TECHNOLOGY

SPRING 2018

FOR

STUD.TECHN. Marius Lien Killi

Hydrodynamic interaction among the pontoons of a floating bridge: effect on global responses
Hydrodynamiske interaksjoner mellom flytebropongtongene: globale effekter

Background:
The floating bridge concepts developed by Statens Vegvesen have many pontoons (20-50, depending on the concept). The dimensions of the pontoons are comparable to the distance between them. Hydrodynamic interaction among these pontoons is therefore expected. The importance of such interaction effects for the global response of the bridge should be investigated.

In the project work, a simple model with few pontoons and a global floating bridge model of one of the Bjørnafjord crossing concepts was developed in the SIMA software (SIMO-RIFLEX coupled model), considering the pontoons as relatively rigid components and using the hydrodynamic coefficients based on a first order potential flow analysis of a single pontoon in Wadam/WAMIT. In the master's thesis work, hydrodynamic interactions between the pontoons will be considered by numerical methods, and the consequences for important bridge responses will be examined. Due to limitations in the software, appropriate approximations and approaches will need to be developed. The work will first consider the simplified bridge model, then the full model, and then examine the parameters which are important for response.

Assignment:
The following tasks should be addressed in the project work:

1. Literature study regarding floating bridge concepts for Bjørnafjord, dynamic loads on floating bridges, and hydrodynamic interactions between rigid bodies. Environmental conditions (particularly waves) at Bjørnafjord should be examined.

2. Carry out first order potential flow analysis of two, three, four pontoons using Wadam or WAMIT. Examine hydrodynamic coefficients and compare to the coefficients for the single pontoon.

3. Incorporate the hydrodynamic coefficients from Wadam/WAMIT in the simplified and global analysis models. Examine the effects of the hydrodynamic interaction on dynamic response in regular waves.

4. Carry out parameter studies to investigate the consequences of hydrodynamic interaction and other modelling choices for the global dynamics of the floating bridge.

5. Report and conclude on the investigation.

The work scope could be larger than anticipated. Subject to approval from the supervisor, topics may be deleted from the list above or reduced in extent.

In the project, the candidate shall present his personal contribution to the resolution of problem within the scope of the project work.

Theories and conclusions should be based on mathematical derivations and/or logic reasoning identifying the various steps in the deduction.

The candidate should utilize the existing possibilities for obtaining relevant literature.

The project report should be organized in a rational manner to give a clear exposition of results, assessments, and conclusions. The text should be brief and to the point, with a clear language. Telegraphic language should be avoided.

The project report shall contain the following elements: A text defining the scope, preface, list of contents, main body of the project report, conclusions with recommendations for further work, list of symbols and acronyms, reference and (optional) appendices. All figures, tables and equations shall be numerated.

The supervisor may require that the candidate, in an early stage of the work, present a written plan for the completion of the work. The plan should include a budget for the use of computer and laboratory resources that will be charged to the department. Overruns shall be reported to the supervisor.

The original contribution of the candidate and material taken from other sources shall be clearly defined. Work from other sources shall be properly referenced using an acknowledged referencing system.

The project report shall be submitted in two copies:
- Signed by the candidate
- The text defining the scope included
- In bound volume(s)
- Drawings and/or computer prints which cannot be bound should be organized in a separate folder.

Erin Bachynski
Trygve Kristiansen
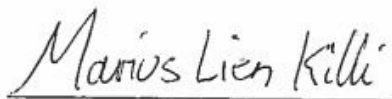Xu Xiang
Supervisors

Deadline: 11.06.2017

2

Preface

This master thesis is the final result of a Master of Science degree in Marin Technology at Norwegian University of Science and Technology. The thesis has a magnitude of 30 ECTS and has been written from January to June 2018. Professor Erin Bachynski and Statens vegvesen developed the scope of the work. Working with this thesis has been a demanding task where some part turned out to be more time consuming than first expected. As a consequence of this, it was not possible to study the hydrodynamic interaction of the complete bridge structure. The model turned out to be too large, and each analysis took many days to complete.

As a preparation for this thesis, a project thesis was written during fall 2017. The project thesis mostly focuses on static and eigenvalue analysis on a previously developed floating bridge concept at Bjornafjorden. Most of the theory is based on the project thesis and it is further developed through this master thesis.

I would like to express my gratitude to Professor Erin Bachynski for guidance and advises during weekly meetings, and Erin always has an answer to all my questions. I also would like to give a special thanks to Xiang Xu working in project-group at Statens Vegvesen. I want to thanks him for information related to the previous investigation within floating bridge concepts.

Trondheim 10.06.2018

Marins Lien Killi

Abstract

The National Public Road Administration has made a plan to establish a ferry-free road connection between Kristiansand and Trondheim. Bjørnafjorden is one of these fjords that have to be crossed, and several solutions are proposed for crossing. The design is developed in a cooperation between COWI, Aas Jakobsen, Johs Holte As and Global Maritime as a part of The Norwegian Public Roads Administrations (NPRA).

The purpose of this master thesis is to examine the effects of hydrodynamic interaction on the dynamic response in regular and irregular waves. The results shows that large oscillations for multibody configuration begins for frequency between 1-2 rad/s. The design chosen in this thesis is a curved floating bridge, with a cable-stayed section in the south end that allows ship traffic to pass under the bridge. It is free floating without mooring lines, and the shear forces are carried through membrane stresses with the curved design. The bridge girder has a total distance from south to north of 5435 meters. In the south end, a navigation channel is placed with a span length of 525 meters. The low bridge has a span length of 100 meters, and the main girder is 16.2 meters above sea-level.

First part of this project was a literature study regarding floating bridge concepts for Bjørnafjorden, dynamic loads on floating bridges and hydrodynamic interactions between rigid bodies. The pontoon model was created in GeniE with a reasonable mesh. The second part was to do a first order potential flow analysis of the different pontoon size in HydroD and Wadam. The curved bridge model was created in SIMA where hydrodynamic interaction between the pontoons was studied. Static analysis and eigenmode analysis was also carried out to verify the model is modeled correctly. The static analysis mainly focuses on bending moment, shear stress and static displacement of the bridge girder and compared to the reference model by The Norwegian Public Roads Administrations.

An eigenvalue analysis was conducted, and large period deflection modes were observed for horizontal bending of the bridge girder. The maximum eigenvalue was found to be 65.4 seconds. The results of the eigenvalue analysis were compared with the reference analysis and were found to correspond well. This gave confidence for the model being able to represent the structural response of the bridge reasonably well.

A simplified floating bridge was established to do further analysis of the effect of hydrodynamic interaction in three different wave directions. The wave heading from the north-west is most critical regarding moments and displacements. That may be because of distribution of all six load components, while waves from the west only have three components In a RIFLEX model the hydrodynamic couplings matrix for radiation data is not included. The interaction problem is therefore based on first order wave force transfer function and radiation data in the diagonal matrix.

In an early stage, I realized how complicated a floating bridge concept is and cover all the aspects are impossible. The complete floating cable-stayed bridge with a total length of more than 5 kilometers turned out to be too large to analysis the hydrodynamic interaction effects. The primary focus was put on studying the response of simple bridge caused by wave loads from different headings.

Sammendrag

Statens vegvesen har i lang tid planlagt å etablere en fergefri veiforbindelse mellom Kristiansand og Trondheim. Bjørnafjorden er en av disse fjordene som må krysses, og det foreslås flere løsninger for kryssing. Designet av broen er utviklet gjennom et tett samarbeid mellom COWI, Aas Jakobsen, Johs Holte As og Global Maritime som en del av Statens vegvesen (NPRA).

Hensikten med denne masteroppgaven er å undersøke effekten av hydrodynamisk interaksjon av den dynamiske responsen i regulære og uregulære bølger. Bølgeindusert respons har blitt undersøkt for relevante bølgelaster og bølgeretninger. Resultatet viser at store svingninger oppstår i de hydrodynamiske koeffisientene i frekvens mellom 1-2 rad/s. Designet valgt i denne oppgaven er en buet flytebro, bestående av en høy kabelbro i sør enden som gjør at skipsfart kan passere under broen. Broen er fritt flytende uten fortøyningslinjer, og skjærkreftene bæres gjennom membranbelastninger med den buede utformingen. Brobjelken har en total avstand fra sør til nord på 5435 meter. I sør enden er en navigasjonskanal plassert med en lengde på 525 meter. Lavbroen har en lengde på 100 meter, og hovedbjelken er 16,2 meter over havoverflaten.

Første del av dette prosjektet var en litteraturstudie om flytende brokonsepter for Bjørnafjorden, dynamiske belastninger på flytende broer og hydrodynamiske interaksjon mellom stive legemer. Pongtongmodellene ble laget i GeniE, mens en første ordens potensiell strømningsanalyse av de forskjellige pongtongstørrelsen ble utført i HydroD og Wadam. Den buede bromodellen ble opprettet i small SIMA hvor hydrodynamisk interaksjon mellom pongtongene ble studert. Statisk analyse og egenmode analyse ble også utført for å verifisere at modellen er riktig modellert. Den statiske analysen fokuserer hovedsakelig på bøyemoment, skjærspenning og statisk forskyvning av brobjelken og er sammenlignet med referansemodellen i regi av Statens vegvesen.

En egenverdianalyse ble utført, og lange egenverdiperioder er observert i horisontal retning. Den største egenverdien er 65.4 sekunder. Resultatene fra egenverdianalysen ble sammenlignet med referansemodellen og korresponderte bra. Dette ga tillit til at modellen kunne representere broens strukturelle respons relativt bra.

En forenklet flytende bro ble etablert for å gjøre ytterligere analyse av effekten av hydrodynamisk interaksjon i tre forskjellige bølge retninger. Innkommende bølger fra nordvest hadde størst momenter og nedbøying. Dette skyldes bidrag fra alle seks lastkomponenter, mens bølger fra vest bare har tre komponenter.

I en tidlig fase skjønte jeg hvor komplisert en flytebro er, og dekke alle aspekter er umulig. Den komplette broen med en total lengde på mer enn 5 kilometer viste seg å være for stor til å analysere de hydrodynamiske interaksjonseffekter. Det primære fokuset ble lagt på å studere responsen på den forenklete broen, forårsaket av bølgelaster fra forskjellige retninger.

Contents

List of Figures

List of Tables

0.1   Nomenclature

SIMO	Software program simulation and analysis of marine operations and floating systems
SIMA	Simulation of complex Marine Operations
RIFLEX	Software program used for analyze of slender structures
Wadam	hydrodynamic analysis program for calculating wave-structure interaction
GeniE	Program for design and analysis of maritime strucures
HydroD	Stability and hydrodynamic analysis of offshore structures
Xtract	FE results presentation postprocessor
NPRA	Norwegian Public Roads Administration

List of Symbols

α	Angle
η	Shielding factor
η	Wave elevation
λ	Wave length or damping ratio
ω	Angular frequency
ϕ	Velocity potential
ρ_a	Mass ensity of air
σ	Stress
λ	Eigenvalue vector
ϕ	Mode shape vector
$\mathbf{v}_c(z)$	Current velocity
A	Added mass
a	accelearation
B	Damping
C	Restroring force
C	Shape coefficient
E	Young's modulus
F	Force
F_D	Diffraction Force

F_W	Wind force
F_{FK}	Froude-Kriloff force
$F_{W,SHI}$	Shielding effects
G	Center of gyration
G	Shear modulus
g	Gravitational aceleration
GM	Metacentric hight
I	Second moment of area
k	Wave number
M	Mass
m	Local mass
N	Axial force
p_D	Dynamic pressure
q	Basic wind pressure
r	Response vector
S	Projected area of the member normal to the direction of the force
T	Wave period
u	Fluid velocity
$U_{T,z}$	Wind velocity averaged over time interval T

Chapter 1

Introduction

In order to improve the infrastructure between Kristiansand and Trondheim, the Norwegian Public Road Administration (NPRA) have ambitions of establishing a continuous coastal highway between Kristiansand and Trondheim during the next 20 years (Vegvesen, 2015). There are many fjords that have to be crossed either by tunnels or bridges, which today have to be crossed by ferries. One of the fjords that have to be crossed is Bjørnafjorden between Os and Stord. The length of this crossing is around 5 km, and the water-depth is down to 550 meters. With this dimension, it is impossible to solve with conventional bridge solution. This project will be looking at the bridge design proposed in the report "Curved Bridge - Navigation Channel in South, developed in cooperation between COWI, Aas Jakobsen, Johs Holte As and Global Maritime. The bridge is floating freely without moorings and has a curved shape to carry shear forces by membrane action. Hydrodynamic interaction among these pontoons is therefore expected and should be investigated.

(a) Bjørnafjorden   **(b)** Nordhordalandsbrua

Figure 1.1: Pictures of potensial crossing of Bjørnafjorden and existing floating bridge Nordhordalandsbrua

1.1   Objective and description of the report

Rest of this chapter presents an overview of floating bridges in general and different floating bridge concepts for Bjørnafjorden. Chapter 2 focus on dynamic loads on floating bridges and relevant theory. This theory includes methods for determining hydrodynamic parameters, beam theory, and potential flow theory.

The first order potential flow analysis of two, three and four pontoons using Wadam are present in Chapter 3. This is followed by a description of the model and the method behind the simulations. The next chapters include static-, eigenvalue,- and dynamic analysis respectively. In the dynamic analysis the choice of which environmental loads that are applied is present. The final chapter includes discussion and conclusion, before recommendations for further work is made.

1.2   Assumptions and Limitation

The scope of the work is described in the problem description. Because of a complex structure and the scope of this thesis, some simplification had to be done.

- Self-weight is the only external load

- Cables at the high bridge are somehow simplified. Wires that are fixed onshore are excluded.

- RIFLEX don't include hydrodynamic coupling effects between the pontoons

- Viscous effects are not considered

Because of these simplifications and limitations of the software, this is not a realistic design of the bridge. After consulting with Supervisor and Professor Erin Bachynski, it was agreed to put the primary focus on the simple bridge. The entire bridge structure turned out to be too comprehensive to solve without using a supercomputer. However, the effect of hydrodynamic interaction on dynamic response can still be carried out.

1.3   Background

E39 stretches over 1100 km, and the route requires multiple crossings of deep and wide Fjords which today had to be crossed by ferries. The Norwegian Government wants to establish a ferry free road connection between Kristiansand in south and Trondheim in the north. The idea is to reduce the traveling time to 12-13 hours, which today takes 19-21 hours depending on the ferries.

The ferry free E39 crossing concept represents Fjord-crossing that are difficult or impossible to solve with conventional existing bridge technology. Many engineers have been working with these technological challenges since the investigation started back in 2010.

Compared with standard land-based bridges, only limited information about floating bridges are available. Currently today it only exists few numbers of floating bridges around the world. The longest floating bridge ever build is the "Evergreen Point Floating Bridge" in Seattle with a floating part of 2310 meters. The bridge consists of 23 longitudinal pontoons, every 11.000 tons and 110 m long (Chandler, 2017).

Figure 1.2: Ferry free E39 from Kristiansand to Trondheim

1.4   Floating Bridges

For Bjørnafjorden, there have been three central concepts that have been studied for possible crossings. The first one is a suspension bridge combined with a Tension Leg Platform (TLP), a submerged floating tunnel and the last one is a floating bridge. This Chapter includes information on existing floating bridges and description of the suggested alternatives of floating bridge over Bjornafjorden.

1.4.1   Floating Bridge Concept

Floating bridge are practical for long crossings of water where the circumstances make it difficult to build a bridge supported by pillars. The basic concept is simple. The foundations are replaced with floating elements with or without mooring lines. The floating elements hold the vertical loading of the bridge by buoyancy. The transverse and longitudinal loading can be supported in two ways: By a curved structural system and/or mooring

lines. For a long straight bridge, it is necessary with mooring lines in order to withstand the lateral loads. For the curved bridge, the lateral loads are carried due to tension or compression. This is an advantage when the seabed is either too deep or the seabed is too soft for anchoring. Due to the fact that the bridge is floating, the response pattern is complex.

1.4.2   The Nordhordland Bridge

The Norhordaland Bridge, see Figure 1.1, was finished in 1994 after many years of planning. The bridge which connects Norhordaland to Bergen is a combined cable-stayed bridge and pontoon bridge with a total cost of 900 million NOK. The total length of the bridge is 1614.75 meters, shaped like an arc with curvature radius 1700 m. (Vegvesen, 1994). In the south end, a 369 m long cable bridge creating a 32 m high underpass for ship traffic. The floating part is 1246 meters supported by ten pontoons. The pontoons are made of concrete with a theoretical span length on 113.25m. The ten pontoons are 42m long, 20.5m wide and 7- 8.6m high with a draft of 4.3 - 5.6m. The pontoons are divided into nine separated cells where two of them can be flooded without risking a danger that the bridge is sinking. The curvature of the box girder has a radius of 1700m. The most significant challenge with the bridge was to identify a simple, robust means to adjusting to tidal movements of the structure of the abutments (Vegvesen, 1994).

The first year after the opening of the bridge, they experienced a 40 % increase in traffic. The following years it was a stable growth of 4.2 % each year, until 2006 when the toll money was removed.

1.4.3   Floating bridge concepts for Bjørnafjord

The investigation of a ferry-free fjord crossing over Bjørnafjorden started back in 2010, (Vegvesen, 2017a). Four different alternatives have been developed which include a submerged floating tunnel, a suspension bridge combined with Tension Leg Platform technology and a floating bridge, Figure 1.3. Statens Vegvensen had decided to go further with two alternatives. The first one is a curved floating bridge of 5530 meters that is fixed in both ends. The bridge is only anchored at the ends and no mooring lines connected to the seabed. The bridge girder has a curvature of 5000 m and is described more detailed in Section 4.4.

The other concept is a straight anchored floating bridge. The bridge is supported by pontoons with a spacing of 203 meters. This solution requires mooring lines connected to the seabed (Vegvesen, 2017b). In both solutions, the navigation channel is located at the south ends supported by a cable-stayed bridge.

As the times goes on a cheaper solution has been developed. The cost is reduced from 20-25 billion to 17 billion NOK (Vegvesen, 2017a). The reduced cost is a result of less material, and the span length of pontoons are changed from 200 meters to 100 meters. The pontoons are made of concrete to resist the corrosive environment in seawater.
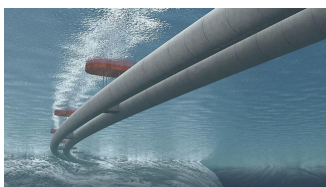
(a) Suspension TLP   (b) Tunnel   (c) Floating bridge

Figure 1.3: Different alternatives for crossing of Bjørnafjorden

Chapter 2

Theory

2.1 Loads acting on a floating bridge

All bridges are continuously exposed to a bunch of different loads due to self-weight of the structure, traffic, and different environmental conditions. A floating bridge is exposed for even more loads due to hydrostatic and hydrodynamic forces acting on the pontoons. In other words, floating bridges are a complex structure where wave and current will affect the stability and the global response. A list of the most important loads are listed in Table 2.1

Table 2.1: Loads to be considered on a floating bridge

Loads:
- Wave loads
- Current loads
- Wind loads
- Self-weight
- Traffic loads
- Marine Growth
- Hydrostatic water pressure
- Collision Loads
- Tsunami, earthquake

2.1.1 Wind Loads

The wind field may contain energy at a frequency near the natural frequencies of the structure, and can possibly lead to catastrophic outcome. Wind loads are important for horizontal motions and vary in time and height above the surface. Wind-induced loads on structures consist of a mean and a fluctuation part. For a bridge stretching more than 5km, the wind loads would vary from position to position depending on where you are on the bridge. A simplification model using the averaging time for wind speeds and a reference height is specified. A commonly used reference height is $H = 10m$ and speed averaged over 1 min or 10 min is often referred to as sustained wind speed. (Veritas, 2010). The basic wind pressure is defined by:

$$q = \frac{1}{2}\rho_a U_{T,z}^2 \qquad (2.1)$$

where q is the basic wind pressure, ρ_a is the mass density of air, and $U_{T,z}$ is the wind velocity averaged over time interval T at a height z meter above the mean water level. The wind force can then be calculated according to

$$F_W = CqS\sin(\alpha) \qquad (2.2)$$

where C is the shape coefficient, S is the projected area of the member normal to the direction of the force, α is the angle between the direction of the wind and the axis of the exposed member or surface, (Veritas, 2010).

For a floating bridge, two or more parallel frames could be located behind each other in the wind direction. Shielding effects may be taken into account:

$$F_{W,SHI} = F_W \eta \qquad (2.3)$$

Where η is the shielding factor.

2.1.2 Current

The most common current types that will be relevant in Bjørnfjorden is wind generated currents and tidal currents. The main factors that affect the current are Reynolds number, roughness number, body form, reduced velocity and direction of ambient flow relative to the structure's orientation (Faltinsen, 1990). Current gives rise to drag and lift forces on submerged structures. The current velocity varies with water-depth, and the total current velocity should be taken as the vector sum of each current component.

$$\mathbf{v}_c(z) = \mathbf{v}_{c,wind} + \mathbf{v}_{c,tide} + ... \qquad (2.4)$$

2.1.3   Wave Loads

The pontoons are located in the sea and will be exposed to a dynamic pressure distribution caused by the presence of waves. Ocean waves are irregular and vary in shape, height, length, and speed. The hydrodynamic problem in regular waves is dealt with as two separate subproblems, diffraction, and radiation, (Faltinsen, 1990). These components causes of pressure and corresponds to different velocity potentials.

- **Problem A**: The forces and moments on the body when the structure is restrained from oscillating and exposed to incident regular waves. The hydrodynamic loads are called wave excitation loads and consists of so-called Froude-Kriloff and diffraction forces and moments.

- **Problm B**: The forces and moment on the body when the structure is forced to oscillate with the wave excitation frequency in any rigid-body motion mode. There are no incident waves. The hydrodynamic loads are identified as added mass, damping and restoring term.

Problem A: Excitation force

First of all, the direction of motion has to be defined. There are six modes of motion, transnational in surge, sway, heave, and rotational modes, roll, pitch, yaw. The excitation forces and moments can be characterized by Froude Krylov load and diffraction load. Froude Krylov is the force introduced by the unsteady pressure field generated by undisturbed waves. The diffraction load is the change in load due to the effect on the structure of the fluid.

$$\phi = \phi_I + \phi_D + \phi_R \tag{2.5}$$

where ϕ_I, ϕ_D and ϕ_R are the velocity potential of the incident wave, diffraction wave, and the radiated wave potential respectively. The diffraction and radiation wave force have a significant effect on large floating pontoons in deep water. The radiation wave represents the wave to be propagated by the oscillating body in calm water and the diffraction wave means the scattering term from the fixed body due to the presence of the incident wave.

In reality, higher order terms have an effect in several cases, but potentials of a higher order than 2nd are rarely used. 2nd order theory is necessary when including mean and slowly varying drift forces from the waves. Higher order wave will give a more contribution with higher crest and shallow water.

Froude-Kriloff Forces:
The dynamic pressure propagation along the positive x-axis in infinite water depth is expressed as (Faltinsen, 1990)

$$p_D = \rho g \zeta_a e^{kz} sin(\omega t - kx) \tag{2.6}$$

Integrating this expression over the wet surface gives the hydrodynamic pressure on the structure.

$$F_{FK} = \iint_S p_D n ds \tag{2.7}$$

Equation 2.7 is called Froude Krylov force where n is the unit vector normal to the body surface. For a rectangular barge the vertical heave forces becomes:

$$F_{FK,3} = \left(\rho g \zeta_A B e^{kz} \right) \left(\frac{2}{k} sin\left(\frac{kL}{2} \right) sin(\omega t) \right) \tag{2.8}$$

This assuming head sea and the dynamic pressure is uniform along the y-axis. Froude Kirloff force in surge and sway can be derived in same way.

Diffraction Forces:
The diffraction loads are the change in load due to the effect on structure on the fluid. This force is related to the acceleration of the fluid.

$$a_3 = -\omega^2 \zeta_a e^{kz} sin(\omega t - kx) \tag{2.9}$$

$$F_{D,3} = A_{33} a_3 \tag{2.10}$$

Where A_{33} is the added mass in heave and a_3 is the vertical acceleration. The diffraction force for heave becomes:

$$F_{D,3} = -\omega^2 A_{33}^{2D} \zeta_a e^k z_m \int_{\frac{-L}{2}}^{\frac{L}{2}} sin(\omega t - kx) \tag{2.11}$$

Poblem B - Radiation force

The radiation forces can be dealt with as a sum of three components.

Mass matrix

The pontoon is symmetric about the XZ-plane with centre of gravity in $(0,0,z_G)$, the mass matrix can be written as:

$$M_{jk} = \begin{bmatrix} M & 0 & 0 & 0 & Mz_G & 0 \\ 0 & M & 0 & 0 & Mz_G & 0 \\ 0 & 0 & M & 0 & 0 & 0 \\ 0 & -Mz_G & 0 & I_4 & 0 & -I_{46} \\ Mz_G & 0 & 0 & 0 & I_5 & 0 \\ 0 & 0 & 0 & -I_{46} & 0 & I_6 \end{bmatrix}$$

The mass is found from the body density

$$M = \iiint_V \rho \, dV \qquad (2.12)$$

Where ρ_b is the density and V is the volume of the body.

When a floating structure is forced to oscillate, the structure is generating radiation waves that are outgoing from the structure. The added mass is the force due to the water that has to be displaced as the structure oscillates, and the damping is the force due to the energy carried away from the structure through radiated waves from the oscillating body (Faltinsen, 1990). Added mass is a 6x6 matrices which depend on the geometry of the body, density of fluid and wave-frequency.

Damping

Damping designates the ability of a structure to dissipate kinetic energy, to transform it into other types of energy such as heat or radiation (Langen, 1979). Assuming potential flow theory it is possible to evaluate the forces acting on a body without the presence of friction by evaluating the velocity potential around the body the generated waves can be evaluated. In structures like floating bridge, there are several sources of damping forces. Structural and viscous damping can be approximated as proportional damping. By assuming damping force is proportional to the velocity of each mass point and damping proportional to strain velocity. Then $\mathbf{C}$ gets proportional to $\mathbf{M}$ and $\mathbf{K}$ and the damping can be expressed as.

$$\mathbf{C} = \alpha_1 \mathbf{M} + \alpha_2 \mathbf{K} \qquad (2.13)$$

The damping ratio λ gives the ratio between the damping ratio between the damping and the critical damping are given by:

$$\lambda_i = \frac{\bar{c}_i}{2\bar{m}_i \bar{\omega}_i} = \frac{1}{2}\left(\frac{\alpha_1}{\omega_1} + \alpha_2 \omega_1\right) \qquad (2.14)$$

The coefficient α_1 and α_2 determines the contribution from each matrix where α_1 damps out the lower mode shapes and α_2 damps out the higher mode shapes. If the damping ratio for two frequencies is known, α_1 and α_2 can be determined as:

$$\alpha_1 = \frac{2\omega_1 \omega_2}{\omega_2^2 - \omega_1^2}\left(\lambda_1 \omega_2 - \lambda_2 \omega_1\right) \qquad\qquad \alpha_2 = \frac{2(\omega_2 \lambda_2 - \omega_1 \lambda_1)}{\omega_2^2 - \omega_1^2} \qquad (2.15)$$

Restoring force

When a body is freely floating, the restoring forces will follow from hydrostatic and mass consideration (Faltinsen, 1990). The only non-zero coefficients for a body that are symmetric in all planes are C_{33}, C_{44}, and C_{55}. Restoring coefficient in heave, roll and pitch is given by:

$$C_{33} = \rho g A_w \qquad\qquad C_{44} = \rho g \nabla GM_T \qquad\qquad C_{55} = \rho g \nabla GM_L \qquad (2.16)$$

$$GM_T = KB + BM_T - KG \qquad\qquad GM_L = KB + BM_L - KG \qquad (2.17)$$

GM is the metacentre height and need to be positive defined for stability.

2.1.4 Regular Waves

Regular waves can be expressed as

$$\zeta = \zeta_a sin(\omega t - kx) \qquad (2.18)$$

Where ζ_a is the wave amplitude, ω is the circular wave frequency and k is the wave number. x and t are two variables where t is the time and x is the horizontal position. This is a linear approximation of ocean waves and is in many situations a good approximation for long crested waves. In this study, both regular and irregular waves will be used.

2.1.5 Slowly varying drift forces

The first order solution is described in Section 2.1.3. In the linear solution, the free surface condition and the boundary condition are satisfied on the mean position of the free surface. The fluid pressure and the velocity of fluid particles on the free surface are linearized. This gives only loads that having the same frequency as the incident waves, but a structure which is exposed to waves will also experience non-linear wave force. Second order theory accounts more properly for the zero-normal flow condition through the body at the instantaneous position of the body. The solution of the second-order problem results in mean forces, and forces oscillating with different frequency and sum frequencies in addition to the linear solution (Faltinsen, 1990, p. 131). Non-linear interaction produces slowly-varying excitation forces and moments which have typical resonance periods of 1-2 minutes.

Slow drift excitation loads are large when the mean wave loads are large (Faltinsen, 1990, p. 155). The general formula for slow-drift excitation loads F_i^{SV}

$$F_i^{SV} = \sum_{j=1}^{N}\sum_{k=1}^{N} A_j A_k \left(T_{jk}^{ic} cos\big((\omega_k - \omega_j)t + (\varepsilon_k - \varepsilon_j)\big) + T_{jk}^{is} sin\big((\omega_k - \omega_j)t + \varepsilon_k - \varepsilon_j)\big)\right)$$

$$(2.19)$$

Where the wave amplitude is denote A_i, wave frequencies ω_i, random phase angles ε_i, t the time instant and number of wave components N. The coefficients T_{jk}^{ic} and T_{jk}^{ic} is the second order transfer functions for the difference frequency loads. $F_{1,2,3}^{SV}$ are respectively x-, y- and z components of the slow-drift force and $F_{4,5,6}^{SV}$ are moments about the x-,y- and z-axes.

Equation 2.19 can be simplified by introducing different assumptions. By using Newman's approximation it is possible to express the off-diagonal terms by the diagonal ones which reduce the computer time significantly. Another desirable consequence is the second-order velocity potential don't need to be calculated.

$$T_{jk}^{ic} = T_{kj}^{ic} = 0.5 \left(T_{jj}^{ic} + T_{kk}^{ic} \right)$$

$$(2.20)$$

$$T_{jk}^{is} = T_{kj}^{is} = 0$$

$$(2.21)$$

$$F_i^{SV} = 2 \left(\sum_{j=1}^{N} A_j (T_{jj}^{ic})^{\frac{1}{2}} cos(\omega_j t + \varepsilon_j) \right)$$

$$(2.22)$$

Equation 2.22 includes high-frequency effects that have no physical background.

2.1.6   The dynamic equation of motion

The equation of motion connects the external forces with mass forces. The global response of a structure can be found by solving the dynamic equilibrium equation given by (Damkilde, 2000)

$$\sum_{k=1}^{6} \left((M_{jk} + A_{jk})\ddot{\eta}_k + B_{jk}\dot{\eta}_k + C_{jk}\eta_k \right) = F_j e^{i\omega t} \quad j = 1, 2.....6$$

$$(2.23)$$

M_{jk} - mass matrix in mode j due to motion in mode k
A_{jk} - added mass matrix in mode j due to motion in mode k
B_{jk} - damping matrix in mode j due to motion in mode k
C_{jk} - restoring matrix in mode j due to motion in mode k
η_k - motion in mode k
$\dot{\eta}_k$ - velocity in mode k
$\ddot{\eta}_k$ - acceleration in mode k

F_j - exciting force in mode j with force given by the real part of $F_j e^{i\omega t}$
ω wave excitation frequency

For mass, added mass, damping and restoring force the dimension of the matrix is a 6x6 and 6x1 vector for the excitation force. When the bridge reacts to incident waves, the pontoons will generate frequency dependent added mass and damping coefficients. The wave can be divided into three different timescales. The first one is wave frequency (WF) motions. The largest wave loads on the bridge take place at the same frequency as the waves. The second one is low frequency (LF) motion. Slowly varying wave and wind loads also named slow-drift motion gives rise to low frequency. The third type is high frequency (HF) motion due to a higher order. Further, it is normally to separate between three cases based on structural behavior and the frequency (Langen, 1979).

- Stiffness dominating system, when $\frac{\omega}{\omega_n} << 1$

- Resonance dominated system system, when $\frac{\omega}{\omega_n} \approx 1$

- Inertia dominated system, when $\frac{\omega}{\omega_n} \gg 1$

Where ω is the applied frequency, and with the relevant eigenfrequency ω_n. The structural response depends on the eigenfrequencies of the structure and is essential factors on how the bridge behave during different loading conditions.

2.1.7   Transfer functions - systems with one degree-of-freedom

The dynamic equlibrium function is given by:

$$(M+A)\ddot{\eta} + B\dot{\eta} + C\eta = Fe^{i\omega t} \tag{2.24}$$

The partical solution:

$$\eta = \bar{\eta}e^{i\omega t} = H(\omega)Fe^{i\omega t} \tag{2.25}$$

Where $\bar{\eta}$ is the complex amplitude of motion. Then the equation can be divided by $e^{-i\omega t}$ into a real and imaginary part. The real part expresses the component of the response which is in-phase with the excitation. The imaginary part expresses the component which is $\pi/2$ out of phase.

$$-\omega(M+A)\bar{\eta} + i\omega B\bar{\eta} + C\bar{\eta} = F \tag{2.26}$$

The frequency-response function can be written as the motion amplitude per unit excitation force

$$H(\omega) = \frac{\bar{\eta}}{F} = \frac{1}{-M\omega^2 + i\omega c + k} \tag{2.27}$$

Where $H(\omega)$ is the complex frequency response function

2.2 Methods for Determining Hydrodynamic Parameters

There are a bunch of different methods for determining the hydrodynamic coefficients. In this section a couple of different methods is present.

2.2.1 Strip Theory

Strip theory is based on that a 3D body can be evaluated as a sum of 2D strips along the body. Strip theory assumes that the variation of the flow in the cross-sectional plane is much larger than the variation of the flow in the longitudinal direction. Today strip theory is a popular approximation for slender ships and other methods are often very complex and may not give significantly better results. Strip theories in an early design stage of a ship which delivers the designer relevant information within a very short computing time. The strip theory is a slender body theory, so one should expect less accurate predictions for ships with low length to breadth ratios. For the pontoon, the length of the body is much greater than the width, so strip theory may give accurate results.
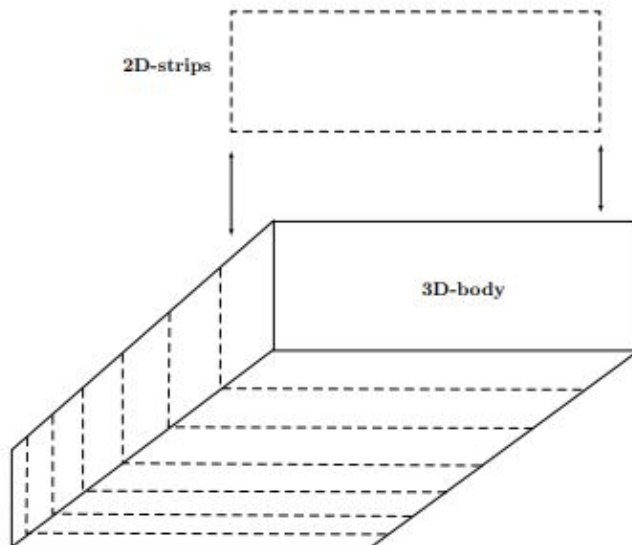

Figure 2.1: Strip theory

2.2.2 Potential Flow Theory

When a flow is both frictionless and irrotational, pleasant things happen. – F.M. White, Fluid Mechanics 4th ed.

Basically, linear theory means that the wave-induced motion and load amplitudes are linearly proportional to ε_a. Using potential theory the fluid can be described by the velocity potential ϕ. In this case, the pontoons are assumed to be a large structure so the first order potential flow effect is dominating. The potential function $\phi(x,z,t)$ is a continuous function that satisfies conservation of mass and momentum, assuming in-compressible, in-viscid and irrational flow.

- Laplace equation:

$$\nabla \times \vec{V} = \frac{\partial^2 \phi}{\partial x^2} + \frac{\partial^2 \phi}{\partial y^2} + \frac{\partial^2 \phi}{\partial z^2} = 0 \qquad (2.28)$$

In an incompressible fluid, the velocity potential has to satisfy the Laplace equation. V is the velocity and ϕ is the potential function. To find the potential velocity, the Laplace equation is solved with different boundary conditions. There are two free surface conditions, which are the dynamic free surface condition and the kinematic free surface condition. In addition, there is a bottom free surface condition.

- Boundary condition at the bottom:

$$\left(\frac{\partial \phi}{\partial z} \right)_{z=-h} = 0 \qquad (2.29)$$

Where h is the water-depth. The boundary condition at the bottom states that there are no normal velocity at the bottom.

- Kinematic Free Surface Condition:

$$\frac{\delta \varepsilon}{\delta t} = \frac{\delta \phi}{\delta z} \quad \text{on z=0} \qquad (2.30)$$

The kinematic states that the particles on the free surface remain on the free surface.

- Dynamic Free Surface Condition:

$$g\varepsilon = \frac{\delta \phi}{\delta t} \quad \text{on z=0} \qquad (2.31)$$

Dynamic condition states that the water pressure on the free surface is constant and equal to the atmospheric pressure p_0.

- Combining the kinematic boundary condition with the dynamic boundary condition result in:

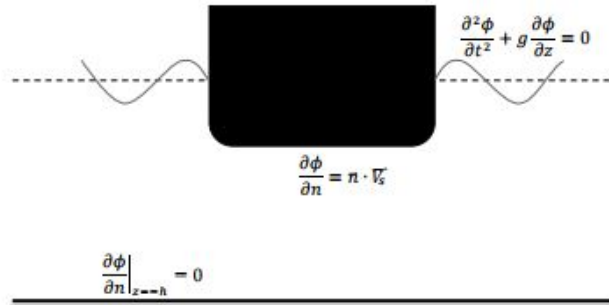$$\frac{\delta^2 \phi}{\delta t^2} + g\frac{\delta \phi}{\delta z} = 0 \quad \text{on z=0} \qquad (2.32)$$

Figure 2.2: Potential theory boundary condition

The velocity potential for deep water are given by:

$$\phi = \frac{\zeta_A g}{\omega} e^{kz} sin(kx - wt) \tag{2.33}$$

The dispersion relation is given as:

$$\omega^2 = kg \tag{2.34}$$

A deep water approximation can be used when h>λ/2. Bjørnafjorden is approximately 500m in the middle of the ocean so deep water assumption is valid. At the bridge end, the water depth is reduced and the effect of shallow water have to be taking into account. However, in this report the deep water approximation is assumed along the whole bridge.

2.3   Beam Theory

Beams are structural elements where the length is several times larger than the dimensions in any of the two other directions. Several different beam theories exist and the difference lies in the simplifications, (Damkilde, 2000). The most simple theory is the Euler-Bernoulli theory that assumes that the cross-section remains orthogonal to the beam axis. The theory treats axial stiffness and bending stiffness but disregards deformations due to shear forces. Torsion is treated separately and is discussed later. Timoshenko beam theory takes the shear deformation into account.

Shear Forces and bending moments in Beams

$$M_{Max} = \frac{wl^2}{12} \qquad M_1 = \frac{wl^2}{24} \qquad V_{Max} = \frac{wl}{2} \qquad \Delta_{max} = \frac{wl^4}{348EI} \tag{2.35}$$

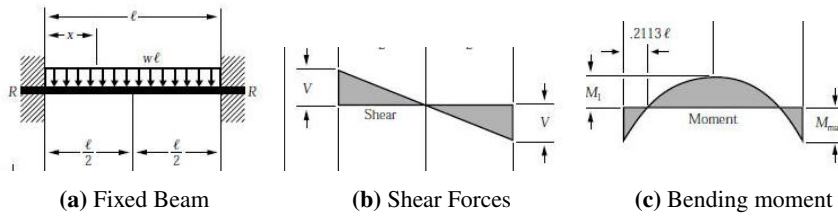**(a)** Fixed Beam   **(b)** Shear Forces   **(c)** Bending moment

Figure 2.3: Shear Force and bending moments for a fixed beam

Stiffness

Axial, bending and torsional stiffness is found by:

$$k_{axial} = EA \qquad\qquad k_{bending} = EI \qquad\qquad k_{tor} = GJ \qquad (2.36)$$

2.3.1 Cable Force

Cables are only capable to carry axial forces in tension. The stress is calculated with Equation 2.37 where A is the cross section area of the cable.

$$\sigma = \frac{F}{A} \qquad (2.37)$$

2.3.2 Center of Gyration

The center of gyration about x,y,z axis can be calculated by:

$$G_x = \sqrt{\frac{I_x}{m}} \qquad\qquad G_y = \sqrt{\frac{I_y}{m}} \qquad\qquad G_z = \sqrt{\frac{I_z}{m}} \qquad (2.38)$$

The moment of inertia for the pontoons is calculated of these formulas.

$$I_x = \frac{m(w^2 + h^2)}{12} \qquad\qquad I_y = \frac{m(l^2 + h^2)}{12} \qquad\qquad I_z = \frac{m(l^2 + w^2)}{12} \qquad (2.39)$$

Where w, h, and l are the width, height, and length of the pontoons. These formulas are applicable for rectangular cylinders. That lead to an overestimation of the center of gyration. However, the center of gyration depend on square-root of the moment of inertia, so the overestimation is neglected in this case.

2.4 Eigenvalue Analysis

The eigenfrequency of a structure are the frequencies the structure tends to vibrate when the structure oscillating freely. For a large structure like the bridge, many such frequencies exist. The dynamic equilibrium is expressed by: (Langen, 1979)

$$\mathbf{M}\ddot{r} + \mathbf{C}\dot{r} + \mathbf{K}r = \mathbf{Q}(t) \tag{2.40}$$

Where:
$\mathbf{M}$ = Mass matrix
$\mathbf{C}$ = Damping matrix
$\mathbf{K}$ = Stiffness matrix
$\mathbf{Q(t)}$ = Time dependent force vector
r = Nodal displacement vector
$\dot{r}$ = Nodal velocity vector
$\ddot{r}$ = Nodal acceleration vector

For free undamped vibration we have $\mathbf{C}=\mathbf{0}, \mathbf{Q}(t) = 0$. This means that there is no damping and no time dependent loading. Equation 2.40 reduces to:

$$\mathbf{M} + \mathbf{K}\mathbf{r} = 0 \qquad\qquad \mathbf{r} = \phi \sin(\omega t) \tag{2.41}$$

Where ϕ is the mode shape or eigenvector. By inserting this function into the equation of motion, the eigenvalue problem on general and special form can be written as:

$$(\mathbf{K} - \omega^2 \mathbf{M})\phi = 0 \qquad\qquad (\mathbf{A} - \lambda \mathbf{I})\mathbf{x} = 0 \tag{2.42}$$

2.4.1 Natural Period

For a floating bridge it is important to identify the eigenvalues and eigenmodes of the structure and check if the coincides with the environmental loads. According to O.M.Faltinsen (1990), the natural period can be given for any structure in any motion mode as:

$$Tn_i = 2\pi \sqrt{\frac{A_{ii} + M}{C_{ii}}} \tag{2.43}$$

Where A_{ii} is the added mass, M is the mass and C_{ii} is the hydro-static stiffness. The equation indicates that increased mass give lower frequencies. An increased stiffness results in higher eigenfrequency.

2.4.2 Eigenvalues of Simple Beams

For a straight beam with constant cross-section, the eigenfrequency $\omega_{n,straight}$ can according to (Young, 2014) be defined by Equation 2.44. This is valid for a fixed beam with a uniform load per unit length. Kn is a constant where n refers to the mode of vibration, see Table 2.2.

$$\omega_{n_straight} = K_n \sqrt{\frac{EI}{ml^4}} \tag{2.44}$$

Table 2.2: A constant where n refers to the mode of vibration.

Kn	Mode 1	Mode 2	Mode 3	Mode 4	Mode 5
Value	22.4	61.7	121	200	299

Equation 2.45 is valid for curved beam, where H is the sagitta of the circular arch. The equation for the curved beam is valid for the first frequency and the bow effect is neglected for higher eigenmodes.

$$\omega_{1,curved} = \sqrt{\frac{\pi^4 EI}{ml^4} \left(1 + \frac{AH^2}{2l}\right)} \tag{2.45}$$

2.5 Dynamic Analysis

2.5.1 Numerical integration of the equation of motion

The dynamic equilibrium equation for one-degree-of-freedom-system

$$m\ddot{u} + c\dot{u} + ku = Q(t) \tag{2.46}$$

Equation 2.46 is an initial-value problem where the solution is determined by the initial values. The time interval is subdivided into time steps with equal length h, see Figure 2.4. When we know the displacement, velocity, and acceleration at the interval and at possible previous time steps, the solution at the end of the interval can be determined by assuming a certain variation of the motion during the interval. The accuracy will, of course, depend on the length of the time steps, but a smaller timestep will cost higher computational time. (Langen, 1979). Langen and Sigbjørnsson (1979) describes two main groups of methods: *The difference formulation* and *numerical integration.* I will present the numerical integration since that is the method used in RIFLEX.
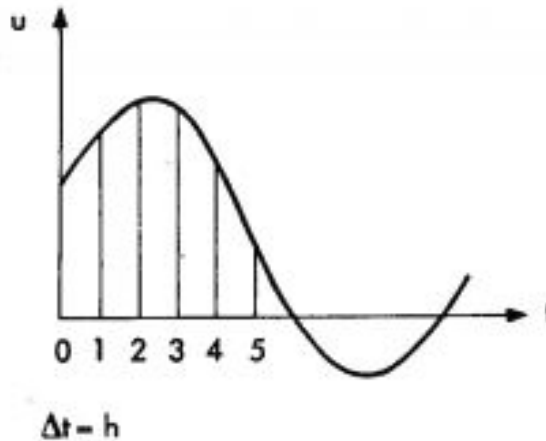
Figure 2.4: The discretisation in time

2.5.2 Numerical Integration

For numerical integration methods, the velocity and displacement are found at each new time step by integrating the acceleration twice.

$$\dot{u}_{k+1} = \dot{u}_k + \int_o^h \ddot{u}(t)dt \qquad (2.47)$$

$$u_{k+1} = u_k + \int_o^h \dot{u}(t)dt \qquad (2.48)$$

Where the velocity is defined as:

$$\dot{u}(t) = \frac{1}{m}(Q(t) - c\dot{u} - ku(t)) \qquad (2.49)$$

By assuming how the acceleration will vary over the interval, the $\dot{u}_{k+1}$ and u_{k+1} can be computed. The difference methods lies in the assumptions and involves constant initial acceleration, constant average acceleration and linear acceleration.
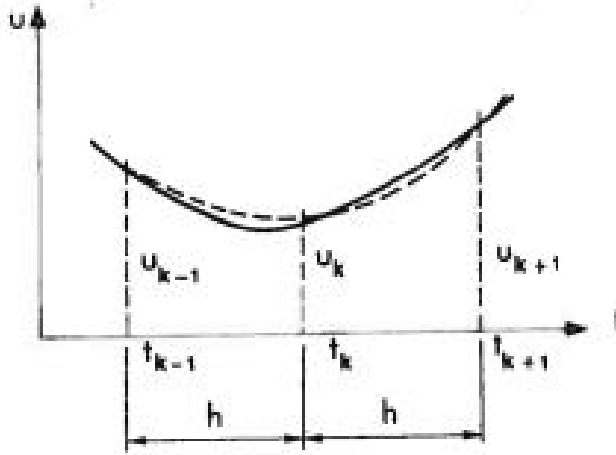
Figure 2.5: Numerical integration

2.5.3   Newmark's β - family

According to (Langen, 1979) the above methods can be regarded as special cases of Newmark's general integral equations

$$\dot{u}_{k+1} = \dot{u}_k + (1-\lambda)g\ddot{u}_k + \lambda h\ddot{u}_{k+1} \tag{2.50}$$

$$u_{k+1} = u_k + h\dot{u}_k + (\frac{1}{2} - \beta)h^2\ddot{u}_k + \beta h^2 \ddot{u}_{k+1} \tag{2.51}$$

The weighting terms λ and β are determined by requirements related to stability and accuracy. The method is in-conditionally stable when

$$\lambda \geq \frac{1}{2} \tag{2.52}$$

$$\beta \geq \frac{1}{4}(\lambda + \frac{1}{2})^2 \tag{2.53}$$

The choise of λ decides if the method has artificail damping or not

$\lambda >$ gives positive artifical damping
$\lambda <$ gives negative artifical damping
$\lambda =$ gives zero artifical damping

According to "RIFLEX 4.8.1 Theory Manual" (2016) $\beta = 1/2$ is normally used to obtain second-order accuracy. The accuracy of the integration method will depend on the dynamic loading, physical parameters of the system and on the step length. According to (Langen, 1979) the integration is accurate when h/T 0.01 for all the methods. For a period of 5 sec, the timestep should be 0.05 s for accurate results. For Newmark $\beta = 1/4$ the period error is 3 % for h=0.1T

2.5.4 Frequency modelling, Power spectrum

The most important characteristic in frequency domain is the powerspectrum.

$$\hat{s}_i = \frac{(a_i^2 + b_i^2)}{2\Delta\omega} \tag{2.54}$$

Where $\Delta\omega$ is the sampling interval in frequency domain.

$$x(t) \approx m + \sum_{i=1}^{N} \sqrt{2\hat{s}_i\Delta\omega} cos(\omega_i t + \theta_i) \tag{2.55}$$

If the sampled signal contains 2N + 1 points then x(t) is equal to its Fourier series at the sampled points. In the special case when N = 2^k, the FFT (Fast Fourier Transform) can be used to compute the spectrum (WAFO-group, 2017). The frequency domain solution is studied to get a better understanding of how the bridge responds for different frequencies.

Chapter 3

Hydrondynamic Interaction

The floating bridge over Bjørnafjorden have a total length of 5440 meters with a spanlength of 100 meters between each pontoon. Hydrodynamic interaction between the pontoons is therefore expected. A simple estimation is referred to (Thomas Viuff and Øiseth, 2016) where two pontoons are considered to interact when the equation is larger than the distance between the pontoons

$$D_{AB} \leq D_{int} = \sqrt{\left(1.5\frac{L_A + L_B}{2}\right)^2 + \left(6\frac{B_A + B_B}{2}\right)^2} \tag{3.1}$$

Where L_A,L_B,B_A and B_B are the length and wide of pontoon A and B. Using spanlength of 100 meters, length and wide equal to 58m and 12m, the D_{int} = 168.4m. This means that hydrodynamic interaction have to be considered.
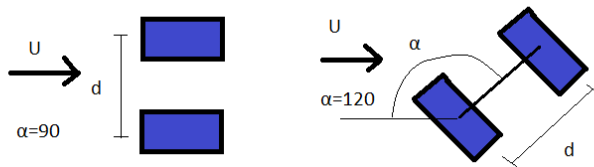
Figure 3.1: Hydrodynamic interaction

Hydrodynamic interactions between multiple pontoons could be a problem if one pontoon is placed in the wake of another. That could affect the drag coefficient and may be

of concern due to large relative motion response between floaters, (Kim and Kim, 2003). Another effect is the sheltering effect which leads to smaller motions on the lee-side than on the weather side (Veritas, 2010). Compared to an isolated body there will be considerably wave forces on multiple bodies. The interaction between the bodies are dependent on many parameters as size, shape, spacing, the angle (α) and environmental conditions. Figure 3.1 shows two pontoons with incident waves in two different angels. The Reynolds number is a quantity which use to estimate the behaviour of the fluid flow (MiT, 2017). At low Reynolds number the fluid flow is laminar, which can be modelled quite accurate by potential theory. When the Reynolds number increases the flow becomes turbulent and the potential theory is not well described because of the viscous effects are important.

The effect of multibody interaction effects have to be taken carefully into consideration for safe operation. Many research have been done regarding this problem. Ohkusu (1974), Kodan (1984) and Fang and Kim (1986) analyzed the hydrodynamic interaction between two side-by-side vessels using two-dimensional theory. Van Oortmerrsen (1979) used the three-dimmensional linear diffraction theory to solve the hydrodynamic interaction problem between two floating structures. Mir Tareque Ali and Yoshiyuki Inoue did a investigation between rectangular barges in regular waves. (Ali and Inoue, 2005) They applied a 3-D source-sink method to compute the hydrodynamic coefficients and wave exciting forces. The result showed that the hydrodynamic causes rapid changes in hydrodynamic loads and responses along the wave frequencies. Choi and Hong analyzed hydrodynamic interactions of a multibody system using higher-order boundary-element method. However, most research of hydrodynamic analysis of multiple bodies is based on potential-flow theory, which neglect the fluid viscosity and energy dissipation, (XU Xin, 2016). Even though the hydrodynamic interaction of multibody system have been much studied, the existing data are far from sufficient for illustrating all aspects from a complex interaction.

The linear coupled motion for four floating bodies can be written as

$$\sum_{k=1}^{24} \Big(-\omega^2 (\mathbf{M} + \mathbf{A}) + i\omega \mathbf{B} + \mathbf{C} \Big) \zeta_j = F_i \tag{3.2}$$

Where ζ_j is the response motion in each of the six degree of freedom for each body. F_i is the wave exciting force on each barge.

3.0.1 Single-body analysis

By analyze added mass, radiation damping, excitation force that are developed during the interaction between the structures, Wadam software is used. The analysis are carried out by using gap distance of 100 meters, and wave direction 0, 15, 30, 45 and 90. The analysis have been performed in constant waterdepth of 500 m and waveperiod from 2- 100s. The number of different bodies varies from one isolated body to four bodies.

For a flow around a single pontoon the velocity will increase in front and around the pontoon. This is due to the viscous effects which cause no-slip on the boundary, (Faltinsen,
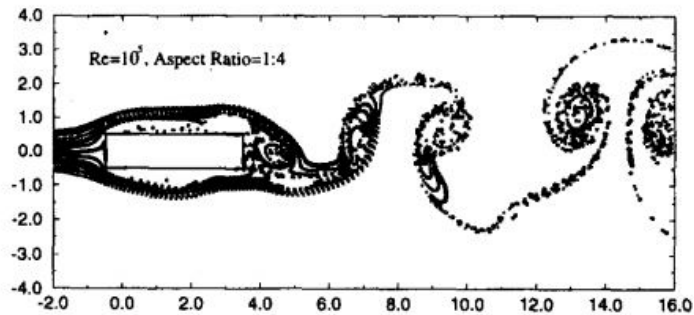
Figure 3.2: Streaklines of flow around rectangular prisms (Yu and Kareem, 1996)

1990). If we look at waves arriving from the x-direction, the forces will not have a motion in y-direction and due to axis symmetry there will be no rotation in yaw.
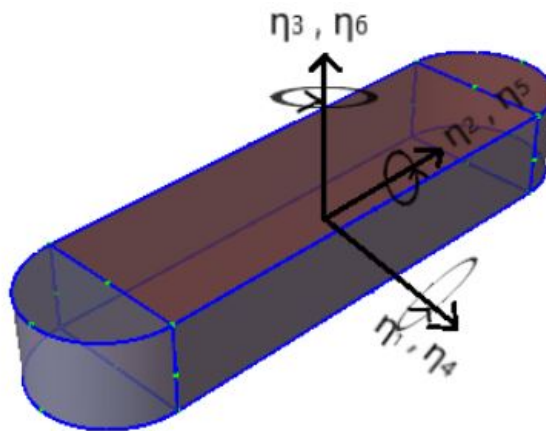

Figure 3.3: Local body motion modes for the pontoon

Regarding Figure 3.3 the pontoon can move in x-, y- and z direction and rotate around the same axes. The local coordinate system on the pontoon is the same for the global coordinate system. The surge motion for the pontoon is defined in the direction of the longitudinal bridge girder.

3.0.2 Assumptions and specifications

When using potential theory many effects have to be neglected. For single body analysis no interaction effects are considered. Viscous effects are not considered, and vortex induced vibrations is neglected. If considering viscous effects, a CFD program solving the Navier-Stokes equation would have to be applied.

Single body analysis is done in frequency-domain using Wadam. To include higher order hydrodynamic effect like slamming loads, a time analysis would be required. Many other effect are also neglected to be able to perform the analysis within the limited time-frame of this thesis. The pontoons that are analysis in Wadam have the same dimensions as Pontoon 2 in Table 4.5. The frequency step is from 0 to 2.5 with frequency step of 0.05. The center of gravity is located at (0,0,-0.5m) according to the local coordinate system. Center of buoyancy (COB) is located 2 m vertically below COG. The design of the pontoon is based of a prismatic shape with smooth edges. The front is cylindrical shaped to reduce forward drag. By adding wave potential, radiated potential and diffraction potential we can get an accurate result of what is going on.

3.0.3 Added mass, damping and excitation force

Figure 3.5 shows the added mass and damping in surge, sway and heave in frequency domain. The same plots are plotted in period-domain in Appendix.

(a) Added mass for single body   **(b)** Damping for single body
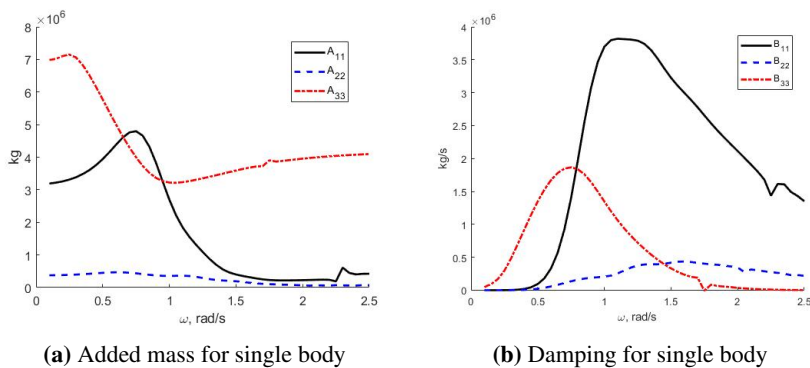
Figure 3.4: Added mass and damping in surge sway and heave

(a) Excitation force, 0 deg   **(b)** Excitation force, 45 deg
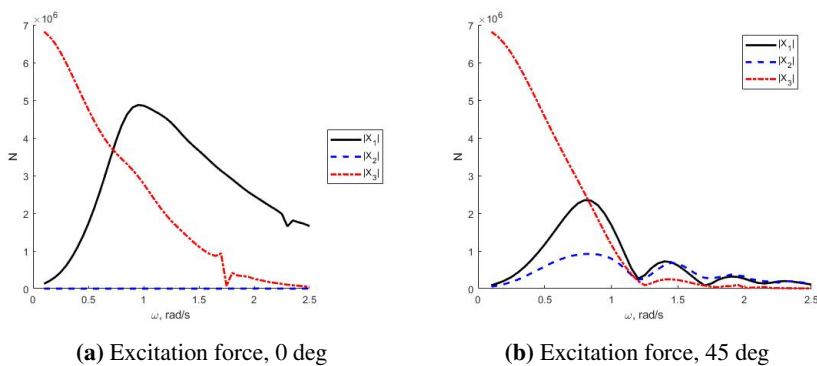
Figure 3.5: Excitation force for waves propagating from 0 and 45 deg

3.1   Multibody analysis

3.1.1   4 Bodies

The analysis of wave interactions with multiple bodies is an important and active field of marine hydrodynamics. In this section comparing the results of a different number of pontoons will be present. Wadam was used to carry out first order potential flow analysis of two, three and four pontoons. The hydrodynamic coefficients are compared to the coefficients for the single pontoon. When the number of bodies becomes large, the solving technique becomes very expensive, because the number of scattered waves that must be accounted for increases rapidly with the number of bodies, (Kagemoto and Yue, 1993).

The results for added mass, damping and excitation force are present for the four body analysis, according to multibody set up in Figure 3.6. Using the same dimension as pontoon 2 in Table 4.5, a multibody analysis is carried out to see how the interaction affects the added mass, damping and excitation force for varying wave headings. The spacing between the pontoons is 100 meters. Figure 3.6 illustrate the analysis with waves propagating in the positive x-direction.
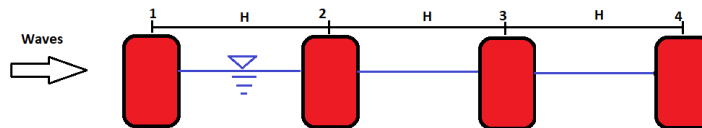
Figure 3.6: Multibody set up

3.1.2   Added mass and damping

Both the added mass and potential damping are plotted in the frequency domain. We can see from the graphs that there is no difference in added mass for low frequencies in the multibody analysis. This is related to the relationship of the length of the pontoons and the corresponding wavelength. When considering deep-water wavelength which corresponds to frequency 0.75 rad/s is 110 meters. This is 11 times larger than the width of the pontoon and longer than its length. That means that it will have little influence on the waves passing the structure and the bodies in the wake will experience the same waves as the first body. For frequency larger than 0.75 rad/s things start to be more interesting. Frequency between 1 and 2 correspond to a wavelength between 61m and 15.4 meters and large oscillations begins. The occurrence of these oscillations will be discussed later. Figure 3.7 and 3.9 shows that the added mass are equal for body 1 and 4 and for body 2 and 3 because of symmetry. The damping in surge, sway and heave follow the same pattern as added mass. Figure 3.8 shows the potential damping in surge and sway motion.

(a) Added mass in surge
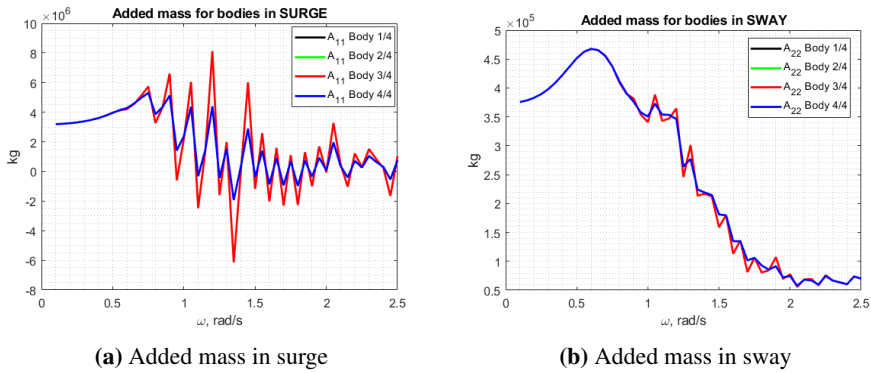
(b) Added mass in sway

Figure 3.7: Added mass in surge and sway

(a) Damping in surge
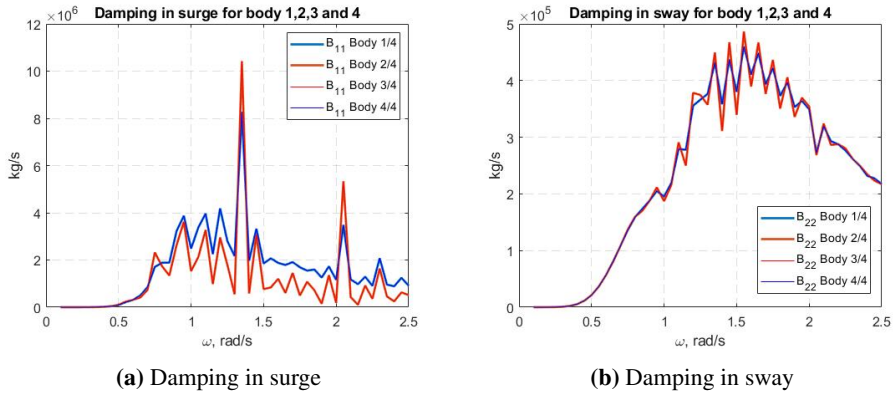
(b) Damping in sway

Figure 3.8: Damping in surge and sway

(a) Added mass in heave

(b) Damping in heave
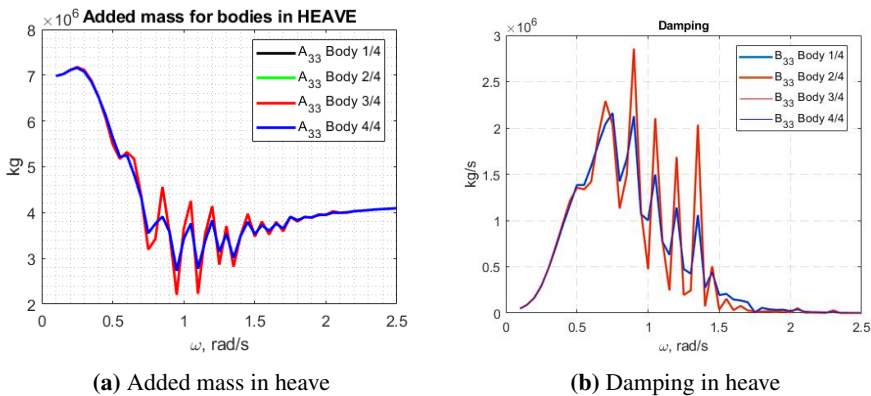
Figure 3.9: Added mass in surge and sway for multibody analysis

3.2   Excitation force

The excitation forces for each pontoon will give a rough estimate of the quasi-static forces going into the bridge structure due to waves. Quasi-static neglecting any dynamic contribution from radiation added mass and damping, (Koo and Kim, 2015). From Figure 3.11 we can see that the difference between the excitation force is not remarkable for the different bodies for waves propagating from the west. This is as expected when waves propagate from the side, each pontoon will be exposed for the same wave force. The exciting force in surge for this wave condition is more or less zero for all frequencies. Due to symmetry the excitation force for body one and four are equal and for body two and three. The excitation force for surge and heave for 0 degrees are presented in Figures 3.10a and 3.10b respectively. Due to shielding effect, amplitudes of wave exciting forces in the lee-side are smaller in magnitude than the one in the weather-side. The exciting force in sway is zero for this wave condition.

(a) Excitation force in surge, 0 degrees

(b) Excitation force in heave, 0 degrees
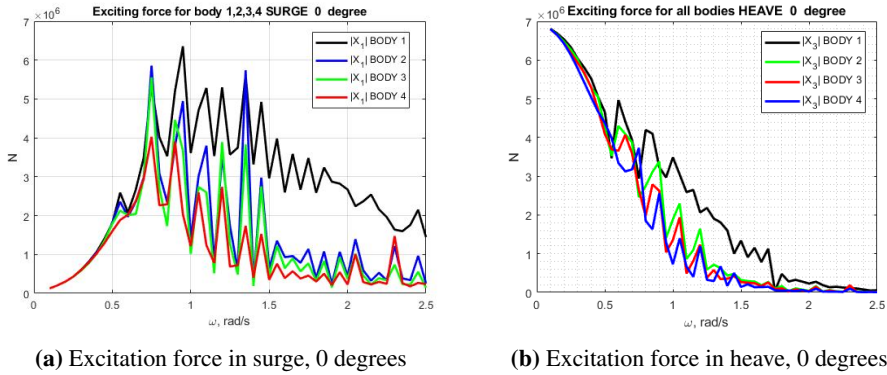
Figure 3.10: Excitation force in sway and heave for 0 degrees

(a) Excitation force in sway, 90 degrees

(b) Excitation force in heave, 90 degrees
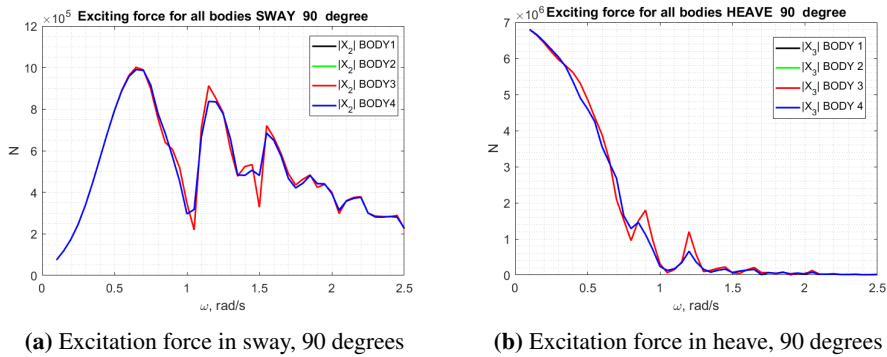
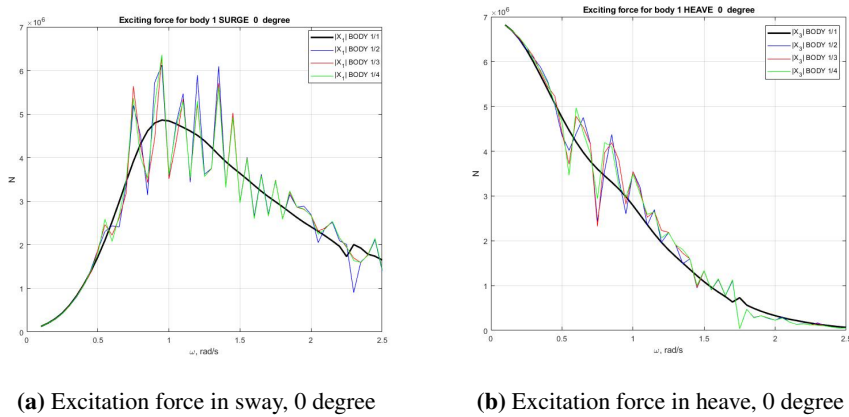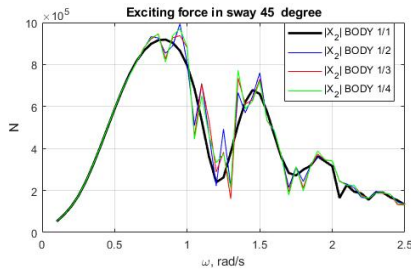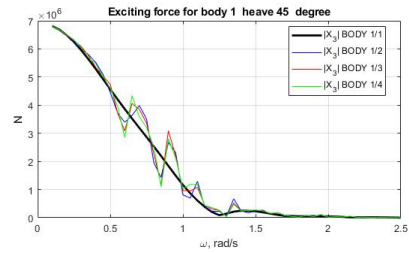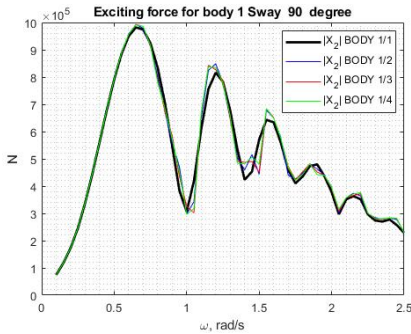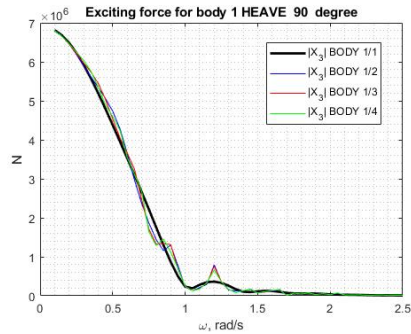**Figure 3.11:** Excitation force in sway and heave for 90 degrees

3.3 Effect of different number of pontoons

In this section, a comparing result of the first pontoon of each analysis will be studied. In this way, we can study the impact of two, three and four pontoons. "Body 1/1" represents the single body analysis, and "Body 1/2" denotes the first pontoon of a two bodies analysis. The purpose of this analysis is to compare interaction effects of two, three and four pontoons. If the interaction effects are similar to each other, we can use the hydrodynamic coefficient of one body to represent the interaction effects for the whole bridge.

3.3.1 Added mass

For the comparison between single body analysis, the influence of hydrodynamic interaction in added mass is clearly shown. The results of added mass in heave and surge motions are larger compare to the results of added mass on sway motion which show that hydrodynamic reactions occur in surge and heave. The added mass in surge oscillating for interacting bodies when $\omega > 0.75$. Especially for added mass in surge, the responses of a multibody analysis are quite different from the responses of a single body without multibody effects. It is important to notice that the different of added mass for multibody analysis is almost the same for all analysis, and the effect of more than two bodies seems to be negligible. The different is due to interaction effect of more than one body.
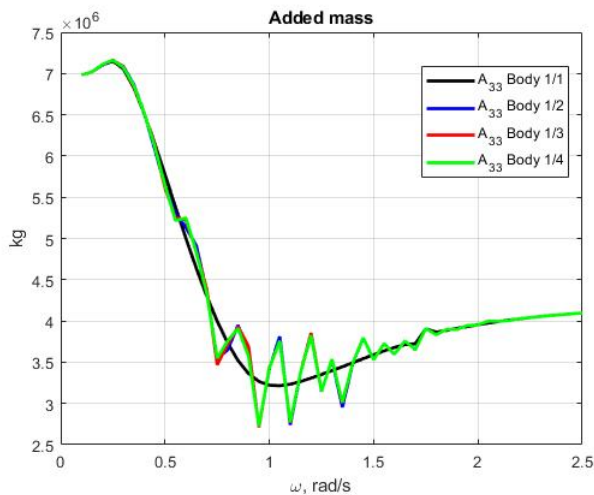
Figure 3.12: Added mass in heave

(a) Added mass in surge
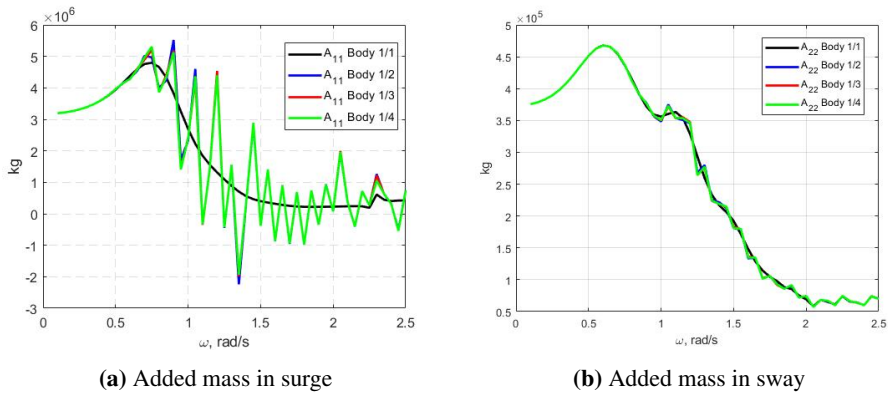
(b) Added mass in sway

Figure 3.13: Added mass in surge and sway

3.3.2 Damping

When the wave period increases, the added mass coefficients gradually converges to a constant value, while the radiation wave damping goes to zero. This can be seen in Appendix where added mass and damping are plotted in the period domain. The damping is close to zero for all frequency lower than 0.5 rad/s. An interesting result is the appearance of fairly sharp oscillations in the predicted amplitudes at specific frequencies. For added mass in heave, sharp oscillations occur in a frequency range from 0.5-1.5. According to Figure 3.14 a peak occur at $\omega \approx 1.3$. Further investigation shows that the peak is an error due to rough frequency step. Wadam can handle maximum 60 different frequency in one simulation. Figure 3.15 shows the same plot with a much smaller frequency step between 1.15-1.55 rad/s (4-5.5 s). The large radiated waves from one body to the other body exhibit a sudden change in sign at these frequencies, resulting in a jump in the total hydrodynamic forces. This is due to the strong interactions effects and will be investigated in Section 3.5.
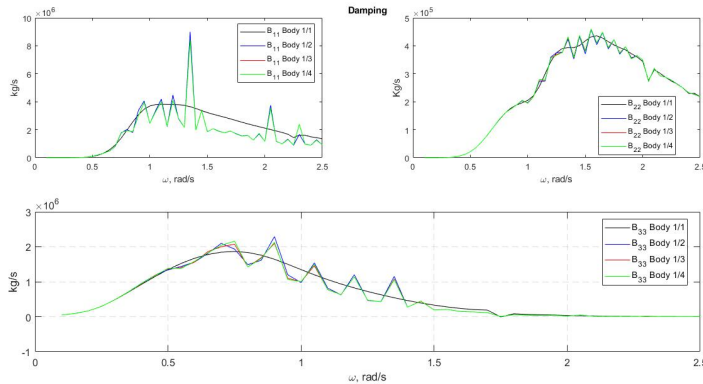
Figure 3.14: Damping in surge, sway and heave

(a) Damping in surge
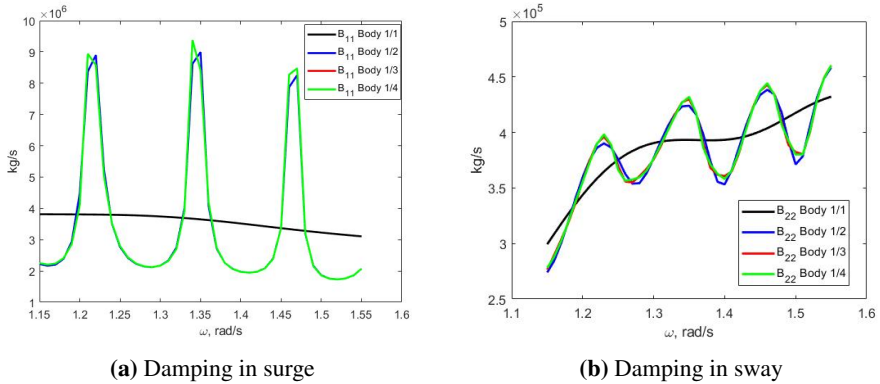
(b) Damping in sway

Figure 3.15: Damping in surge and sway for frequency between 1.15-1.55 rad/s

3.3.3   Excitation force

The hydrodynamic interaction also affects the diffraction problem. The noticeable inter-
action effect is observed for surge comparison with heave. The reason may be that the
resonance mainly dominates the heave response and as a result of this, the interaction ef-
fect is not so prominent in heave mode, (Ali and Khalil, 2005). Figures 3.18a and 3.18b
show the excitation force in surge and heave for 90 degrees respectively. For this wave
condition, the interaction effects are similar to the single body analysis when waves are
propagating from the west. When waves are propagating from north and northwest, the
interaction effects are clearly shown, see Figure 3.16 and 3.17. This is as expected since
the pontoons are placed in the wake of the waves

(a) Excitation force in sway, 0 degree

(b) Excitation force in heave, 0 degree

Figure 3.16: Excitation force in sway and heave for 0 degree

(a) Excitation force in sway, 45 degree

(b) Excitation force in heave, 45 degree

Figure 3.17: Excitation force in sway and heave for 45 degree

(a) Excitation force in sway, 90 degree

(b) Excitation force in heave, 90 degree

Figure 3.18: Excitation force in sway and heave for 90 degree

To give a better insight into interaction effects, the next sections will describe various interactions effects which affect the added mass, damping and excitation force for multiple bodies. The peaks are exaggerated because of potential theory neglect the fluid viscosity and energy dissipation. According to Equation 3.1 interaction effect is expected because of the small distance between the pontoons. In following section coupling effects, linear sloshing, piston-mode resonance, and influence of mesh size will be discussed.

3.4 Coupling effects

RIFLEX do not take hydrodynamic coupling effect into account when calculating the radiation data. It is therefore important to detect which contribution radiation data from other pontoons affects the total added mass. Figure 3.19a and 3.19b shows the contribution of coupling effect from different bodies. "Body 1 and Body 2" denotes the contribution from *Body 2* on *Body 1*. The result is as expected where the neighboring body has a larger

distribution than the bodies that are further away. The coupling effects following an irregular pattern and the contribution vary from frequency to frequency. For coupling effect in heave, the contribution from *Body 2* is around 20% for frequency 0.8. This corresponds to a wavelength that is equal to the distance between the pontoons. Because of the eigenperiods depend on the square root of the added mass the coupling effect is neglected even though the effect is important for some frequencies. RIFLEX have a plan to implement coupling effects into the model, but right now there is no easy way to implement the couplings effect into RIFLEX.

(a) Coupling effects in sway   **(b)** Coupling effects in heave
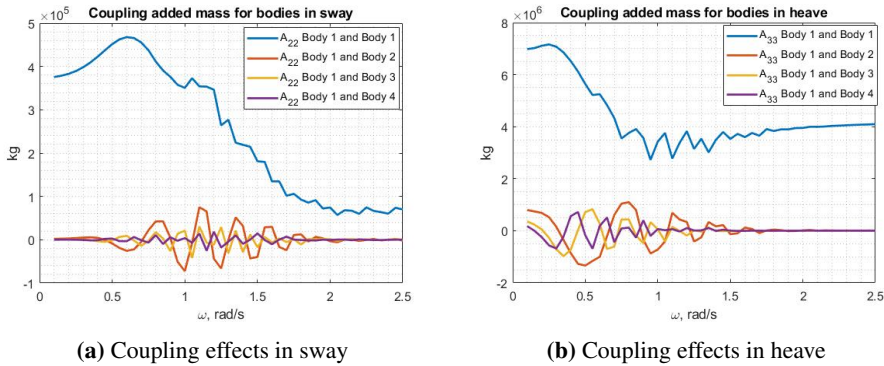
Figure 3.19: Coupling effects in sway and heave

3.5   Linear Natural Sloshing

This section describes how to estimate linear natural sloshing frequencies without using CFD methods. The sloshing phenomena occur for any moving tank with a free surface, especially widely studied in large LNG tanks and anti-roll tanks. However, sloshing may occur as an interaction problem between the pontoons. Figure 3.20 illustrates the section between two pontoons as a sloshing problem. The effect is important to consider during design, because of the danger of uncontrolled resonant excitation, (Faltinsen and Timokha, 2009). Sloshing has been extensively studied using many analytically, numerically and experimental methods. The phenomena are hard to predict, and in this section, only natural linear sloshing will be described. Faltinsen and Timokha describe linear natural sloshing frequencies and modes by the potential flow theory of in-compressible liquids without surface tension effects. The simplest 2D case with exact analytically natural modes and frequencies is sloshing in a planar rectangular tank. Figure 3.20 shows the gap between two pontoons with the water depth **h** and the horizontal distance **L** between the pontoons.

Nodal and antinodal vertical lines pass through the liquid volume, see Figure 3.20. A liquid particle moves horizontally at a nodal line and vertical at an antinodal line. The lowest natural mode (i=1) has a node in the middle between the two pontoons and antinodal lines coinciding with the vertical walls. The number of nodal lines is equal to the mode number, i. The natural frequencies depend on the depth and breadth ratio.
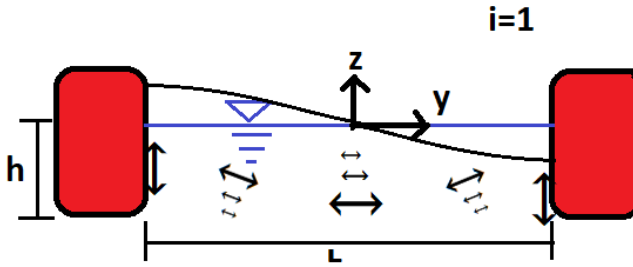
Figure 3.20: Mean liquid shape and notations used for a "2D rectangular tank

$$\omega_i = \sqrt{g\frac{\pi i}{l}tanh\left(\frac{\pi i}{l}h\right)} \tag{3.3}$$

$$T_i = \frac{2\pi}{\sqrt{\frac{g\pi i}{l}tanh(\frac{\pi ih}{l})}} \quad i = 1,2... \tag{3.4}$$

The highest natural periods are most important in assessing the severity of sloshing. This is where the largest sloshing occurs. A standing wave with a wavelength twice the tank breadth and a node in the middle of the tank is dominant according to the linear theory for a 2D rectangular tank flow in resonant conditions at the highest natural period. When viscous damping effects are neglected, a linear theory based on the potential flow of an incompressible liquid predicts infinite steady-state response for a forcing frequency equal to a natural frequency of the liquid motion, (Faltinsen and Timokha, 2009). The reason is zero damping.
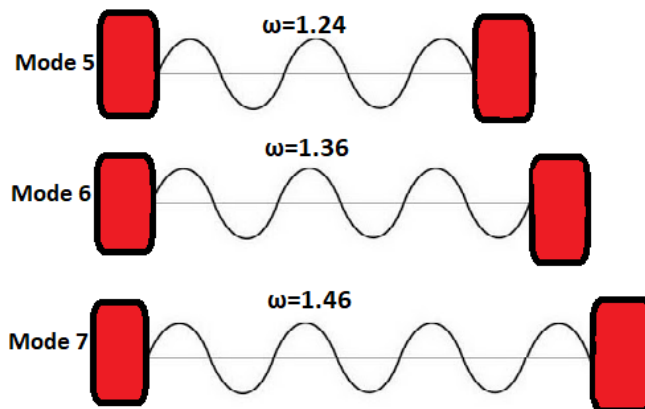
Figure 3.21: Sloshing with infinte waterdepth

The eight first natural sloshing modes in Equation 3.3 are plotted together with the damping and excitation force to investigate the peaks. The vertical lines indicates the eight first natural modes in a 2D rectangular tank. According to Figure 3.22 and 3.23 mode three to eight correspond approximately to local minimum in damping in surge. Added mass, damping and excitation force following the same pattern and is depending on each other with peaks at the same frequency. Of course, one should also keep in mind that the peaks are mostly overestimated. Although, the conventional potential theory is found to overpredict the actual motion response and wave elevation.

The liquid depth can have a significant influence on the natural period. For floating pontoons, the tank depth has been defined as the draft of the pontoons. It is also interesting to see how the natural periods change for deep liquid conditions. Figure 3.21 shows the natural sloshing frequency for infinite water depth. Mode 1 corresponds to wavelength twice the tank breadth with frequency 0.55 rad/s. It is observed some irregularities for Figure 3.10a and Figure 3.12 at frequency 0.55 rad/s. It is hard to say if this is due to sloshing effects or other interaction effects, but it is clear that peaks occur for the natural sloshing frequencies. The second frequency is at 0.79 rad/s, and same peaks are observed in added mass and excitation force. For sloshing with a water depth of 5 meters the first sloshing mode is 0.22 rad/s. For this frequency, no irregularities are observed. This implies that sloshing is more accurate in deep liquid conditions. This gives sense since this is not a tank put floating bodies with a free surface.
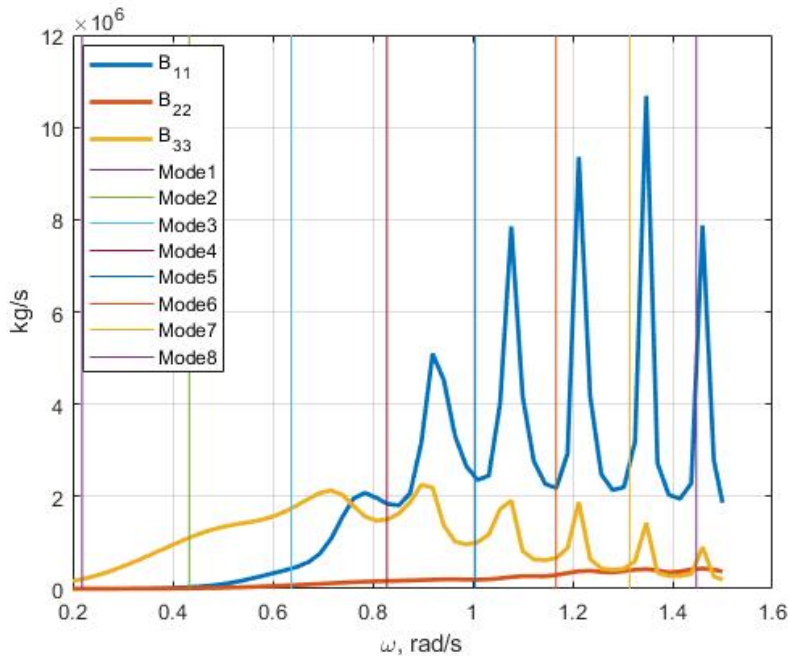
Figure 3.22: Damping force in surge, sway and heave for the eight first natural sloshing modes
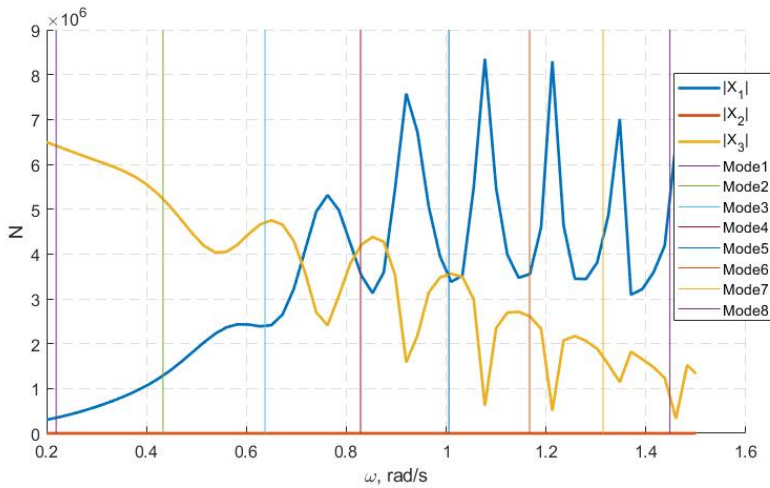
Figure 3.23: Exciting force in surge, sway and heave for the eight first natural sloshing modes

3.6 Piston-mode resonance in a 2-D moonpool

Moonpools are vertical openings through the deck and hull of ships or barges. The most important resonance is called piston-mode oscillation, Molin (2001). The piston-mode resonance frequency occurs in a frequency range with large vertical ship motions that act as excitation.
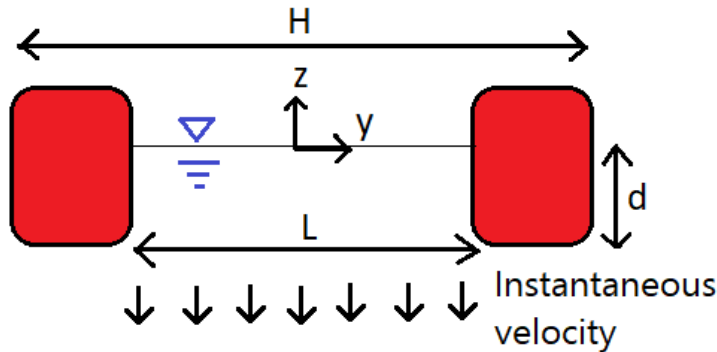
Figure 3.24: Piston-mode resonance between the two hulls, illustrated by instantaneous water velocity vectors

$$\omega \simeq \sqrt{\frac{g}{h + \frac{L}{\pi}\left(\frac{3}{2} + ln(\frac{B}{2L})\right)}} \tag{3.5}$$

The natural frequency is obtained by Equation 3.5 with a solution $\omega = 0.52$. The natural piston-mode frequency is equal to the first natural sloshing frequency for infinite water depth.

Linear theory in general overpredict the resonant fluid motions rather severely. When multiple bodies floating close to each other, large resonant elevations of the free surface occurs in the gap. Most of the programs using linear theory overpredict the free surface elevation between the bodies. For example, if the piston-mode amplitude is found to be five times that of the incoming wave, the linear theory may typically predict a factor of ten - twenty, or even more, (Faltinsen and Timokha, 2009).

3.7   Sesam Xtract

How the surface elevation is changing due to the pontoons are interacting is possible to study using off-body points in Wadam. SESAM Xtract is a postprocessing tool specialized in presenting Wadam output.

To estimate the free surface elevation in the gap, the waves are simulated by SESAM Xtract using Wadam off-body points. Xtract is not able to simulate multibody motion, so the visualization only illustrates the wavefield before and after hitting the body, and possible sloshing effects are ignored. HydroD has a limitation of 2000 off-body points in the grid. In a CFD point of view this is a ridiculously small number of off-body points, but in this case, 2000 off-body points are enough to show how the wave field altered due to potential theory. The dimension of the pontoons and the spacing between is the same as the previous analysis.

(a) Offbody mesh with one pontoon   **(b)** Offbody mesh with two pontoons
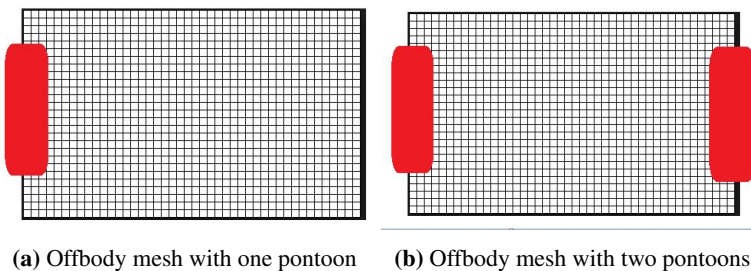
Figure 3.25: Offbody mesh

A range of different wave frequencies has been evaluated, but the most relevant is wave period between 3-8 seconds. All figures below have a wave frequency of 0.3 Hz, which correspond to wave period of 3.33 sec. The colors indicate the surface elevation from still

water level. The highest elevation is indicated with red color, and the mean water surface is indicated with green color.
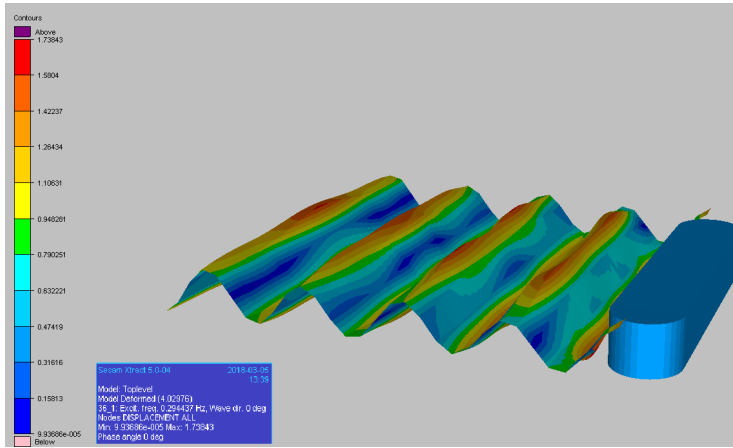
Figure 3.26: Incomming Wave
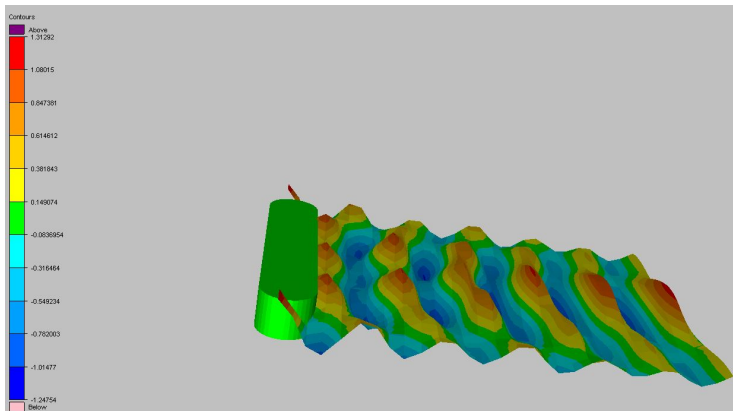
Figure 3.27: Wake between the pontoons

The visualization shows the wave field between the structures. To be able to compare the wave field between the pontoons to the incoming waves, a reference analysis with one pontoon has been run. When the waves hit the pontoon, the wavefield is changed. By analyzing the wave field in front of the single pontoon with the wave fields in the wake, we can observe sharp peaks and an evident reduction in the wave heights behind the pontoons. The reduced wave height corresponds to a lower response of the lee-side. When multiple bodies floating close to each other, large resonant elevations of the free surface may occur in the gap. Most of the programs using linear theory overpredict the free surface elevation between the bodies, (Xin Xu, 2014).

3.8   Convergence Study

Doing analysis using the finite element method, much time can be saved by dividing the model into more substantial and fewer elements. Too large elements can lead to losing accuracy and miss valuable information. Convergence studies can therefore be carried out to find the point where the analysis is sufficiently accurate and time efficient. By running the simulation several times with smaller and smaller mesh size, the result should become more and more similar in each run.

The element size convergence was determined through a static analysis where element size between 0.25m and 2m. HydroD has a restriction on a maximum number of elements in panel model, so a more beautiful mesh than 0.25 was not possible. All analysis was run with the same wave direction and frequency of 1.25 rad/s.

For each run, the added mass in surge and heave and damping in heave are determined. The result of the convergence study can be seen in Table 3.8 and 3.8. When decreasing the element size to 1m, the difference is less than 1 % for heave and surge. This was considered to be sufficiently accurate, and an element size of 0.5 m was used as mesh size in GeniE.

Element-size	Added mass, surge	Added mass, heave	Damping - heave
2	1.077E+06	3.425E+06	6.786E+05
1	1.063E+06	3.357E+06	7.087E+05
0.5	1.060E+06	3.326E+06	7.209E+05
0.25	1.060E+06	3.326E+06	7.209E+05

Element-size	Added mass, surge	Added mass, heave	Damping - heave
2m-1m	1.32%	2.03%	4.25%
1m-0.5m	0.28%	0.93%	1.69%
0.5m-0.25m	0	0	0

The elements were divided into relatively large elements. A convergence study could be carried out and check the result for various element size in SIMA. Because of an enormous structure, I considered that element size of 10 meters in the horizontal beam and 3 meters for the towers were adequately to get reasonable results without further investigations. However, it might be interesting to looking into smaller elements at critical points in the model.

Modeling and calculation software

In this chapter, I will present the different software used in this thesis. The whole analysis started with creating the structure for each pontoon type in GeniE. The structural mesh was taken into HydroD for hydrodynamic analysis, and then the entire bridge was modeled in SIMA/RIFLEX.

4.1   Genie

Sesam GeniE is a software tool for design and analysis of offshore and maritime structures developed by DNV GL. The pontoon bodies were created and meshed using Genie software. The mass model created in GeniE was then exported (.FEM) file and then used in the further analysis in Wadam to examine hydrodynamic coefficients. The mesh was determined according to the convergence test in Section 3.8, with a size of 0.5 m, something that seems reasonable for large floating structures. In total, four different sized pontoons were created in Genie. The dimensions of different pontoons can be seen in Table 4.5 and Figure 4.1 shows a meshed pontoon in Genie. The coordinate system is defined with y-axis longitudinal and z-axis in the vertical direction. This is because it corresponds to the global coordinate system in SIMA.

4.2   HydroD - Wadam analysis

The pontoons modeled in Genie were analyzed in HydroD for calculating added mass and hydrostatic stiffness data using panel method. By solving the green integral equation for each element the value of the velocity potential over each element is found. An advantage
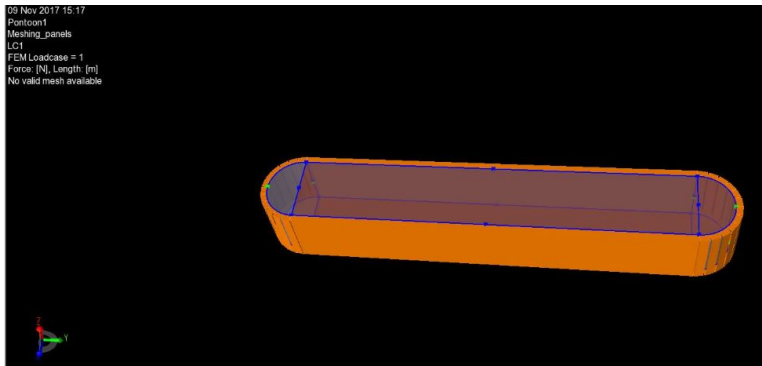
Figure 4.1: Mass model made in GeniE

of using panel method, accurate results are obtained in short time, and the required computer power is not so comprehensive. A disadvantage using panel method is that viscous damping cannot be found because this method assumes inviscid, irrational and incompressible fluid. This program is able to estimate the added mass quickly, restoring and potential damping, compared to CFD which takes much time and processor power.

The guidance of Wadam Wizard ("Wave Analysis by Diffraction And Morison theory") were used to create direction set and frequency set. The required input for Wadam is a panel model, mass model, radius of gyration and environmental data. The lowest period was set to 2 sec and the largest to 100 sec. Because of limited numbers of different periods obtained in HydroD the different periods have to be chosen carefully. The first period was set to 2 sec with a timestep of 0.2 sec to 12 sec. After 12 sec the timestep was set to every 10 sec to last value 100 sec. In project thesis, I observe that SIMA just considered added mass for infinite frequency for calculation of eigenfrequency.

The incoming wave direction is varied between $0°$-$90°$, with an interval of $15°$ and then using double symmetry to cover the whole specter of directions. Further, a constant water-depth was set to 500 meters for the entire structure. The draft of the pontoon is defined according to (NorconsultAS, 2017) as 5 meters. The mass model is defined as well as the center of gravity, radius of gyration according to Section 2.3.2.

To analyze the interaction between the pontoons a multi-body configuration was used. The interaction effect of two, three and four floating pontoons was carried out using the same hydro model and loading condition in the HydroD workspace. The results from the multibody models are reported separately, in the body system for each model.

4.3 SIMA/RIFLEX

RIFLEX is an efficient program for hydrodynamic and structural analysis of slender marine structures (often applied to risers) developed by SINTEF Ocean. Slender structures
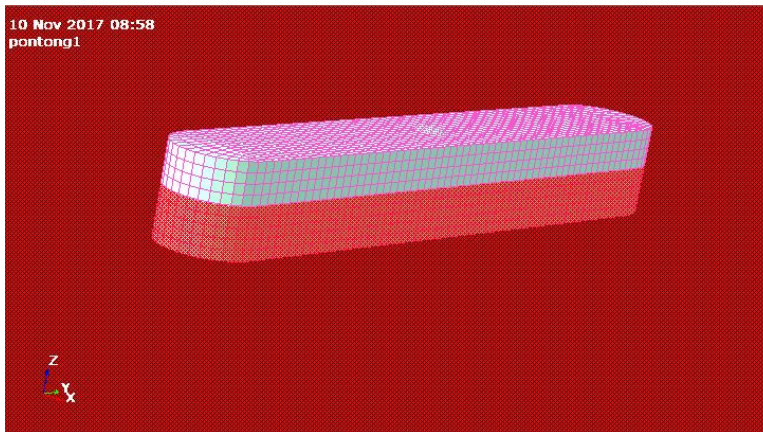
Figure 4.2: Model made in HydroD

are characterized by small bending stiffness and large deflections. RIFLEX have high flex-ibility in modeling and analysis for a wide range of structures, including floating bridge (MARINTEK, 2011). SIMO (Simulation of Marine Operations) is a program for simula-tion of complex multibody marine operations.

The program system consists of four programs or modules communicating via the file sys-tem as shown in the Figure 4.3 The INPMOD module reads input data, such as supernodes,
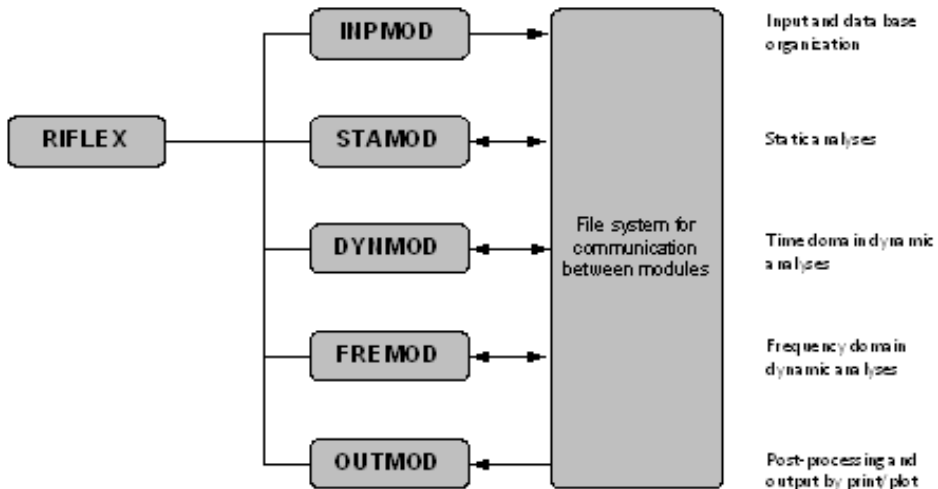
Figure 4.3: Structure of program system

lines, and cross-sections and organizes a database for use during subsequent analyses. The STAMOD module performs static analysis and is used to define the initial configuration for the dynamic analysis Key data for finite element analysis are also generated by STAMOD

based on system data given as input to INPMOD (Veritas, 2014b). DYNMOD performs the time domain dynamic analysis based on the static configuration and environmental data. DYNMOD module also calculates the natural frequencies and mode shapes. OUTMOD performs postprocessing of selected results generated by STAMOD and DYNMOD.

4.3.1   SIMA - modeling

In this section a overview of modelling in SIMA will be present. Figure 4.4 shows the configuration of one pontoon-section.
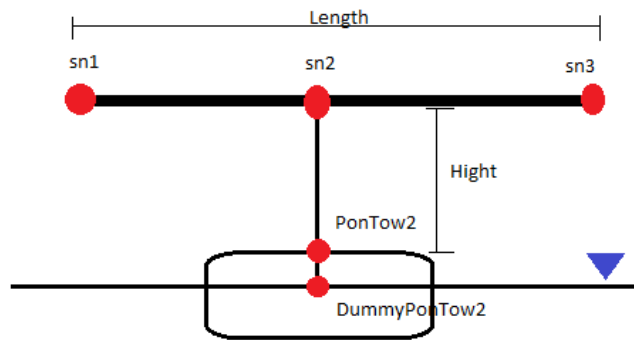
Figure 4.4: One pontoon section

Supernodes:
First supernodes are defined at every beam connection in an ascending order starting from sn1 at $x = 0$ to sn=49 at $x = 5435$. The same procedure is done for pontoon towers, starting with PonTow2. Further, constraints to every supernode had to be defined. The supernodes in each end are fixed, and the nodes between are free. The supernodes that connect the pontoons with the pontoon tower is slaved to the motion of pontoon towers.

Lines and line type:
Lines are defined between two different supernodes with a characteristic line type. The different lines are defined in same ascending order as the supernodes. Each line type has a unique length, cross-section and element length. As a result of a long structure, the element length needs to be large. For the low bridge, the element length is 10 meters, and for pontoon towers, the element length is approximately 5 meters depending on tower height. For a long and simple structure, there will be no significant changes in stresses for a small change in length. This is also to reduce the computing time.

Cross-sections:
Each line-type need to have a corresponding cross-section. Here is mass, area, gyration, and stiffness properties defined according to parameters in Section 4.4

Bodies:
The bodies are imported from Wadam through a (.SIF) file. The SIF file including all physical properties like hydro-static stiffness data and linear damping data. The pontoons are connected to the tower by a dummy-line. The dummy-lines have no physical properties and the mass is set to zero and the stiffness very large. For the model contains hydrodynamic interaction the pontoon body 2 is used for the whole model, find in Section 3.1. That is because of the hydrodynamic coefficient does not change within the bodies in a multibody analysis. For the model without interaction effects the pontoons are modeled according to Table 4.5.

Specifeid force:
The analysis in SIMA is a coupled SIMO/RIFLEX analysis which the RIFLEX part contains the bridge structure and a SIMO part for floating bodies. For the floating bridge the neutrally buoyant position includes the RIFLEX elements, but in SIMO, the assumption is that the floating body is neutrally buoyant without the RIFLEX element. To compensate for this a specified force acting on the center of buoyancy is applied. In SIMA, a specified force equal to the specified force equal to the buoyancy force of the body is added in CoB (center of buoyancy) at each pontoon.
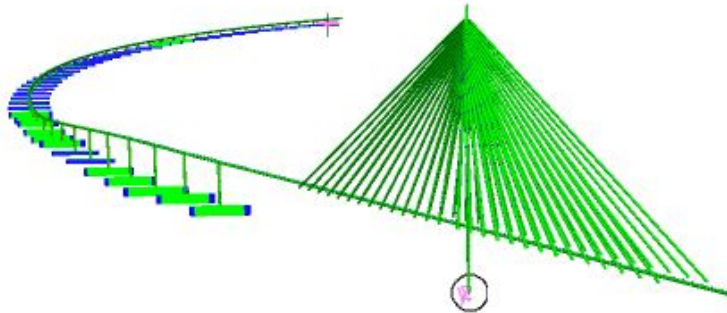
Figure 4.5: Model made in SIMA

4.4 Modelling Description

An overall description of the concept is present in this section. For this analyze, the same dimensions and parameters as a previous report produced by project group leading by Norconcult AS are used. Figure 4.6a and 4.6b shows an XY- and XZ-plot of the initial geometry of the bridge, where the blue dots represent pontoon towers. The navigation channel requires minimum 45 meters from water surface to the bridge deck. In this concept, the horizontal clearance between tower two and three is 525 m to provide the navigation channel. The maximum vertical slope down from the navigation channel is 4.97%. The curved shape of the bridge has a radius of 5 km, and the distance between the two ends of the bridge is around 5 km and enables the transverse loading to be taken as membrane stress

in the bridge girder.

The end of the right-hand side of Figure 4.6a is referred as north end support and will be used further in this thesis.

(a) xy-plot of initial position

(b) xz-plot of initial position
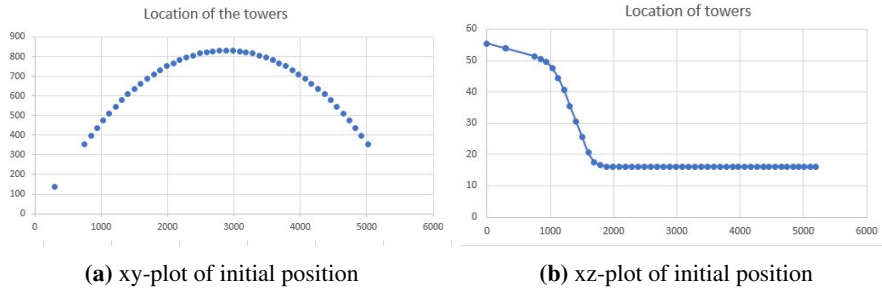
Figure 4.6: xy- and xz-plot of initial position of pontoon towers

4.4.1   Cable Stays

Two planes of stay cables support the high bridge. There are total 56 cables in total, 2x14 on each side of the tower and support the bridge girder at every 20 meters. The main span is 510 meters and provides the navigation channel.

The wires are pre-tensioned, to support the weight of the bridge girder in the navigation channel. When applying weight to the structure, the pre-tensioned wires will prevent deflection of the bridge girder. By inducing initial pretension to the cables, it can reduce the moments acting on the girders and make a long span bridge possible. The calculation of the initial pretension of the cables can be difficult and complicated and was done with "trial and error" until the bridge girder have reasonable deflection.
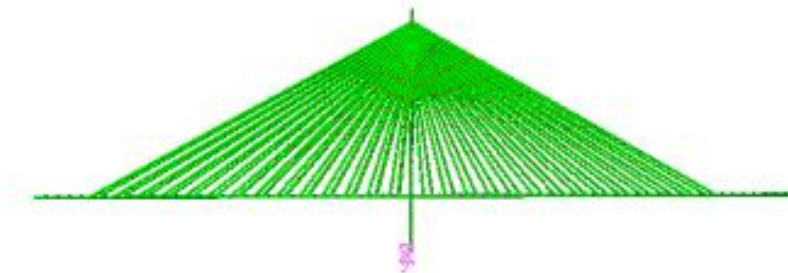
Figure 4.7: Cross-section of main gider

4.4.2   Bridge girder

The bridge girder is supported by two different parts, a floating part, and a cable-stayed section. In the cable stay bridge, the back span is 325 m and the second span 510 m connected with a tower in the middle. For the floating part, permanent loads are supported by the buoyancy provided by the 48 pontoons. A cross-section of the bridge main girder is shown in Figure 4.8 (NorconsultAS, 2017).
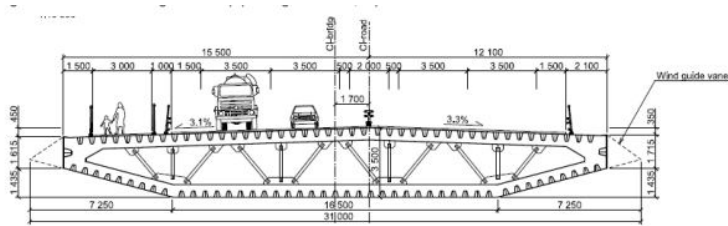
Figure 4.8: Cross-section of main gider

Cross sections of the three different girders used in the analyses are given in the following tables:

Table 4.1: Main girder cross section

Parameter	Value	Unit
E-modulus	210 000	N/mm^2
G-modulus	80769	N/mm^2
Poission ratio	0.3	m^4
Alfa	1.2E-5	1/K

Table 4.2: Main girder cross section

Parameter	Main Girder 1	Main Girder 2	Main Girder 3	Unit
Iz	115.62	132.47	181.1	m^4
Iy	2.68	3.2	5.049	m^4
It	6.10	7.32	10.86	m^4
Area	1.43	1.68	2.634	m^2
Width	31	31	31	m
Max hight	3.5	3.5	3.5	m
Mass per meter	17836	19798	27287	kg/m
Wt	2.3	2.76	3.61	m^3
Position	0-835 1935-5465	835-1935.5	0	m

*Angel of incident = 0 degree

4.4.3   Pontoon towers

Each tower starts at the top of each pontoon (4 meters above sea level) and ends below the main girder. Three different towers are used along the bridge. For the low bridge, the height of the tower is 12.2 meters and the highest tower applied for the high bridge is 49.8 meters.

Table 4.3: Material input pontoon towers

Parameter	Value	Unit
E-modulus	210 000	N/mm^2
G-modulus	80769	N/mm^2
Poission ratio	0.3	m^4
Alfa	1.2E-5	1/K

Table 4.4: Input pontoon towers

Parameter	Tower 1	Tower 2	Tower 3	Unit
Iz	5.53	10.23	14.369	m^4
Iy	5.53	10.23	14.369	m^4
It	11.06	20.46	28.738	m^4
Area	0.872	0.977	1.158	m^2
Mass/m	7200	7956	9429	kg/m
Diameter	7.16	9.185	10	m
Drag coefficient	1.05	1.05	1.05	-
Position	11-46	5-10	2-4	-

4.4.4   Pontoons

The pontoons must be large enough to provide enough buoyancy for the entire structure. The floating bridge is supported by 48 pontoons with spans 100 meters. It is total three different pontoons types that have been used. All types have same length and draft but vary in width and stiffness. For the low bridge, where the pontoons carry the weight of one small girder segment and one tower, the small pontoon is used. For the high bridge, the girder segment is longer and a pontoon with more buoyancy is applied. The local coordinate system of the pontoon is defined in the same direction as the global axis. Surge is the motion in the transverse direction of the pontoon, while sway is longitudinal to the pontoon.

Table 4.5: Pontoon parameters

Parameter	Pontoon 1	Pontoon 2	Pontoon 3	Unit
Length	58	58	58	m
Width	10	12	14	m
Radius end	5	6	7	m
Draft	5	5	5	m
Total Volume	5027	5986	6929	m^3
Displacement	2793	3325	3850	m^3
Marine growth	560	615	669	kN
Roll stiffness	-1.66E7	3.22E6	3.79E7	m
Pitch stiffness	1.404E9	1.64E9	1.86E9	m
Heave stiffness	5.61E9	6.68E6	7.73E6	m
mass	754	898	1039	ton
Position	12-46	6-11	2-5	-

4.5   Simple Bridge

A simple bridge is designed to perform an investigation of hydrodynamic interaction. The simple bridge consists of four pontoons, girders with the same span-length as the low bridge and fixed in both ends.

1. The pontoons are analyzed in Wadam without the interaction effects. This implies that forces with equal magnitude are acting on each pontoon, as the first order wave force transfer functions are the same for all pontoons.

2. The pontoons are analyzed in Wadan including the effect of interaction. The hydro-dynamic coefficients are obtained for a four-body analysis.

Chapter 5

Eigenvalue Analysis

5.1 Eigenvalue simple bridge

An eigenvalue analysis was performed for the simple bridge in order to see how the bridge respond. Vertical motion dominates the first mode shape. The vertical mode shapes are important around the wave period of the fjord. For fjords, the wave period is relatively short, around 4-8 sec. For the simple bridge, the three first eigenperiods corresponds to the wave period. From the equation of eigenfrequency 5.2 the eigenfrequency depend on the stiffness and mass. Having eigenperiods in the same range of wave period could be critical, and may lead to large oscillations.

The mode shapes are plotted in XY-plane and XZ-plane together with static position. Figure 5.1a and 5.1b shows the motion of the first mode shape that consists of one-half wave. SIMA considering added mass for infinite frequency, the eigenperiods are the same for interaction problem and the single pontoon.

Table 5.1: First 5 eigenperiods for the simple bridge

	Mode 1	Mode 2	Mode 3	Mode 4	Mode 5
Periode [s]	6.0	4.3	3.9	3.2	2.1

(a) Mode 1 XY-plot

(b) Mode 1 XZ-plot
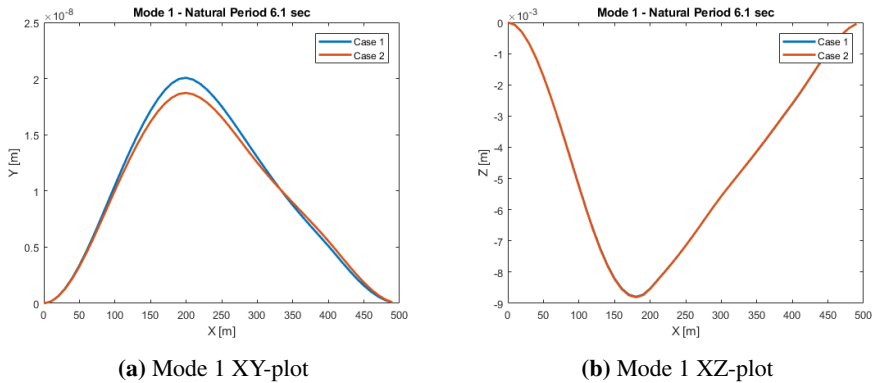
5.2 Eigenvaue Analysis

According to Section 2.4 the eigenvalue analysis is based on the mass and stiffness matrices of the structure. The eigenvalue analysis was carried out in order to ensure that the eigenfrequency was close to the reference model. This would be a good starting point for the dynamic analysis. Table 5.2 present the 10 first eigenperiods calculated in SIMA with the corresponding dominating motion. These first eigenmodes are essential due to drift loads and wind loads while Mode 9 and 10 is important due to wind-generated waves which coincide with the wave periods of Bjørnfjorden.

The first eigenmodes are dominating by horizontal motion illustrated in Figure 5.2a to 5.5b. Mode 1 consist of a one-half wave, Mode 2 of two half waves and Mode 3 of four half waves. After the seven first eigenmodes the eigenperiod decrease very slowly. The results compared to (COWI, 2016a) is some differently. The first mode is 61 seconds for the initial model of the bridge determined from (COWI, 2016a). The deviation between the reference model and computed one can be justified by the relationship between the mass and stiffness is different. Other explanation of why the eigenvalues are larger could be the simplification of the bridge girder. According to 2.4.2 the first eigenperiod is larger for a straight beam than a curved beam. A curved beam will have a smaller period than a straight beam as the arch shape makes it stiffer. In this model the bridge model is curved but the actual bridge girder is modeled as straight between the columns. Therefore it is reasonable to think that the actual eigenperiod is closer to the reference bridge. In the reference analysis, the bridge is modeled with some differences than in this theses. High bridge, pontoons, are factors that will influence the mass and stiffness.

Table 5.2: 10 Eigenperiods calculated using SIMA

Mode	Eigenperiod [s]	Motion
Mode 1	65.4	Horizontal
Mode 2	37.4	Horizontal
Mode 3	21.7	Horizontal
Mode 4	15.4	Horizontal
Mode 5	10.9	Horizontal
Mode 6	8.6	Horizontal
Mode 7	7.9	Horizontal
Mode 8	7.0	Horizontal
Mode 9	6.5	Horizontal
Mode 10	6.4	Vertical
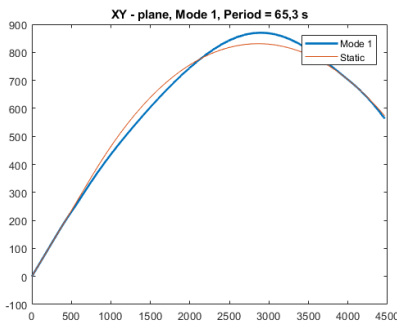
(a) Mode 1 XY-plot
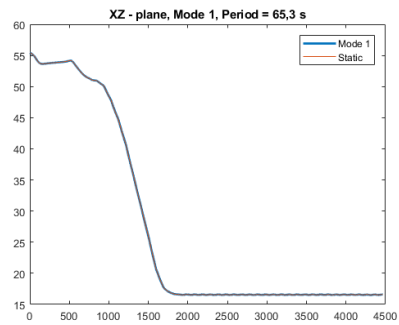
(b) Mode 1 XZ-plot

Figure 5.2: Mode 1
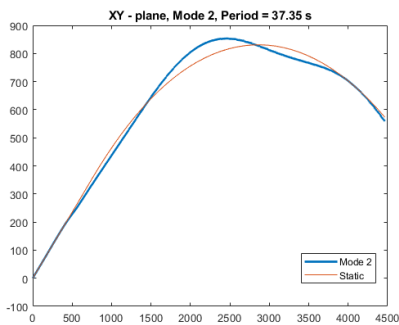
(a) Mode 2 XY-plot
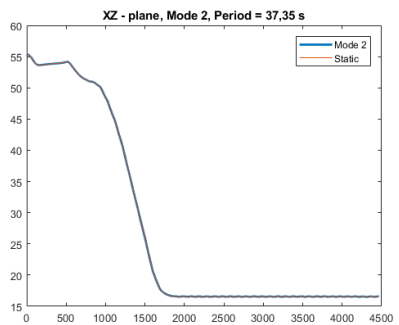
(b) Mode 2 XZ-plot

Figure 5.3: Mode 2

(a) Mode 3 XY-plot

(b) Mode 3 XZ-plot

Figure 5.4: Mode 3

(a) Mode 4 XY-plot

(b) Mode 4 XZ-plot
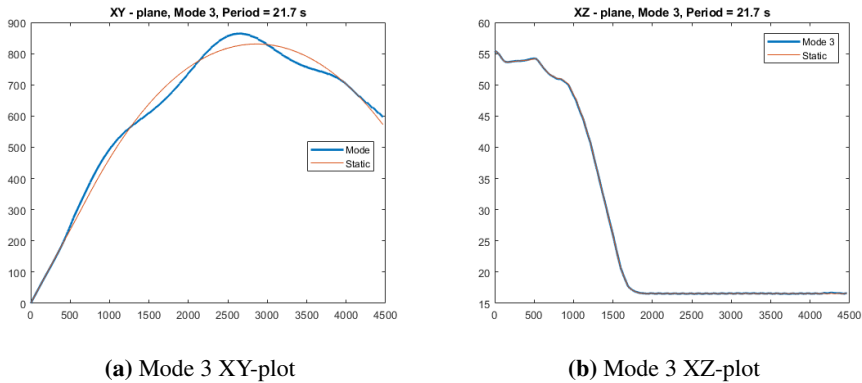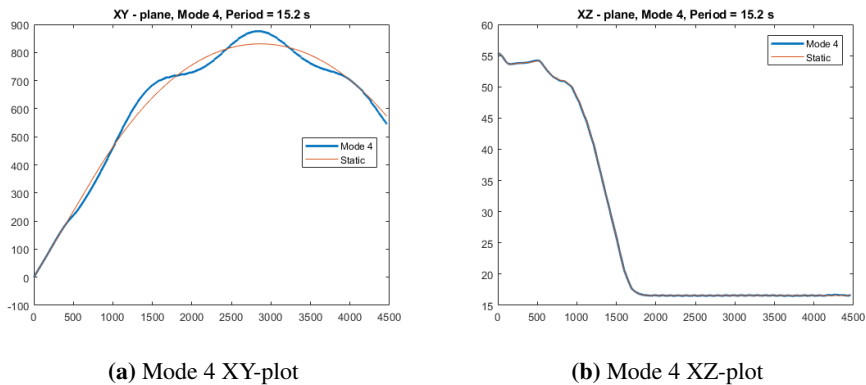
Figure 5.5: Mode 4

Aas Jacobsen, COWI, Global Maritim and Johs Holt (2016) get more eigenperiods around 11 seconds. Eigenperiods in this thesis decreases faster than the reference model. This may be due to a different number of elements for the different parts, and some differences in modeling. That could also be related to the number of half waves. More half waves mean more considerable stiffness and lower eigenperiods. The added mass of the pontoons is frequency dependent. SIMA using added mass for infinite frequency, and using different frequencies components will lead to different results. All these factors will affect the mass and stiffness.

Ideally, to avoid resonance, the eigenfrequency should be outside the range of wave frequency. For a sizeable floating bridge structure, it is impossible to have all eigenperiods outside the range of wave frequency.

Chapter 6

Static Analysis

6.1 Main Girder

Static analysis was carried out to ensure that the bridge can withstand self-weight without large deflections and stresses. The most significant part of the loads is carried as bending moments in the main girder. Figure 6.1 shows the static bending moment about the y-axis. Only the bridge self-weight is taken into consideration when calculating the bending moment, and there is no traffic loads or other external loads included. The most considerable bending moment is not surprisingly located at the high bridge and is a result of a large free span-length and large self-weight.

For the low bridge, the maximum bending moment is located at the connection of pontoon towers. The deviation between SIMA result and hand-calculation of maximum bending moment for a fixed end beam is 1.1%.

Table 6.1: Sima Vs Handcalculation

Location	Sima	Hand-calculation	different
$M_{max}[10^8 Nm]$	1.445	1.461	1.1%

Figure 6.2a shows the displacement of the main girder for the low bridge together with the initial position. The bridge keeps the initial position and shows that right buoyancy force is applied. For the low bridge, the maximum vertical deflection is located in the middle of the two towers and is approximately 0.075 m at each of the spans. According to the theory, maximum deflection in the middle is calculated to be 0.082 m. The horizontal deflection of the towers is negligible. According to (Vegvesen, 2015) maximum deflection is given by $L/350$ where L is the span-length. With a span-length of 100 meters, this corresponds to maximum deflection of 0.28 meters. For self-weight, only the vertical deflection satisfies the requirements of Statens Vegvesen.
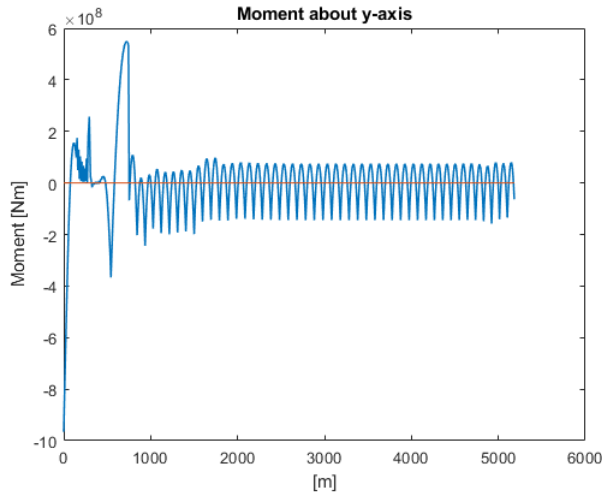
Figure 6.1: Moment about Y-axis

Figure 6.2b shows the shear force for the main girder and the largest shear force for the low bridge occurs at the end of each beam section. That matches the hand-calculation for a fixed beam described in Section 2.3 with self-weight as the only external load.
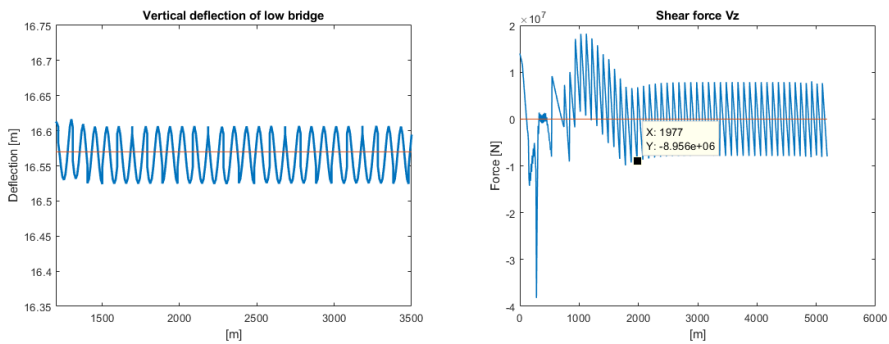
(a) main girder displacement

(b) Shear force of main girder

Figure 6.2: Main girder displacement and shear force of main bridge girder

Table 6.2: Sima Vs Handcalculation

Location	Sima	Hand-calculation	different
$V_{max}[10^6 N]$	8.956	8.763	0.98%

Chapter 7

Dynamic Analysis

7.1 Environmental Conditions at Bjornafjorden

Relevant environmental conditions at Bjørnafjorden involves wave, wind, tide, and current. In this thesis, I will put attention on waves. Various 100-year sea state for different wave headings are described in Table 3-7,p.19 in (COWI, 2016a). The sea states are described with the peak period T_p and significant wave height H_s occurring from north to north-west. The cable-stayed part is located in the south, while the other end is referred to as the north end support.

Table 7.1: 100-year sea states for wind generated waves and swells

	$H_s[m]$	$T_p[s]$
Wind generated wave	3	6
Swell wave	0.4	12-16

100-year current speed are defined as 0.7 m/s for draft of 5 meters, given in table 7.2. Current is not accounted for in the analysis but could easily be included in SIMA by defining the current in environmental conditions. However, (COWI, 2016a) concludes that loads from the current are small comparing to wave loads.

Table 7.2: Current profile according to (COWI, 2016a)

Depth [m]	100 year current velocity V_0 [m/s]
0-5	0.70

7.1.1   Tidal variations

The tidal variation given in (COWI, 2016a) is +/- 0.75 m from mean sea level. To simulate tidal variations, a load could be implemented on each pontoon equals the vertical increase or decrease in pontoon displaced volume. Tidal variations may be crucial for the moment about y-axis in the bridge girder. However, tidal variations will only provide a static contribution, and it was determined to rather focus on the response from wave loads, as these have frequency components in the same range as the eigenperiods of the bridge.

7.1.2   Sea Spectrum

The wind generated sea is described using a JONSWAP spectrum described in (Veritas, 2010).

$$S_j(\omega) = A_\gamma S_{PM}(\omega) \gamma^{exp-0.5(\frac{\omega-\omega_p}{\sigma\omega_p})} \tag{7.1}$$

Where S_{PM} is the Pierson-Moskowitz spectrum defined in (Veritas, 2014a, p.49). γ is a shape parameter defining the shape of the spectrum peak. A higher γ gives a higher spectrum peak, i.e. wave energy is more concentrated around T_p. $\omega_p = 2\pi/T_P$ is the spectral peak frequency, σ describes width of the peak. Figure 7.1 shows the resulting JONSWAP-spectrum that is used for wind generated waves. The parameters are chosen according to (Veritas, 2014a), represented in table 7.3

Table 7.3: Parameters used to describe the JONSWAP spectrum for wind generated sea

Parameter	Value
γ	3.3
$\sigma\_omega, for \omega > \omega\_p$	0.07
$\sigma\_\omega, for \omega > \omega\_p$	0.09
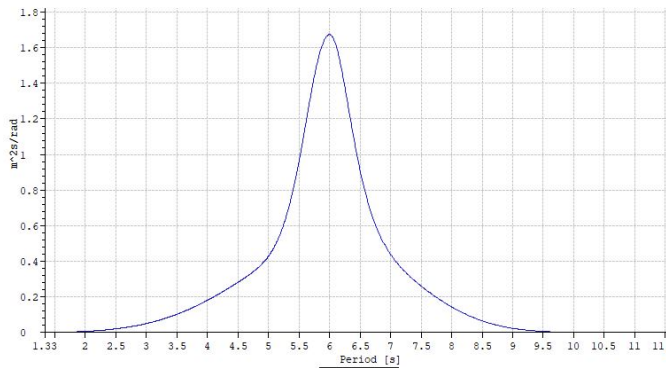
Figure 7.1: JONSWAP spectrum used to describe the wind generated sea.

7.2   Dynamic Analysis

The results from the time domain analysis of the bridge response will be present in this section. The dynamic calculations turned out to be extremely time-consuming. The massive structure has an arc length of more than 5000 m, 49 pontoons and cables lead to too many elements. To decrease the computer time, the element size was adjusted to larger elements, using symmetry when modeling the bodies in Genie and when calculating the wave force in SIMA. Still, One 1 h analysis took 62 hours to finish. With the purpose of investigating the effect of hydrodynamic interaction, it was determined to rather focus on the simple bridge structure. However, one dynamic analysis for the entire bridge structure was run to get an indication of what is going on.

7.2.1   Initial analysis of the bridge motion

This wave condition is generated from (COWI, 2016a), and it used to verify that the bridge model behaved similarly. The waves are propagating from the side with significant wave height $Hs = 3m$ and peak period $Tp = 6s$. When the waves propagating from the west, the force acting on the pontoons are excitation force in heave, sway and roll moment.

The motions of the bridge seem to follow an irregular displacement pattern. The irregular motions could be a consequence of differences in the geometry at the north and south part of the bridge. The variation in column height in addition to the high bridge will result in different stiffness properties for the two ends. The waves load only act on the floating part, and the frequency of pontoons are higher at the north end, could also be a source of the observed behavior.
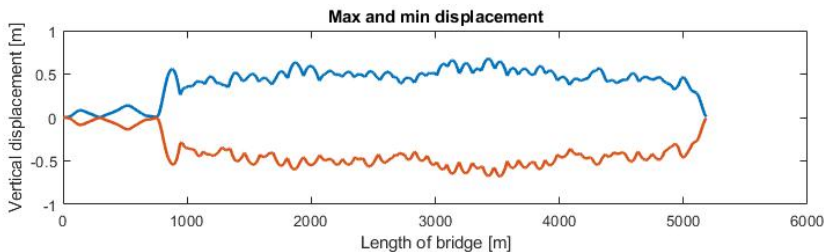
Figure 7.2: Maximum and minimum envelopes of vertical displacement

In order to get an indication of how the bridge responds due to wave loads, a short analysis of 300 seconds was studied. This was done to decide which parts of the bridge that would be studied more closely. Figure 7.18 illustrates the vertical displacement for the north and south part of the bridge, with a simulation length of 300 seconds. The behavior seems to be irregular and horizontal motion seems to be the dominating motion. It is logical that the horizontal displacement is the dominating motion when waves are propagating from the side. In addition, there is a higher stiffness in the vertical direction due to the pre-tensioned cables.

Maximum vertical displacement is around 0.5 meters and occurs at the south end. For this wave condition, the horizontal oscillating period tends to be around 50 seconds which is close to critical eigenperiod. The horizontal displacement is around 2 meters which are significant for this wave condition. The maximum and minimum displacement are present in Table 7.4. These results are larger than compared to (COWI, 2016a, p. 85). This was not expected since the results from COWI is obtained from 10 x 3hours analysis, while this result is obtained from only a 300 seconds irregular analysis. However, the extreme values seem to appear in the south end, while the north end is more similar to the reference model. An explanation of the irregular motion could be the difference in geometry is different at the north and south side of the bridge. At the south side, the navigation channel results in a high column height. The column height reduces with a slope of 5% after the high bridge and are constant in the south end, and this results in different stiffness properties along the bridge. The vertical and horizontal displacement seems to be most significant at the south end. In addition, the pontoon has a shorter span length in the north end. This could be a result of variation column height.
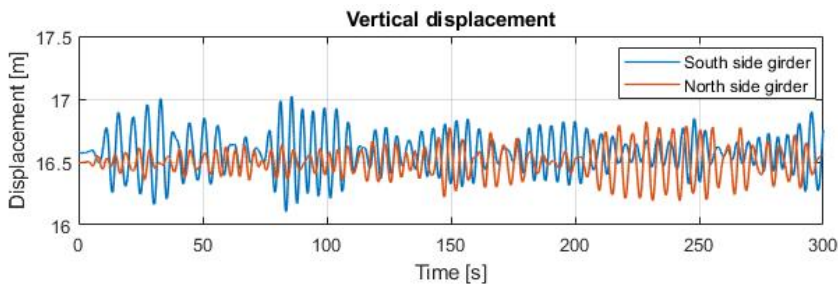
Figure 7.3: The vertical displacement in the north and south side girder
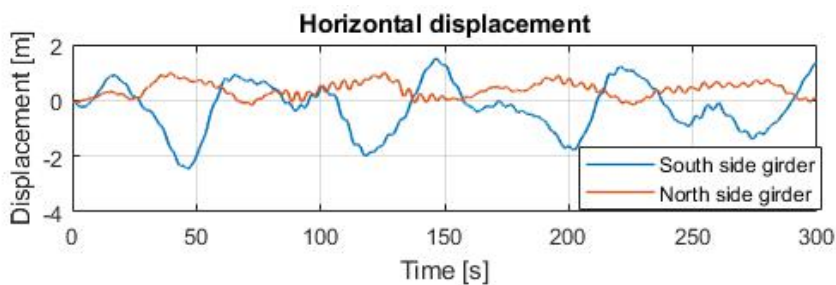
Figure 7.4: The vertical displacement in the north and south side girder

Table 7.4: Largest displacements for fully correlated waves from west

	Max/Min (south end)	Max/ Min (north end)	COWI	Unit
Vertical displacement	0.5 -0.3	0.3 -0.29	0.24 -0.28	[m]
Horizontal displacement	1.6 -2	1 -0.1	0.8 -0.85	[m]

The largest forces due to wave-induced load are present in Table 7.5, together with the location of occurrence. The largest stresses are caused by bending moment about the strong and weak axis. The bending moment appears to be most critical for yielding and its most relevant to focus on influencing moment for different load conditions.

Table 7.5: Lagest axial, torsosinal, moment and shear force, with respective occurance

Force Component	Maximum	Location
Axial	30.9 MN	Line 2
Torsinal Moment	55.3 MNm	Line 2
Moment about y-axis	311 MNm	Line 4
Moment about z-axis	826 MNm	Line 2
Shear force in z-direction	9.9 MN	Line 2

7.3   Simple Bridge

In cooperation with the supervisor, it was decided to focus on the simple bridge and run a various analysis with varying load conditions. An alternative was to use a supercomputer with more capacity. This was not given priority since the time consumption was considered as too large compared to the value of the learning outcome by doing it. The objective of this thesis could be obtained by the simple model.

The analysis is run with regular and irregular waves. With regular waves, it is reasonable to investigate the response for certain wave height and wave period combinations in a much shorter time. The following section contains results where the simple model is exposed to regular and irregular waves. The response is measured for a range of wave heights and directions.

Two analysis for each load condition is applied with different hydrodynamic coefficients. In the "interaction" analysis the result from the multibody analysis in Wadam is used. For the "no interaction" analysis of the hydrodynamic parameters for a single body without including the effect of adjacent bodies, the wave experienced by each pontoon is exactly the same. This implies that forces with equal magnitude are acting on each pontoon. All other properties are equivalent to the two models and difference in results must come

from the hydrodynamic coefficients. The propose is to check the effect of interaction and compare the result with the model without interaction effects.

7.4 Regular Waves

In this section, the simple model is exposed to regular waves. Figure 7.5 shows the maximum moment in the bridge girder for wave height from 1-6 m with a period of 6 seconds and waves propagating from the west. The simulation length is set to 300s, but only results after 150 s are studied to avoid transient effects. The model behaves more or less linearly for bending moment about the weak axis. As the figure shows, the bending moment follows the same pattern indicating that there is a linear relationship between the wave height and the response. The maximum bending moment is bigger for the single body analysis in regular waves.
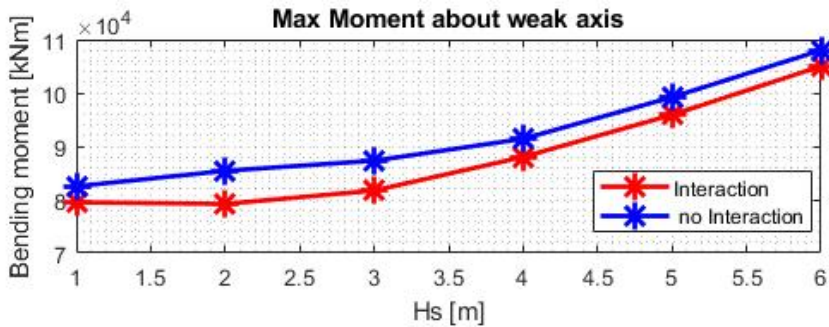
Figure 7.5: Maximum moment for different wave height
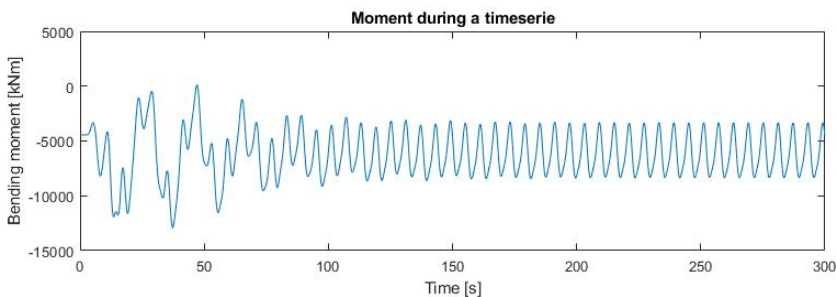
Figure 7.6: Response for a timeserie showing transient state before reaching steady sate

Figure 7.7 shows the pontoon location in a long wave period. Because a short bridge with fixed ends, the pontoon does not follow the wave elevation for long wave periods exactly.
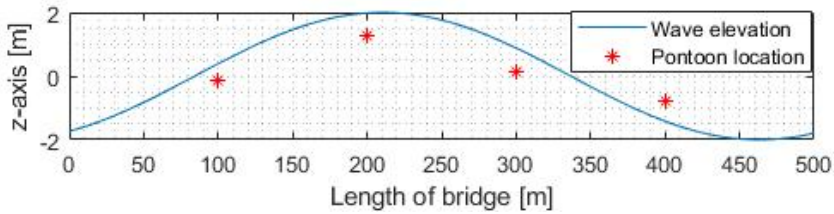
Figure 7.7: Pontoon location in a regular wave with wavelength of 500 m

7.5 Load Condition 1

"Load Condition 1" have a significant wave height and peak period of H_s = 3m and T_p = 6s respectively. The waves approaching from the west will give rise to excitation force in sway and heave. The load condition 1 will be studied more in-depth than the others. This is because this wave condition is the most common wave condition at Bjørnafjorden. According to Figure 3.19 the excitation force in sway and heave follows the same pattern for all bodies. However, the excitation force is very frequency sensitive, which mean a small change in frequency lead to a large difference in excitation force. The purpose of this chapter is to observe what effect added mass and excitation force affect the forces and displacements. Afterward, a parameter study will investigate what kind of hydrodynamic coefficients affect the response most.
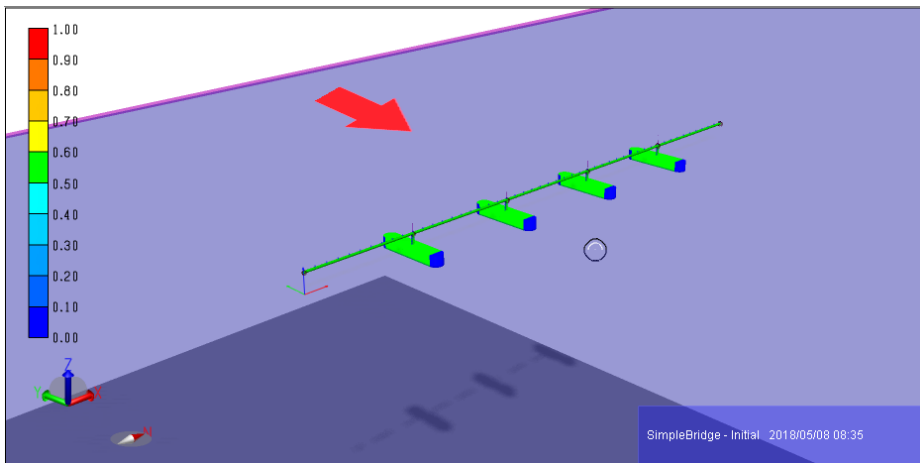
Figure 7.8: Maximum and minimum vertical displacement for 3h simulation with incoming waves from 270 degree

7.5.1 Dispacement

The envelopes for the response for each point of the bridge is shown. The plots are made by extracting BIN files from RIFLEX and plotted in Matlab. The displacement plots are obtained from the maximum and minimum values obtained at each integration point along the bridge girder for every timestep. Figure 7.9b and Figure 7.9a illustrates the maximal and minimum displacement on each integration point during a 3 hours analysis. The results from the model accounted for hydrodynamic interaction the maximal and minimum displacement is larger than for the model without interaction. Figure 7.10a shows the actual distribution during a 3-hour analysis located in the middle of the bridge.
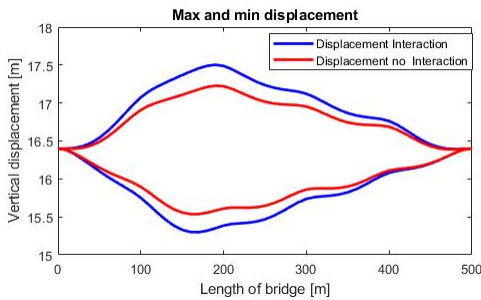
(a) Vertical displacement
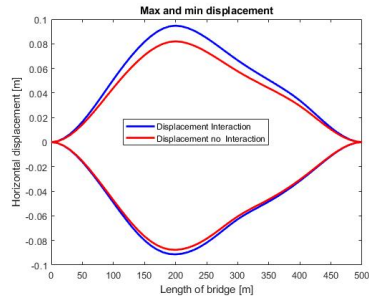
(b) Horizontal displacement
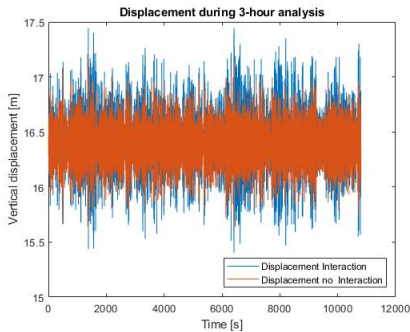
(a) Displacement in bridge girder
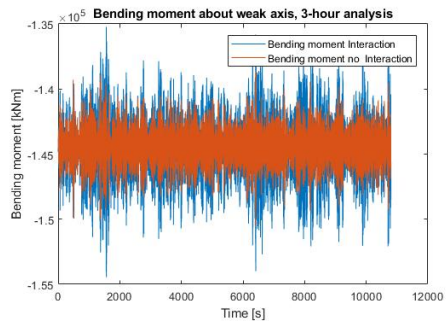
(b) Bending moment in bridge girder

Forces and Moments

The maximum axial force and moment are shown in Figure 7.18. One should notice that the maximum plots only present the largest response that occurs at each integration point during a time series. The difference in the maximum bending moment for bending moment is approximately 13 % located between pontoon 2 and 3. Figure 7.11 shows the maximum and m.inimum static and dynamic axial force and bending moment

(a) Max min bending moment

(b) Max min axial force
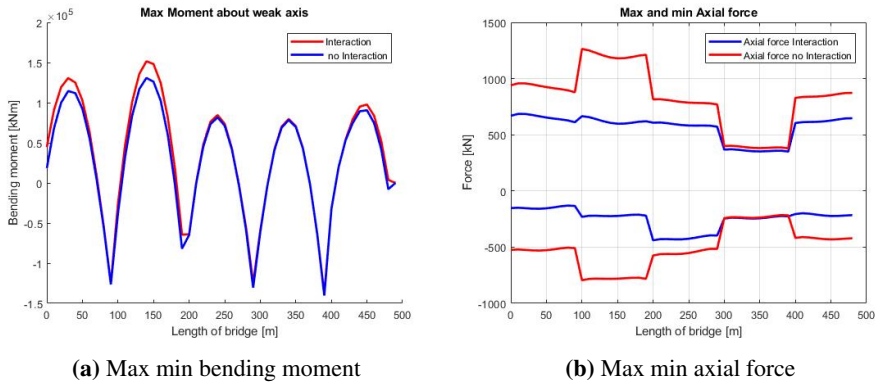
Figure 7.11: Maximum and minimum axial force and bending moment for Load Condtion 1

7.5.2 Dominating motions

The frequency domain solution of the vertical displacement for the two models are present in Figure 7.12a and 7.12b. The frequency domain solution is carried out according to Section 2.5.4 in order to understand how the bridge girder responds due to wave loads. Frequency domain solution for bending moment is present in Appendix for the same location at the bridge. The point is located at the second pontoon and is plotted using the WAFO toolbox.

The vertical displacement is extremely irregular with sharp peaks at distinct frequencies. The largest peak is for both conditions at 1.13 rad/s, which correspond to a period of 5.5 sec. This is close to the first eigenmode of 6 seconds which consist of vertical motions. This corresponds also to T_p=6 sec for this load condition. For the single body the vertical motion consists of wide range of frequencies between 0.7-1.3 rad/s, and for the multibody configuration, the vertical displacement is between 1.1-1.2 rad/s.

However, the peak is expected since the first eigenmode coincides with wave period. The difference between the two models are somehow unexpected and need to be further investigated. In order to understand the sharp peak at frequency 1.13 in Figure 7.12b, the added mass and excitation force were studied at frequency 1.13 rad/s. Table 7.6 shows the added mass and excitation force for single body and multibody analysis for the critical frequency.

(a) Vertical displacement   **(b)** Vertical displacement.
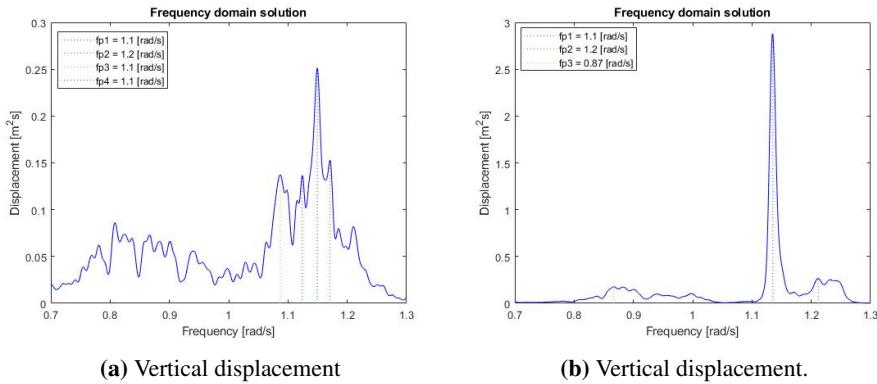
Figure 7.12: Frequency domain solution for vertical displacement

Table 7.6: Added mass and excitation force at critical frequency of 1.13

Added mass for frequency 1.13 rad/s			
	Interaction	No interaction	Diffrence
Surge	1.45e06	1.55e06	6.9%
Sway	3.53e05	3.54e05	0.3%
Heave	3.38e06	3.27e06	3.4%
Excitation Force for frequency 1.15 rad/s			
	Interaction	No interaction	Difference
Sway	8.24e05	7.56e05	9%
Heave	3.2e05	3.48e05	8%

The difference in added mass is largest in surge with a deviation of 6.9 %. The deviation in excitation force is 9% and 8 % in sway and heave respectively. There is no exciting force component in sway for this wave condition. To understand how much the added mass affects the eigenperiods a simulation without added mass has a natural period that was 34% higher. The natural period depends on the square root of the sum of mass and added mass. Small changes in added mass should, therefore, lead to a smaller change in eigenperiods.

Added mass lead to longer natural period, which corresponds to Equation 2.43. SIMA does not account for frequency-dependent added mass and only considered added mass for infinite frequency. To get correct results, frequency depended added mass has to be taken into consideration.

The next step is to perform a parameter study to investigate what coefficients affect the response most. This is done by using the added mass and excitation force for the multibody analysis into the single body analysis and see how it will affect the result.

7.5.3   Effect of Diffraction Force

The excitation force for the multibody configuration is used in the single body analysis to see how the bridge respond. The vertical displacement is the sum of static and dynamic displacement and is almost identically to the multibody configuration. The maximum vertical displacement for the single body analysis is 0.7m and 1m with the diffraction force from the multibody analysis. According to Section 3.3.3, the result for the excitation force in this wave condition is similar to each other. The result is more different than expected. That shows that the response is sensitive to a small change in excitation force.

(a) Vertical displacement   **(b)** Horizontal displacement
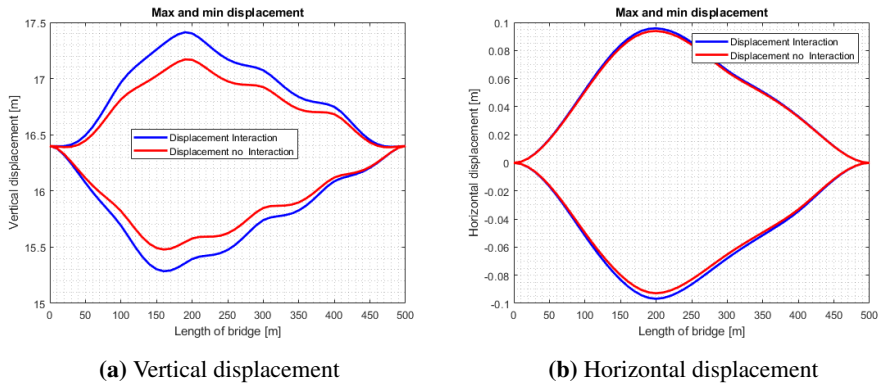
Figure 7.13: Impact of excitation force on vertical and horizontal displacement

(a) Vertical displacement   **(b)** Bending moment about weak axis
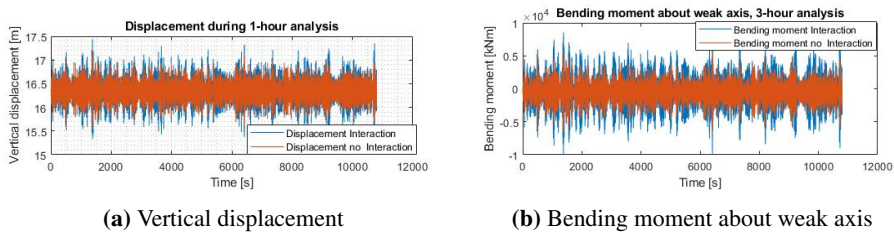
Figure 7.14: Vertical displacement and bending moment during a 3h analysis

7.5.4   Effect of added mass

The added mass for the multibody configuration is used in the single body analysis to see how the bridge respond. The horizontal displacement is identical to the single body analysis. The maximum vertical displacement for the single body analysis is 0.7m and 1.3m with the added mass from the multibody analysis. The result is expected because of sharp oscillation in added mass for the relevant frequency.

(a) Vertical displacement
(b) Horizontal displacement
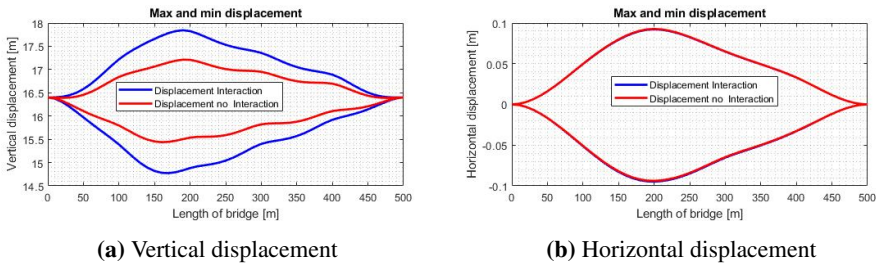
Figure 7.15: Effect of added mass on vertical and horizontal displacement

(a) Different added mass
(b) Different excitation force
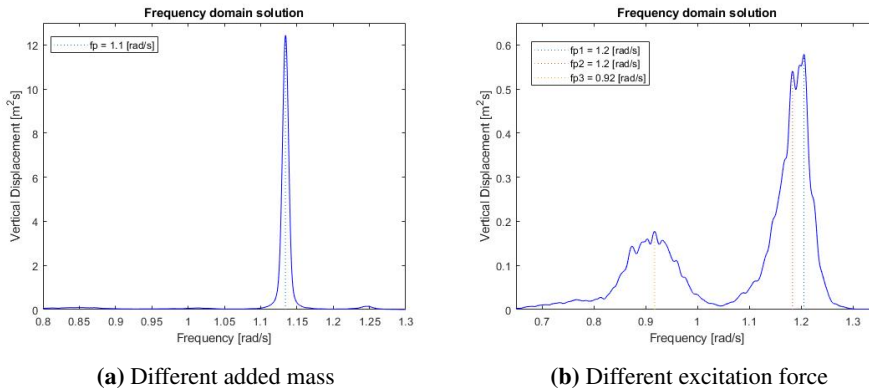
Figure 7.16: The impact of added mass and excitation force in frequency domain solution for

The impact of added mass and excitation force in the frequency domain are present in Figure 7.16. The largest peak is at 1.18 rad/s for the model with different excitation force and a second peak at 0.9 rad/s. For the model with different added mass, the response pattern is similar to Figure 7.12b. The result shows that the added mass contributes to a concentrated displacement response at frequency 1.13 rad/s. The added mass was analysis for the critical frequency of 1.13 rad/s without extreme values for exactly that frequency.

However, sharp peaks in added mass occur in the interval around and will affect the total response. For frequency 1.1 rad/s the frequency depending added mass in heave is 2.2E6 kg and 4.2E6 kg for frequency 1.2 rad/s, while the value is almost constant on 3.3E6 kg for the single body, in interval 1.1-1.2 rad/s. Interaction is a complex problem, and the frequency domain solution depending on many factors that affects the peak frequency response.

(a) Bending moment (b) Vertical displacement
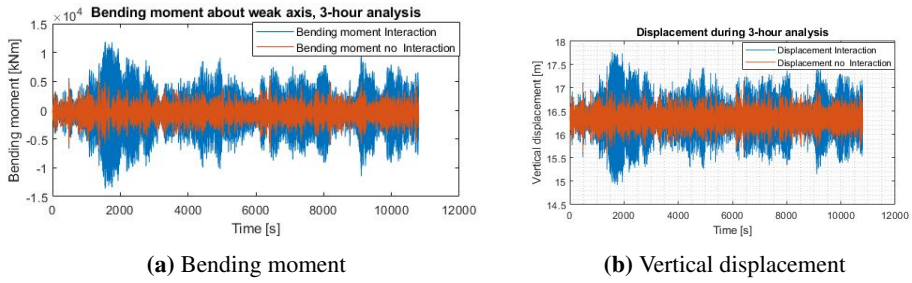
Figure 7.17: Bending moment and vertical displacement during a timeserie

7.6 Wave condition 2

Wave Condition 2 have a significant wave height and peak period of Hs= 3m and Tp= 6s. The waves coming from the north will give rise to excitation force in surge and heave. As shown in Section 3.2 the amplitudes of exciting wave force in lee-side are smaller than the one on the weather side.
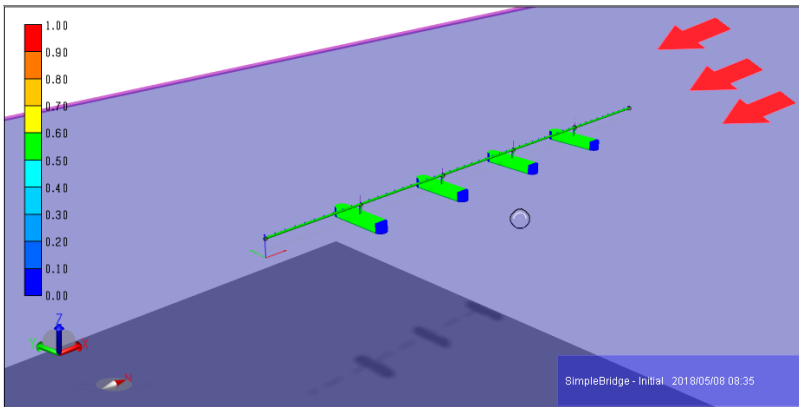
Figure 7.18: Incoming waves from 0 degrees

7.6.1 Displacement

For this wave condition, the displacement for the single body is larger than the multibody configuration. That is because of shielding effects, and the excitation force is smaller in the lee-side. When the waves hit the pontoon, the wavefield is changed, according to the visualization shown in Section 3.7. The reduction in the wave heights behind the pontoon corresponds to a lower response in the lee-side.

(a) Vertical Displacement

(b) Horizontal displacement
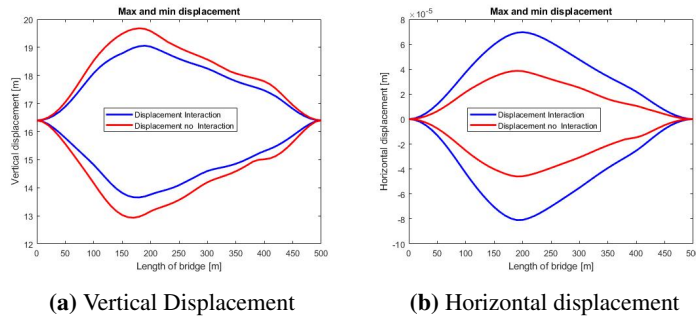
Figure 7.19: Vertical and horizontal displacement

7.6.2   Forces and moments

The maximum bending moment is larger for this wave condition. The design of the body is based on a prismatic shape with smooth edges. When waves propagate from the north, the bending moment will be larger because of hitting the longest side of the pontoons.

(a) Bending moment

(b) Max bending moment
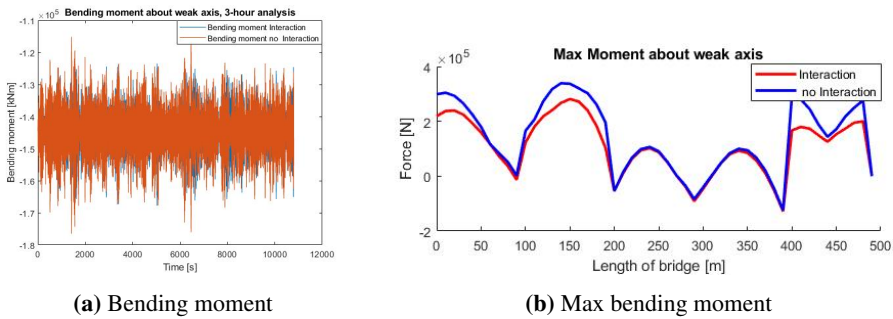
Figure 7.20: Bending moment during a timeserie and max bending moment

(a) Vertical displacement

(b) Vertical displacement
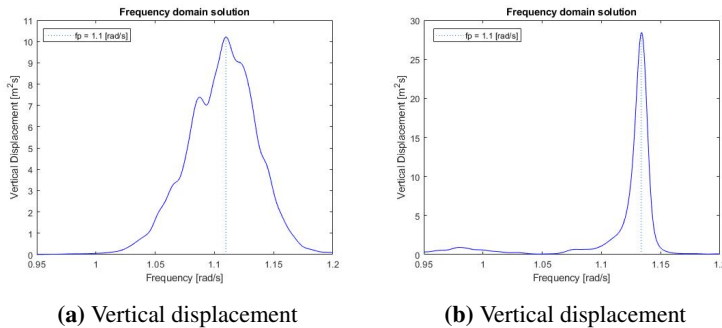
Figure 7.21: Frequency domain solution for vertical displacement

7.7 Wave Condition 3

In this wave condition, the waves come from the north-west (315 degrees) and will, therefore, include wave force component in surge, sway and heave in addition to pitch, roll and yaw moment. The response in this wave condition turned out to be much larger than Wave Condition 1. That may be because of distribution of all six load components, while waves from the north and west only have three components.

7.7.1 Displacement

The most substantial displacement of the bridge girder during a 3-hour analysis is shown in Figure 7.22. This shows the absolute maximum and minimum at each integration point in the bridge girder. The maximum vertical displacement analysis is 0.6m and 2.0m for the multibody analysis, respectively.

(a) Incoming waves from 315 degrees

(b) Incoming waves from 315 degrees
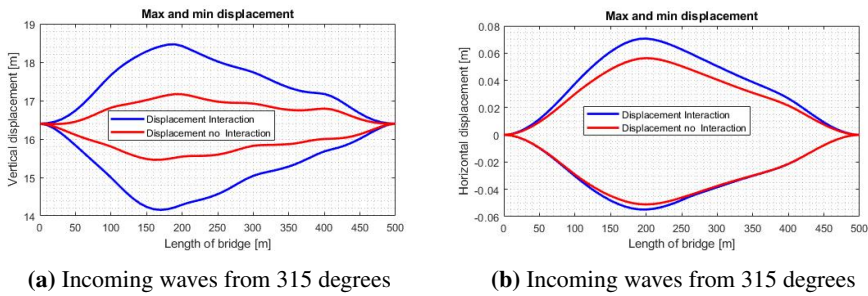
Figure 7.22: Vertical and horizontal displacement
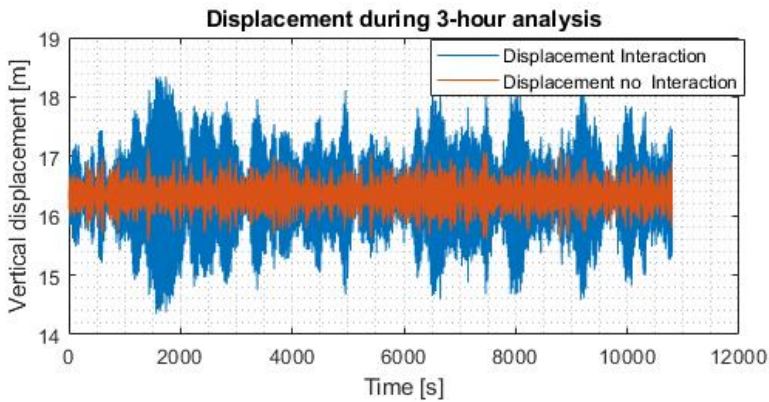
Figure 7.23: Incoming waves from 315 degrees
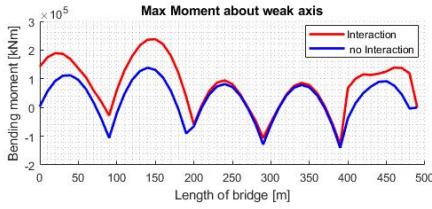
(a) Incoming waves from 315 degree
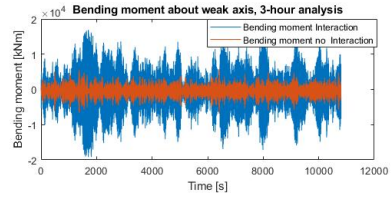
(b) Incoming waves from 315 degree
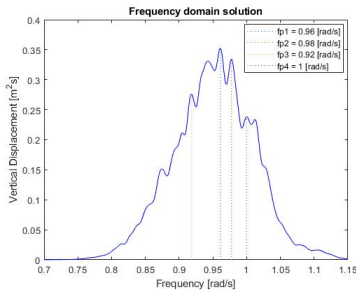
(a) Incoming waves from 315 degree
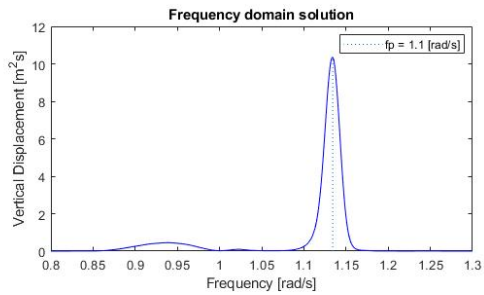
(b) Incoming waves from 315 degree

Table 7.7: Max vertical and horizontal displacement for single body and multibody configuration

	Interaction		No interaction	
Wave condtition	Max Vertical	Max Horizontal	Max Vertical	Max Horizontal
Wave condition 1	1m	0.09m	0.6m	0.08m
Wave condtion 2	2.4m	0	2.9m	0
Wave condition 3	2.0m	0.07m	0.6m	0.055m

Chapter 8

Conclusion

In the static analysis, I primarily look into bending moment and shear forces in the main girder with self-weight only. The results correspond to hand-calculation with a deviation of 1.1 % and 0.98% for the maximum moment and maximal shear force respectively. The most considerable bending moment was located at the high bridge and is a result of a large span length and large self-weight. The vertical deflection of the pontoons were all approximately zero. This indicates that the applied specified force was modeled correctly.

The main objective of eigenmode analysis was to check if the eigenfrequencies of the bridge were outside the range of environmental load frequencies. For the first eigenmodes the wind loads are the most crucial. These modes are slowly varying forces and can probably cause fatigue. For mode 9 and 10 might coincide with the wave frequency. For lower modes, the vertical modes are dominating. This could be a problem according to the response of the bridge and could damage the structure. Ideally, the eigenfrequencies should be outside the range of wave frequency. For sizeable floating bridge structure, it is impossible to have all eigenperiods outside the range of wave frequencies. One feasible solution could be increasing the added mass by attaching a flange to the pontoons. The attached flange could be placed on the bottom to increased the added mass in heave. With the flange attached the heave motion can be out of the range where wave loads are dominating. This is already suggested in the report compiled by Cowi.(COWI, 2016b)

The hydrodynamic interaction of multiple bodies is a complex problem and is hard to elucidate. There was no difference in added mass, damping and excitation force for low frequencies. For frequencies between 1 and 2 large oscillations for multibody configuration begins, and the influence of hydrodynamic interaction is clearly shown. Especially for added mass in surge, the responses of a multibody analysis are quite different from the responses of a single body without multibody effects. The oscillations are a result of strong interaction effects due to sloshing and other interaction effects. The natural sloshing frequencies correspond to local maxima and minima for the hydrodynamic coefficients. By investigating the waves in the wake, we see a reduction in wave height behind the pontoon.

The dynamic analysis turned out to be too time-consuming, only a short analysis of 300 seconds was studied. Horizontal displacement was the dominating motion with a maximum displacement of 2 meters in extreme environmental conditions. For this wave condition, the bridge would not be safe for traffic. The most significant force components occur at the south side of the bridge. At the south end, the navigation channel, long span length leads to large force components. However, the force component is far beyond yield strength of the structure.

For the simple bridge, single body and multibody analysis in regular waves have been presented in the frequency domain. The single body and multibody analysis in regular waves show that the hydrodynamic interaction can be observed from added mass, potential damping, and exciting forces. The vertical displacement is dominant for all wave conditions compared to horizontal displacement. The vertical displacement is larger for the multibody configuration when waves are coming from the west. When waves are propagating from the south, the vertical displacement is largest for the single body due to shielding effects of the multibody analysis. The maximum horizontal displacement is observed in the middle of the bridge for both models. The weak axis moment was the component that gives the most significant contribution of stress.

The dominating motion is centered around the first eigenperiod and wave loads. For the multibody analysis, the vertical displacement has a much more sharp peak at a frequency of 1.13 rad/s. Further investigation shows that the sharp peak was due to added mass. Using the added mass into the single body analysis, the dominating motion is more concentrated around the wave period and lead to larger displacement.

It is interesting to observe how the wave heading caused a significantly different response of the bridge girder. The wave heading from the north-west is most critical regarding moments and displacements. That may be because of distribution of all six load components, while waves from the west only have three components. The analysis of the bridge exposed to linear wave loads creates substantial load effect at the bridge girder for several headings. The accurate prediction of hydrodynamic coefficients, such as added mass, damping and excitation force is crucial in analyzing the motion response of a floating structure in waves. Changing one of this coefficient lead to a different response. When the hydrodynamic coefficients are computed, the use of complicated mathematical analysis or state-of-the-art numerical tools are required, which can be expensive and time-consuming. In my case, the process was too time-consuming for the whole bridge structure.

The representation of the simple bridge cannot be compared to the complete bridge structure and is much more different than I first thought. First of all, the long bridge structure has very long eigenperiods of more than 60 seconds, and the eigenmodes are dominating by horizontal motions. For the simple bridge, the eigenmodes dominating of vertical motions and the first eigenmodes is close to the wave conditions at Bjørnafjorden.

Wadam can handle 60 different frequencies, and in an interaction problem where the hydrodynamic coefficients are strongly dependent on a small change in frequency, this is a source of error. RIFLEX do not take coupling effects into account when calculating the radiation data. Coupling effects for some distinct frequency contain up to 20% for some distinct frequencies.

Chapter 9

Recommendation for Further Work

It is no doubt that the floating bridge over Bjørnafjorden is a very large and complex structure which requires expertise from many different disciplines. Many improvements should be implemented. For instance, the contribution from other force components than the linear wave load such as slowly varying loads should be implemented. It could also be interesting to use another software for calculation of the interaction effects. To consider VIV, the potential theory solver Wadam can no longer be used, and a computational fluid dynamics (CFD) analysis would have to be performed. However, doing a CFD analysis in time domain requires a lot of computing power.

For further studies, viscous fluid models can be developed to simulate the fluid flow around multiple bodies to examine the excitation due to the resonance. Sensitivity analyses of the gap width, barge length, barge breadth, and draft should be performed.

Self-weight was the only external load included. Traffic load and other external loads should also be looked into. Wind, wave, and current should be investigated from every different direction, magnitude, and direction.

Using a more powerful computer is necessary to run the analysis for the whole bridge structure. This is just a numerical study based on linear theory, and many effects are neglected. It could also be interesting to do a model testing of multiple floating pontoons. The model testing will be able to investigate the interaction effects and could be performed as an alternative to CFD analyses.

References

Ali, M. T., Inoue, Y., 2005. ON HYDRODYNAMIC INTERACTION BETWEEN TWO RECTANGULAR BARGES FLOATING SIDE-BY-SIDE IN REGULAR WAVES, 1st Edition. Naval Architecture and Marine Engineering, Bangladesh.

Ali, M. T., Khalil, G. M., 2005. ON HYDRODYNAMIC INTERACTION BETWEEN SEVERAL FREELY FLOATING VERTICAL CYLINDERS IN WAVES, 1st Edition. Halkidiki, Greece.

Chandler, N., 2017. How floating bridges work.

COWI, 2016a. CURVED BRIDGE – NAVIGATION CHANNEL IN SOUTH, 1st Edition. COWI AS.

COWI, 2016b. STRAIGHT BRIDGE – NAVIGATION CHANNEL IN SOUTH, 1st Edition. COWI.

Damkilde, L., 2000. Euler-Bernoulli beam theory, 1st Edition. Stress and stiffness analysis of beam sections.

Faltinsen, O., 1990. Sea loads on ships and offshore structures, 1st Edition. Cambridge University Press.

Faltinsen, O. M., Timokha, A. N., 2009. Sloshing, 1st Edition. Cambridge Universisy Press.

Kagemoto, H., Yue, D. K. P., 1993. Hydrodynamic Interaction Analyses of Very Large Floating Structures, 1st Edition. Cambridge.

Kim, M-S., H. M.-K., Kim, B.-W., 2003. Relative motions between LNG-FPSO and side-by-side positioned LNG carriers in waves, 13th Edition. ISOPE Conference, Honolulu.

Koo, W., Kim, J.-D., 2015. Simplified formulas of heave added mass coefficients at high frequency for various two-dimensional bodies in a finite water depth, 1st Edition. Department of Naval Architecture and Ocean Engineering, Inha University, Incheon, Korea Hyundai Heavy Industries.

Langen, S. ., 1979. Dynamisk analyse av konstruksjoner, 1st Edition. Stress and stiffness analysis of beam sections.

MARINTEK, 2011. Riser System Analysis Program, 1st Edition. MARINTEK.

MiT, 2017. Reynolds number pipe flow.

NorconsultAS, 2017. Ferry free E39 –Fjord crossings Bjørnafjorden, 1st Edition. Norconsult AS.

Thomas Viuff, Bernt Leira, X. X., Øiseth, O., 2016. Methods for preliminary analysis of floating bridges structures, 1st Edition. NTNU and NPRA.

Vegvesen, S., 1994. The nordhordland bridge.

Vegvesen, S., 2015. Bruprosjektering, Håndbok N400, 1st Edition. Statens Vegvesen.

Vegvesen, S., 2017a. E39 stord-os.

Vegvesen, S., 2017b. E39 stord-os (hordfast) blir 8 milliardar billigare.

Veritas, D. N., 2010. ENVIRONMENTAL CONDITIONS AND ENVIRONMENTAL LOADS, 1st Edition. Det norske Veritas.

Veritas, D. N., 2014a. Environmental Conditions and Environmental Loads, 1st Edition. Det Norske Veritas AS.

Veritas, D. N., 2014b. SIMA User Guide, 1st Edition. Marintek.

WAFO-group, 2017. A Matlab Toolbox for analysis of Random Waves and Loads, 1st Edition. Lund University.

Xin Xu, Jian-Min Yang, X. L. . L. X., 2014. Hydrodynamic performance study of two side-byside barges, 1st Edition. Taylor Francis.

XU Xin, Li Xin, Y. J.-m. . X. L.-f., 2016. Hydrodynamic Interactions of Three Barges in Close Proximity in A Floatover Installation, 1st Edition. Chinese Ocean Engineering Society and Springer-Verlag Berlin Heidelberg.

Young, W. C., B. R. G., 2014. Roark's Formulas for Stress and Strain, 7th Edition.

Yu, D., Kareem, A., 1996. Two-dimensional simulation of flow around rectangular prisms, 1st Edition. University of Notre Dame, Notre Dame.

Appendices

Appendix A

Hydrodynamic Coeffisients

(a) Added mass for single body

(b) Damping for single body
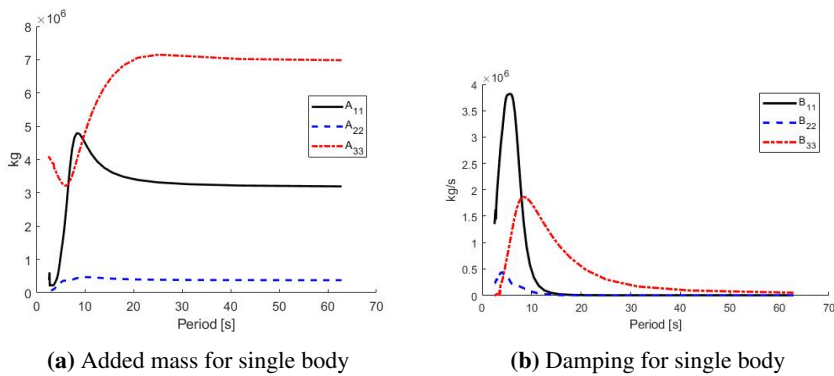
Figure A.1: Added mass and damping for single body
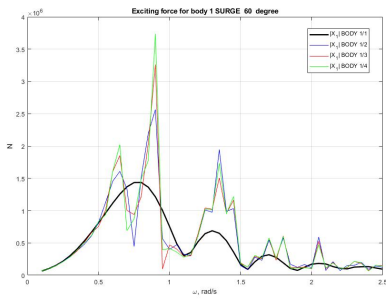
(a) excitingforce surge 60 deg
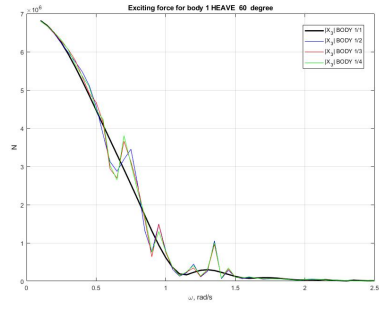
(b) exciting force heave 60 deg

Figure A.2: Excitingforce for surge and heave for waves propagating from 60 deg
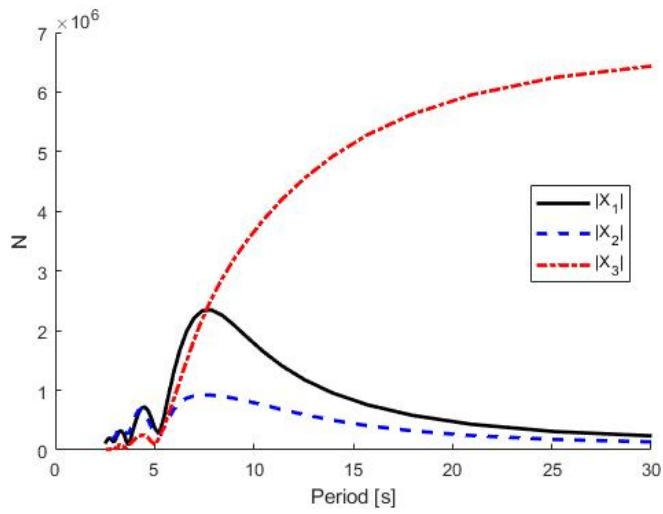
Figure A.3: Added mass in surge, sway and heave
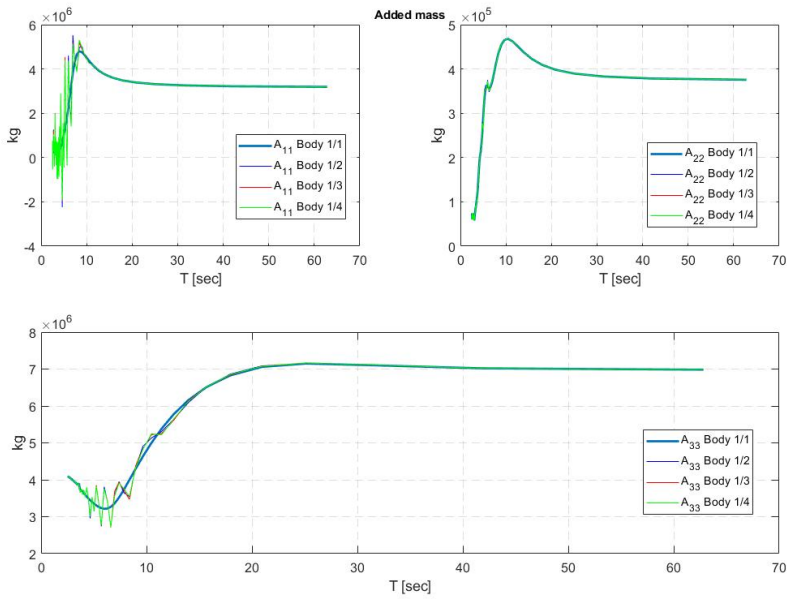
Figure A.4: Added mass in surge, sway and heave
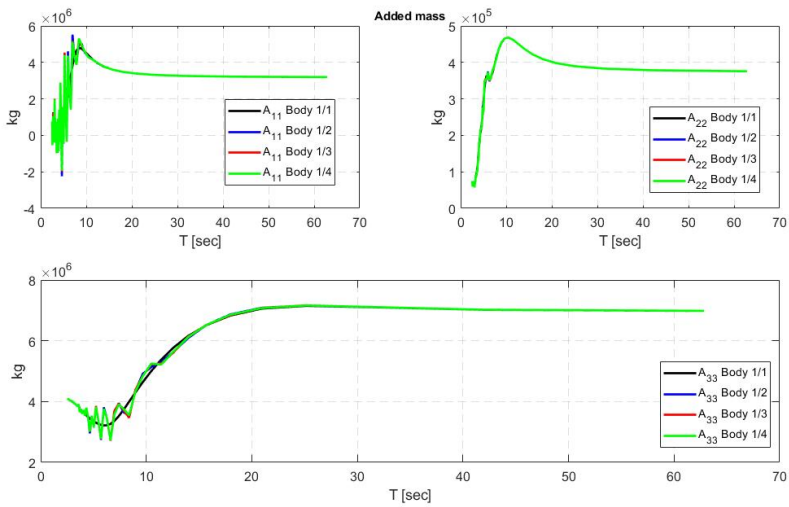
Figure A.5: Added mass in surge, sway and heave
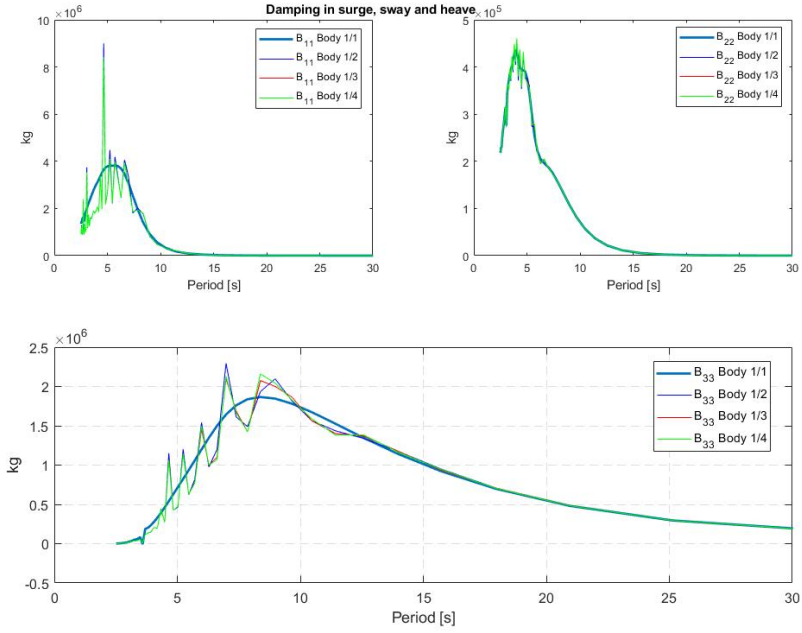
Figure A.6: Damping in surge, sway and heave
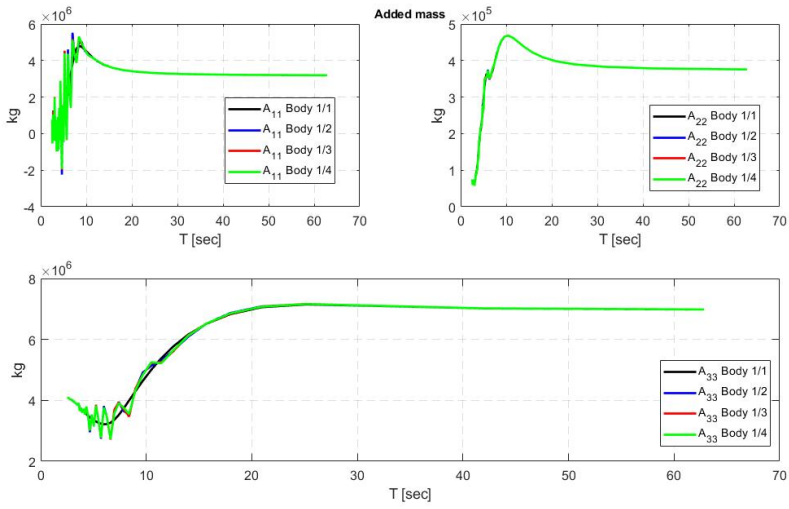
Figure A.7: Added mass in surge, sway and heave
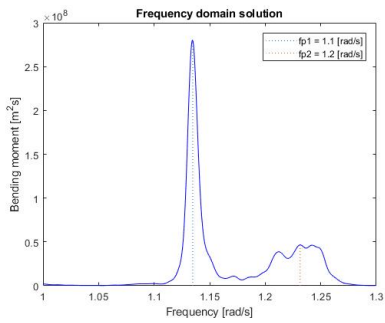
(a) Vertical displacement
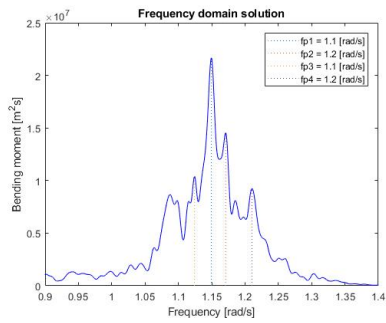
(b) Vertical displacement.
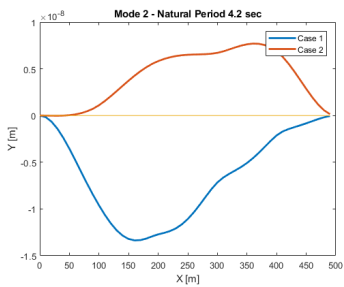
(a) Mode 2 XY-plot
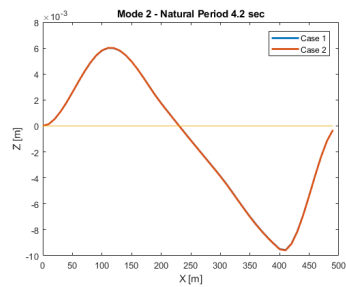
(b) Mode 2 XZ-plot
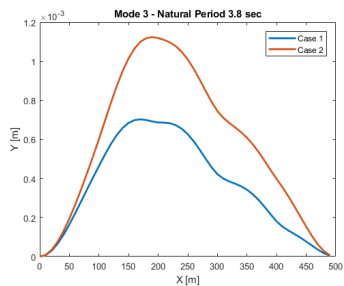
(a) Mode 3 XY-plot
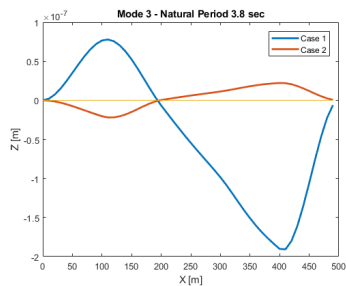
(b) Mode 3 XZ-plot

Appendix B

Matlab Code

Matlab Code

```matlab
close all
clear all
clc

%%%%%------------------------INFO-----------------------------%%%%%%
%This script is a modified script given by Erin Bachynski. The
    script is
%read the LIS-file from WADAM for multiple bodies. The script
    plots
%added mass, damping and excitation force in surge and heave for
    all
%bodies. In addition, added mass, damping and excitation force
    for a
%spesific body which is determined in input parameters
%%%%%------------------------------------------------------------%%%%%%

%INPUT PARAMETERS
WaveHeadInd = 5; % index of the wave heading
fname='WADAM2.LIS' %File name
body=4; %Number of bodies in your analysis
plot_body=3; %Decide wich spesific body you want to plot added
    mass, damping and excitation force

number_body=1:1:body;
fid = fopen(fname);
A = textscan(fid,'%s','Delimiter','\n');
data = A{1};
```

```
23
24  n=0;
25  ii = 1;
26  found = 0;
27  while ii<length(data) && found == 0
28      k = strfind(data(ii), 'ENVIRONMENTAL DATA:');
29      if ~isempty(k{1})
30          n = ii;
31          found = 1;
32          C = textscan(data{ii+3},'%s %s %s %f %s');
33          waterdepth = C{4};
34          C = textscan(data{ii+4},'%s %s %s %s %s %f ');
35          numwavelengths = C{6};
36          C = textscan(data{ii+5},'%s %s %s %s %s %f ');
37          numheadangles = C{6};
38          WaveDat = zeros(numheadangles,numwavelengths,5);
39          for jj = 1:numheadangles
40          for kk = 1:numwavelengths
41              WaveDat(jj,kk,:) = str2num(data{ii+kk+12});
42          end
43          end
44      end
45      ii = ii+1;
46  end
47  ii = n;
48  found = 0;
49  while ii<length(data) && found == 0
50      k = strfind(data(ii), 'THE OUTPUT IS NON-DIMENSIONALIZED
            USING');
51      if ~isempty(k{1})
52          n = ii;
53          found = 1;
54          C = textscan(data{ii+8},'%s %s %f');
55          RO  = C{3};
56          C = textscan(data{ii+9},'%s %s %f');
57          G   = C{3};
58          C = textscan(data{ii+10},'%s %s %f');
59          VOL = C{3};
60          C = textscan(data{ii+11},'%s %s %f');
61          L   = C{3} ;
62          C = textscan(data{ii+12},'%s %s %f');
63          WA  = C{3} ;
64      end
65      ii = ii+1;
66  end
67
68  % ADDED MASS
69  for iii=1:body
70      ii=1;
71      n=1;
```

```matlab
72   nstart = ii;
73   ADDMASS = zeros(numwavelengths,6, 7);
74   for nn = 1:numwavelengths
75       ii = n;
76       found = 0;
77       while ii<length(data) && ~found
78           k = strfind(data(ii), ['ADDED MASS MATRIX FOR BODY '
                    num2str(number_body(iii)) ' AND '
                    num2str(number_body(iii))]);
79           if ~isempty(k{1})
80               found = 1;
81               n = ii + 1;
82               ADDMASS(nn,1,:) = str2num(data{ii+4});
83               ADDMASS(nn,2,:) = str2num(data{ii+5});
84               ADDMASS(nn,3,:) = str2num(data{ii+6});
85               ADDMASS(nn,4,:) = str2num(data{ii+7});
86               ADDMASS(nn,5,:) = str2num(data{ii+8});
87               ADDMASS(nn,6,:) = str2num(data{ii+9});
88           end
89           ii = ii+1;
90       end
91   end
92   ADDMASS_TOT{iii}=ADDMASS
93   end
94
95   for iii = 1:body
96   ADDMASS_TOT{iii} = ADDMASS_TOT{iii}(:,:,2:7);
97   ADDMASS_TOT{iii}(:,1:3,1:3) = ADDMASS_TOT{iii}(:,1:3,1:3)*RO*VOL;
98   ADDMASS_TOT{iii}(:,1:3,4:6) =
           ADDMASS_TOT{iii}(:,1:3,4:6)*RO*VOL*L;
99   ADDMASS_TOT{iii}(:,4:6,1:3) =
           ADDMASS_TOT{iii}(:,4:6,1:3)*RO*VOL*L;
100  ADDMASS_TOT{iii}(:,4:6,4:6) =
           ADDMASS_TOT{iii}(:,4:6,4:6)*RO*VOL*L*L;
101  end
102  %%%DAMPING%%%
103  for iii=1:body
104  ii=1;
105  n=1;
106  ii = nstart;
107  DAMPING = zeros(numwavelengths,6,7);
108  for nn = 1:numwavelengths
109      found = 0;
110      while ii<length(data) && ~found
111          k = strfind(data(ii), ['DAMPING MATRIX FOR BODY '
                    num2str(number_body(iii)) ' AND '
                    num2str(number_body(iii))]);
112          if ~isempty(k{1})
113              found = 1;
114              n = ii + 1;
```

```matlab
115            DAMPING(nn,1,:) = str2num(data{ii+4});
116            DAMPING(nn,2,:) = str2num(data{ii+5});
117            DAMPING(nn,3,:) = str2num(data{ii+6});
118            DAMPING(nn,4,:) = str2num(data{ii+7});
119            DAMPING(nn,5,:) = str2num(data{ii+8});
120            DAMPING(nn,6,:) = str2num(data{ii+9});
121        end
122        ii = ii+1;
123    end
124 end
125 DAMPING_TOT{iii}=DAMPING
126 end
127
128 for iii=1:body
129 DAMPING_TOT{iii} = DAMPING_TOT{iii}(:,:,2:7);
130 DAMPING_TOT{iii}(:,1:3,1:3) =
        DAMPING_TOT{iii}(:,1:3,1:3)*RO*VOL*sqrt(G/L);
131 DAMPING_TOT{iii}(:,1:3,4:6) =
        DAMPING_TOT{iii}(:,1:3,4:6)*RO*VOL*sqrt(G*L);
132 DAMPING_TOT{iii}(:,4:6,1:3) =
        DAMPING_TOT{iii}(:,4:6,1:3)*RO*VOL*sqrt(G*L);
133 DAMPING_TOT{iii}(:,4:6,4:6) =
        DAMPING_TOT{iii}(:,4:6,4:6)*RO*VOL*L*sqrt(G*L);
134 end
135
136 %%%%%%%%%%%%%%%%%%%%%%%%%%%%%%%%%%%%%%%%%%%%%%%%%%%%%%%%%%%%%%%%%%%%%%
137 % TOTAL EXCITING FORCES AND MOMENTS
138 for iii = 1:body
139    ii=1;
140 ii = nstart;
141 WAVEEX = zeros( numheadangles,numwavelengths,6, 4);
142 MOTIONS = zeros( numheadangles,numwavelengths,6, 4);
143 for nn = 1:numwavelengths
144    for mm = 1:numheadangles
145        found = 0;
146        while ii<length(data) && ~found
147            k = strfind(data(ii), ['EXCITING FORCES AND MOMENTS FROM
                INTEGRATION OF PRESSURE FOR BODY '
                num2str(number_body(iii))]);
148            if ~isempty(k{1})
149                found = 1;
150                n = ii + 1;
151                for qq = 1:6
152                    dat = textscan(data{ii+2*qq+1+2},'%s %f %f %f %f');
153                    WAVEEX(mm,nn,qq,:) = [dat{2} dat{3} dat{4} dat{5}];
154                end
155            end
156            ii = ii+1;
157        end
158    end
```

94

```matlab
159  end
160  WAVEEX_TOT{iii}=WAVEEX
161  end
162
163  for iii = 1:body
164  WAVEEX_TOT{iii}(:,:,1:3,1:3)=
         WAVEEX_TOT{iii}(:,:,1:3,1:3)*RO*VOL*G*WA/L;
165  WAVEEX_TOT{iii}(:,:,4:6,1:3)=
         WAVEEX_TOT{iii}(:,:,4:6,1:3)*RO*VOL*G*WA;
166  %MOTIONS_TOT{iii}=MOTIONS{iii}
167  end
168
169  %%%%%%%%%%%%%%%%%%%%%%%%%%%%%%%%%%%%%%%%%%%%%%%%%%%%%%%%%%%%%%%%%%%%%%
170  % HORIZONTAL MEAN DRIFT FORCES AND MOMENT
171  ii = nstart;
172  MEANDRIFT = zeros( numheadangles,numwavelengths,3);
173  for nn = 1:numwavelengths
174      for mm = 1:numheadangles
175          found = 0;
176          while ii<length(data) && ~found
177              k = strfind(data(ii), 'HORIZONTAL MEAN DRIFT FORCES AND
                    MOMENT');
178              if ~isempty(k{1})
179                  found = 1;
180                  n = ii + 1;
181                  for qq = 1:3
182                      C = textscan(data{ii+3+qq},'%s %s %s %s %s %s %f');
183                      MEANDRIFT(mm,nn,qq) = C{7};
184                  end
185              end
186              ii = ii+1;
187          end
188      end
189  end
190  MEANDRIFT(:,:,1:2) = MEANDRIFT(:,:,1:2)*RO*G*L*WA*WA;
191  MEANDRIFT(:,:,3) = MEANDRIFT(:,:,3)*RO*G*L*L*WA*WA;
192  fclose(fid);
193
194  %%%%%%%%%%%%%%%%%%%%%%%%%%%%%%%%%%%%%%%%%%%%%%%%%%%%%%%%%%%%%%%%%%%%%%
195  % PLOT ADDED MASS
196  %%%%%%%%%%%%%%%%%%%%%%%%%%%%%%%%%%%%%%%%%%%%%%%%%%%%%%%%%%%%%%%%%%%%%%
197  styles = {'k','b','r','g','b','r'
198      'k--','b--','r--','g--','b--','r--'
199      'k-.','b-.','r-.','g-.','b-.','r-.'
200      'k','b','r','g','b','r'
201      'k--','b--','r--','g--','b--','r--'
202      'k-.','b-.','r-.','g-.','b-.','r-.'};
203
204  f=figure(1);
205  set(f,'Position',[200 200 1200 800])
```

```matlab
subplot(2,2,1)
hold on
n = 1;
legent = cell(9, 1);
for ii = 1:3
    for jj = 1:3
        plot(WaveDat(WaveHeadInd,:,5),ADDMASS_TOT{plot_body}(:,ii,jj),styles{ii,j
        legent{n} = ['A_' num2str(ii) '_' num2str(jj)];
        n = n+1;
    end
end
grid
% xlabel('\omega, rad/s')
xlabel('\omega, rad/s')
legend(legent{1},legent{2},legent{3},legent{4},legent{5},legent{6},...
legent{7},legent{8},legent{9},'Location','EastOutside')
ylabel('kg')
set(gca,'FontSize',12)
set(gca,'GridLineStyle','--')

subplot(2,2,3)
hold on
n = 1;
legent = cell(9, 1);
for ii = 1:3
    for jj = 4:6
        plot(WaveDat(WaveHeadInd,:,5),ADDMASS_TOT{plot_body}(:,ii,jj),styles{ii,j
        legent{n} = ['A_' num2str(ii) '_' num2str(jj)];
        n = n+1;
    end
end
grid
xlabel('\omega, rad/s')
legend(legent{1},legent{2},legent{3},legent{4},legent{5},legent{6},...
    legent{7},legent{8},legent{9},'Location','EastOutside')
ylabel('kg-m')
set(gca,'FontSize',12)
set(gca,'GridLineStyle','--')

subplot(2,2,2)
hold on
n = 1;
legent = cell(9, 1);
for ii = 4:6
    for jj = 4:6
        plot(WaveDat(WaveHeadInd,:,5),ADDMASS_TOT{plot_body}(:,ii,jj),styles{ii,j
        legent{n} = ['A_' num2str(ii) '_' num2str(jj)];
        n = n+1;
    end
end
```

```matlab
256  grid
257  xlabel('\omega, rad/s')
258  legend(legent{1},legent{2},legent{3},legent{4},legent{5},legent{6},...
259      legent{7},legent{8},legent{9},'Location','EastOutside')
260  ylabel('kg-m^2')
261  set(gca,'FontSize',12)
262  set(gca,'GridLineStyle','--')
263
264  subplot(2,2,4)
265  hold on
266  n = 1;
267  for ii = 4:6
268      for jj = 1:3
269          plot(WaveDat(WaveHeadInd,:,5),ADDMASS_TOT{plot_body}(:,ii,jj),styles{ii,j
270          legent{n} = ['A_' num2str(ii) '_' num2str(jj)];
271          n = n+1;
272      end
273  end
274  grid minor
275  xlabel('\omega, rad/s')
276  legend(legent{1},legent{2},legent{3},legent{4},legent{5},legent{6},...
277      legent{7},legent{8},legent{9},'Location','EastOutside')
278  ylabel('kg-m')
279  set(gca,'FontSize',12)
280  set(gca,'GridLineStyle','--')
281  set(gcf,'NextPlot','add');
282  axes;
283  set(gca,'Visible','off');
284  h = title('Added mass for body 1/3','fontweight','b');
285  set(h,'Visible','on');
286
287  %%%%%%%%%%%%%%%%%%%%%%%%%%%%%%%%%%%%%%%%%%%%%%%%%%%%%%%%%%%%%%%%%%%%%%%%%
288  % PLOT DAMPING
289  %%%%%%%%%%%%%%%%%%%%%%%%%%%%%%%%%%%%%%%%%%%%%%%%%%%%%%%%%%%%%%%%%%%%%%%%%
290  f=figure(2);
291  set(f,'Position',[200 200 1200 800])
292  subplot(2,2,1)
293  hold on
294  n = 1;
295  legent = cell(9, 1);
296  for ii = 1:3
297      for jj = 1:3
298          plot(WaveDat(WaveHeadInd,:,5),DAMPING_TOT{plot_body}(:,ii,jj),styles{ii,j
299          legent{n} = ['B_' num2str(ii) '_' num2str(jj)];
300          n = n+1;
301      end
302  end
303  grid
304  xlabel('\omega, rad/s')
305  legend(legent{1},legent{2},legent{3},legent{4},legent{5},legent{6},...
```

```
306  legent{7},legent{8},legent{9},'Location','EastOutside')
307  ylabel('kg/s')
308
309  subplot(2,2,3)
310  hold on
311  n = 1;
312  legent = cell(9, 1);
313  for ii = 1:3
314      for jj = 4:6
315          plot(WaveDat(WaveHeadInd,:,5),DAMPING_TOT{plot_body}(:,ii,jj),styles{ii,j
316          legent{n} = ['B_' num2str(ii) '_' num2str(jj)];
317          n = n+1;
318      end
319  end
320  grid
321  xlabel('\omega, rad/s')
322  legend(legent{1},legent{2},legent{3},legent{4},legent{5},legent{6},...
323  legent{7},legent{8},legent{9},'Location','EastOutside')
324  ylabel('kg-m/s')
325
326  subplot(2,2,2)
327  hold on
328  n = 1;
329  legent = cell(9, 1);
330  for ii = 4:6
331      for jj = 4:6
332          plot(WaveDat(WaveHeadInd,:,5),DAMPING_TOT{plot_body}(:,ii,jj),styles{ii,j
333          legent{n} = ['B_' num2str(ii) '_' num2str(jj)];
334          n = n+1;
335      end
336  end
337  grid
338  xlabel('\omega, rad/s')
339  legend(legent{1},legent{2},legent{3},legent{4},legent{5},legent{6},...
340  legent{7},legent{8},legent{9},'Location','EastOutside')
341  ylabel('kg-m/s^2')
342
343  subplot(2,2,4)
344  hold on
345  n = 1;
346  for ii = 4:6
347      for jj = 1:3
348          plot(WaveDat(WaveHeadInd,:,5),DAMPING_TOT{plot_body}(:,ii,jj),styles{ii,j
349          legent{n} = ['B_' num2str(ii) '_' num2str(jj)];
350          n = n+1;
351      end
352  end
353  grid
354  xlabel('\omega, rad/s')
355  legend(legent{1},legent{2},legent{3},legent{4},legent{5},legent{6},...
```

```matlab
356        legent{7},legent{8},legent{9},'Location','EastOutside')
357   ylabel('kg-m/s')
358   set(gcf,'NextPlot','add');
359   axes;
360   set(gca,'Visible','off');
361   h = title('Damping for body 1/3','fontweight','b');
362   set(h,'Visible','on');
363
364   %%%%%%%%%%%%%%%%%%%%%%%%%%%%%%%%%%%%%%%%%%%%%%%%%%%%%%%%%%%%%%%%%%%%%%%%
365   % PLOT EXCITING FORCES BODY 1
366   %%%%%%%%%%%%%%%%%%%%%%%%%%%%%%%%%%%%%%%%%%%%%%%%%%%%%%%%%%%%%%%%%%%%%%%%
367   f=figure(3);
368   set(f,'Position',[200 200 1200 800])
369   subplot(2,2,1)
370   hold on
371   n = 1;
372   for ii = [1,3]
373       plot(WaveDat(WaveHeadInd,:,5),WAVEEX_TOT{plot_body}(WaveHeadInd,:,ii,3),style
374       legent{n} = ['|X_' num2str(ii) '|'];
375       n = n+1;
376   end
377   legend(legent{1},legent{2},'Location','EastOutside')
378   grid
379   xlabel('\omega, rad/s')
380   ylabel('N')
381
382   subplot(2,2,2)
383   hold on
384   n = 1;
385   for ii = [1,3]
386       plot(WaveDat(WaveHeadInd,:,5),WAVEEX_TOT{plot_body}(WaveHeadInd,:,ii,4),[styl
387           '.'])
388       legent{n} = ['\theta(X_' num2str(ii) ')'];
389       n = n+1;
390   end
391   legend(legent{1},legent{2},'Location','EastOutside')
392   ylim([-180 180])
393   grid
394   xlabel('\omega, rad/s')
395   ylabel('deg')
396
397   subplot(2,2,3)
398   hold on
399   n = 1;
400   for ii = [4,5]
401       plot(WaveDat(WaveHeadInd,:,5),WAVEEX_TOT{plot_body}(WaveHeadInd,:,ii,3),style
402       legent{n} = ['|X_' num2str(ii) '|'];
403       n = n+1;
404   end
405   legend(legent{1},'Location','EastOutside')
```

```
405  grid
406  xlabel('\omega, rad/s')
407  ylabel('N')
408
409  subplot(2,2,4)
410  hold on
411  n = 1;
412  for ii = [4,5]
413      plot(WaveDat(WaveHeadInd,:,5),WAVEEX_TOT{plot_body}(WaveHeadInd,:,ii,4),[styl
            '.'])
414      legent{n} = ['\theta(X_' num2str(ii) ')'];
415      n = n+1;
416  end
417  legend(legent{1},'Location','EastOutside')
418  ylim([-180 180])
419  grid minor
420  xlabel('\omega, rad/s')
421  ylabel('deg')
422  set(gcf,'NextPlot','add');
423  axes;
424  set(gca,'Visible','off');
425  h = title('Exciting force for body 1/3','fontweight','b');
426  set(h,'Visible','on');
427
428  %%%%%%%%%%%%%%%%%%%%%%%%%%%%%%%%%%%%%%%%%%%%%%%%%%%%%%%%%%%%%%%%%%%%%%%%%%%%
429  % PLOT EXCITING FORCES FOR ALL BODIES - SURGE
430  %%%%%%%%%%%%%%%%%%%%%%%%%%%%%%%%%%%%%%%%%%%%%%%%%%%%%%%%%%%%%%%%%%%%%%%%%%%%
431  f=figure(4);
432  set(f,'Position',[10 10 800 700])
433  for iii = 1:body
434   plot(WaveDat(WaveHeadInd,:,5),WAVEEX_TOT{iii}(WaveHeadInd,:,1,3),styles{1,iii})
435   legent{iii}=['|X_', num2str(iii) , '| BODY 2'];
436  hold on
437  end
438  legend(legent,'Location','EastOutside')
439  set(gcf,'NextPlot','add');
440  axes;
441  set(gca,'Visible','off');
442  h = title(['Exciting force for all bodies SURGE ',
        num2str(WaveHeadInd*15-15) ' degree' ]);
443  set(h,'Visible','on');
444  grid minor
445  xlabel('\omega, rad/s')
446  ylabel('N')
447  hold off
448
449  %%%%%%%%%%%%%%%%%%%%%%%%%%%%%%%%%%%%%%%%%%%%%%%%%%%%%%%%%%%%%%%%%%%%%%%%%%%%
450  % PLOT EXCITING FORCES FOR ALL BODIES - SWAY
451  %%%%%%%%%%%%%%%%%%%%%%%%%%%%%%%%%%%%%%%%%%%%%%%%%%%%%%%%%%%%%%%%%%%%%%%%%%%%
452  f=figure(5);
```

```matlab
set(f,'Position',[10 10 800 700])
for iii = 1:body
 plot(WaveDat(WaveHeadInd,:,5),WAVEEX_TOT{iii}(WaveHeadInd,:,2,3),styles{1,iii})
 legent{iii}=['|X_', num2str(iii) , '| BODY 2'];
hold on
end
legend(legent,'Location','EastOutside')
set(gcf,'NextPlot','add');
axes;
set(gca,'Visible','off');
h = title(['Exciting force for all bodies SWAY ',
    num2str(WaveHeadInd*15-15) ' degree' ]);
set(h,'Visible','on');
grid minor
xlabel('\omega, rad/s')
ylabel('N')
hold off
%%%%%%%%%%%%%%%%%%%%%%%%%%%%%%%%%%%%%%%%%%%%%%%%%%%%%%%%%%%%%%%%%%%%%%%%%%%%%%%%
% PLOT EXCITING FORCES FOR ALL BODIES HEAVE
%%%%%%%%%%%%%%%%%%%%%%%%%%%%%%%%%%%%%%%%%%%%%%%%%%%%%%%%%%%%%%%%%%%%%%%%%%%%%%%%

f=figure(6);
set(f,'Position',[10 10 800 800])
for iii = 1:body
    plot(WaveDat(WaveHeadInd,:,5),WAVEEX_TOT{iii}(WaveHeadInd,:,3,3),styles{1,iii
    legent{iii} = ['|X_' num2str(iii) '| BODY 1'];
hold on
end
legend(legent,'Location','EastOutside')
grid minor
xlabel('\omega, rad/s')
ylabel('N')
set(gcf,'NextPlot','add');
axes;
set(gca,'Visible','off');
h = title(['Exciting force for all bodies HEAVE ',
    num2str(WaveHeadInd*15-15) ' degree' ]);
set(h,'Visible','on');
hold off

%%%%ADDED MASS FOR ALL BODIES IN SURGE
f=figure(7);
set(f,'Position',[200 200 1200 800])
n = 1;
for iii = 1:body
    n = 1;
        plot(WaveDat(WaveHeadInd,:,5),ADDMASS_TOT{iii}(:,1,1),'linewidth',2)
        hold on

```

```matlab
        legent{iii} = ['A_' num2str(iii) '_' num2str(iii) ' Body '
            num2str(iii) '/' num2str(body)'];
end
legend(legent,'Location','EastOutside')
title('Added mass for bodies in SURGE')
grid minor
xlabel('\omega, rad/s')
ylabel('kg')
set(gca,'FontSize',12)
set(gca,'GridLineStyle','--')

%%%%ADDED MASS FOR ALL BODIES IN HEAVE
f=figure(8);
set(f,'Position',[200 200 1200 800])
n = 1;
for iii = 1:body
    n = 1;
        plot(WaveDat(WaveHeadInd,:,5),ADDMASS_TOT{iii}(:,3,3),'linewidth',2)
        hold on

        legent{iii} = ['A_' num2str(iii) '_' num2str(iii) ' Body '
            num2str(iii) '/' num2str(body)'];
end
legend(legent,'Location','EastOutside')
title('Added mass for bodies in HEAVE')
grid minor
xlabel('\omega, rad/s')
ylabel('kg')
set(gca,'FontSize',12)
set(gca,'GridLineStyle','--')

%%%%PLOT DAMPING FOR ALL BODIES IN SURGE%%%%%
figure(9);
for iii = 1:body
    n = 1;
        plot(WaveDat(WaveHeadInd,:,5),DAMPING_TOT{iii}(:,1,1),'linewidth',2)
        hold on
        legent{iii} = ['B_' num2str(iii) '_' num2str(iii) ' Body'
            num2str(iii) '/' num2str(body)];
end
legend(legent,'Location','EastOutside')
grid minor
xlabel('\omega, rad/s')
ylabel('kg/s')
set(gca,'FontSize',12)
set(gca,'GridLineStyle','--')
title('Damping in surge for all bodies')
axes;
set(gca,'Visible','off');
hold off
```

```
547
548  %%%%PLOT DAMPING FOR ALL BODIES IN SURGE%%%%%
549  figure(10);
550  for iii = 1:body
551      n = 1;
552          plot(WaveDat(WaveHeadInd,:,5),DAMPING_TOT{iii}(:,3,3),'linewidth',2)
553          hold on
554          legent{iii} = ['B_' num2str(iii) '_' num2str(iii) ' Body'
                  num2str(iii) '/' num2str(body)];
555  end
556  legend(legent,'Location','EastOutside')
557  grid minor
558  xlabel('\omega, rad/s')
559  ylabel('kg/s')
560  set(gca,'FontSize',12)
561  set(gca,'GridLineStyle','--')
562  title('Damping in heave for all bodies')
563  axes;
564  set(gca,'Visible','off');
565  hold off
```